

Structural and Functional Studies On Human PHD Finger Protein 2

Xian Deng

Wolfson College

Master of Science (by Research) Thesis 2014

Supervised by Professor Christopher Schofield

Abstract

Histone lysine methylation is an important post-translational modification (PTM) that can regulate gene expression in eukaryotic genomes. Histone methylation states are dynamically altered by the activity of methyl-transferases and demethylases, including the Jumonji C-domain-containing histone demethylases (JHDMs). The JHDM enzymes are members of the Fe(II) and 2-oxoglutarate (2OG) dependent dioxygenases superfamily, which utilise Fe(II) as a cofactor, and 2OG and oxygen as co-substrates to catalyse oxidative demethylation.

This thesis presents structural and functional studies on an unusual JHDM, PHF2, which has an interesting metal binding site. The proposed substrate for PHF2 is histone H3K4me3K9me2 although no definitive *in vitro* demethylation activity for PHF2 has yet been demonstrated. Due to the unusual composition of the catalytic site of PHF2, it is questionable whether PHF2 is able to productively bind metal ions and catalyse demethylation reactions, as do other JHDMs. In this thesis, work investigating the cofactor/co-substrate binding ability of PHF2 and its substrate peptide recognition mechanism is described. The studies used a combination of biochemical/biophysical assays and structural methods including X-ray crystallography. The results confirmed that PHF2 is able to bind to a transition metal ion and 2OG/NOG. Further investigations revealed that substrate peptide binding is mostly determined by the PHD finger; and biochemical assays suggested that the JmjC domain is not involved in peptide binding, which offers a possible explanation for the difference between the results of *in vitro* and cell-based demethylation activity assays.

Inhibitor screening was also carried out for PHF2, and a list of initial hits was

generated. Although the results of this work are preliminary, the initial hits will serve as templates for future development of PHF2 specific inhibitors, which could be used for both drug development and as probes to investigate the biological function of PHF2.

Acknowledgements

I would like to thank Professor Christopher Schofield, my supervisor without whom I could not have carried out any of the work in this project. I would like to thank Louise Walport as well; her constant support and endless patience were essential throughout my project. My thanks also go to Richard Hopkinson for his help in NMR, to Hanna Tarhonskaya for her help on non-denaturing ESI-MS, to Akane Kawamura for her help in T_m shift assays, to Michael McDonough, Shoichiro Horita, Rasheduzzaman Chowdhury, John Scotti and Weishen Aik for guidance on X-ray crystallography, and the rest of the CJS group who made my Masters project a very enjoyable experience.

List of Abbreviations

2OG	2-Oxoglutarate
ABH	Human AlkB homologue
Acetyl-CoA	Acetyl coenzyme-A
AdoHcy	*S*-Adenosyl-*L*-homocysteine
AdoMet	*S*-Adenosyl methionine
ARID5B	AT rich interactive domain 5B
CHCA	α-Cyano-4-hydroxycinnamic acid
CODD	*C*-Terminal oxygen-dependent degradation domain
CPH	Collagen prolyl hydroxylase
DAOCS	Deacetoxycephalosporin C synthase
DSBH	Double-stranded β-helix
DSF	Differential scanning fluorimetry
DTT	Dithiothreitol
EDTA	Ethylenediaminetetraacetic acid
FIH	Factor inhibiting HIF
FITC	Fluorescein isothiocyanate
FTO	Fat mass and obesity-associated protein
GFP	Green fluorescent protein
HAT	Histone acyltransferase
HDAC	Histone deacetylase
HEPES	4-(2-Hydroxyethyl)-1-piperazineethanesulfonic acid
HIF	Hypoxia-inducible factor
IEX	Ion exchange chromatography

IPTG	Isopropyl β-D-1-thiogalactopyranoside
JHDM	Jumonji domain-containing histone demethylase
JmjC	Jumonji domain C
LIC	Ligation-independent cloning
LRR domain	Leucine-rich repeat domain
LSD1	Lysine-specific demethylase 1
MALDI	Matrix-assisted laser desorption/ionization
NMR	Nuclear Magnetic Resonance
NODD	*N*-Terminal oxygen-dependent degradation domain
NOG	*N*-oxalylglycine
PADI4	Peptidyl arginine deiminase 4
PCR	Polymerase chain reaction
PHD Finger	Plant homeodomain
PHD	Prolyl hydroxylase domain
PHF2	PHD finger protein 2
PMSF	Phenylmethylsulfonyl fluoride
PRMT	Protein arginine methyltransferases
pVHL	Von Hippel–Lindau tumor suppressor
SDM	Site-directed mutagenesis
SDS	Sodium dodecyl sulfate
SDS-PAGE	Sodium dodecyl sulfate polyacrylamide gel electrophoresis
SEC	Size-exclusion chromatography
TCA cycle	Tricarboxylic acid cycle
TCEP	Tris-(2-carboxyethyl)phosphine
TEMED	Tetramethylethylenediamine

TET	Ten-eleven translocation family enzyme

List of Figures

Figure 1 Views from a crystal structure of the nucleosome (PDB 1EQZ).

Figure 2 Summary of histone modifications.

Figure 3 The chemical mechanisms by which three different classes of enzymes reverse lysine methylation.

Figure 4 The outline mechanisms of 2OG oxygenases.

Figure 5 Examples of modifications catalysed by 2OG oxygenases.

Figure 6 The domain architecture of KDM7 enzymes and the structures of PHF2 PHD and the JmjC domain.

Figure 7 Expression trial of wild-type PHF2 protein at 37 °C, 1 mM IPTG, 3 hours and 18 °C, 0.1 mM IPTG, overnight.

Figure 8 Purification of wild-type PHF2 and the Y321H variant proteins.

Figure 9 MALDI *In vitro* demethylation assay.

Figure 10 The use of non-denaturing ESI-MS to investigate the interactions between metal ions, 2OG/NOG and wild-type PHF2.

Figure 11 View from a crystal structure of PHF2 showing its active site and the tryptophan fluorescence studies on the metal binding affinities of PHF2.

Figure 12 The peptide binding affinity of wild-type PHF2 and the Y321H variant determined by fluorescence polarisation assays.

Figure 13 The peptide binding affinity of wild-type PHF2 (JmjC only) and wild-type PHF2 (PHD finger + JmjC) determined by fluorescence polarisation assays.

Figure 14 The effect of Ni^{2+} ions on the peptide binding affinity of wild-type PHF2 determined by fluorescence polarisation assays.

Figure 15 The peptide binding affinity of PHF2 determined by fluorescence polarisation assays.

Figure 16 Inhibitor screening for PHF2 using differential scanning fluorimetry (DSF) assay and the chemical structures of initial hits and 2OG.

Figure 17 NaCl concentrations screen for PHF2 using DSF assay.

Figure 18 T_m shift screen of various metal ions.

Figure 19 Diffraction image of a PHF2 crystal taken at Diamond Light Source beamline I04-1.

Figure 20 Structures of PHF2 JmjC domain and SDS-PAGE analysis.

List of Tables

Table 1 Summary of KDM subfamilies.

Table 2 Peptide substrate tested in the MALDI assay.

Table 3 Optimisation conditions of PHF2.

Table 4 Peptide substrate tested in the MALDI assay.

Table 5 Crystallographic data and refinement statistics.

Contents

Chapter 1 Introduction 1

1.1. DNA packing 1

1.2. Histone modification and relating enzymes 2

1.2.1. Histone acetylation 2

1.2.2. Histone phosphorylation 3

1.2.3. Histone ubiquitination 3

1.2.4. Histone methylation 4

1.2.5. Histone demethylase 7

1.3. 2OG-dependent oxygenases 10

1.3.1. Prolyl hydroxylases 12

1.3.2. DNA demethylase 13

1.4. JHDM KDM7 subfamily 15

1.5. PHD finger protein 2 (PHF2) 16

1.5.1. Domain architecture of PHF2 16

1.5.2. The biological relevance of PHF2 17

1.5.3. The structure of PHF2 18

1.6. Aim of this project 20

Chapter 2 Materials and Methods 21

2.2. Cloning 25

2.3. Protein Production 30

2.3.1. Expression Optimisation 30

2.3.2. Large Scale Protein Expression 31

2.4. Protein Purification 31

2.4.1. Affinity Chromatography 32

2.4.2. Ion-exchange Chromatography 33

2.4.3. Size exclusion chromatography 33

2.5. 2OG Turnover Assays using NMR 34

2.6. *In vitro* Demethylase Assays using MALDI 34

2.7. Non-denaturing ESI-MS Analyses 36

2.8. Tryptophan Fluorescence Analyses 36

2.9. Fluorescence Polarisation Analyses 37

2.10. Differential Scanning Fluorimetry (DSF, or T_m shift) Analyses 39

2.11. X-ray crystallography 40

Chapter 3 Cloning, Expression, and Protein Purification 42

Chapter 4 Biochemical Characterisation of PHD Finger Protein 2 (PHF2) 46

4.1. 2OG Turn Over Assays by NMR 46

4.2. *In vitro* demethylation assay by MALDI 47

4.3. Non-denaturing ESI-MS Analyses 50

4.4. Tryptophan Fluorescence Analyses 53

4.5. Fluorescence Polarisation Analyses 56

4.6. Differential Scanning Fluorimetry (DSF, or T_m shift) Analysis 62

Chapter 5 X-ray crystallography 66

5.1. Screening of the most stabilising conditions for PHF2 by DSF assay 66

5.2. X-ray crystallography 69

Conclusions 74

References 78

Supplementary figures and tables 92

Chapter 1 Introduction

1.1. DNA packing

A normal human cell is estimated to contain about 2 metres of linear DNA, which needs to be densely packed to fit into the nuclei with a diameter of around 6 μm (Parker 1997; Alberts, Johnson, and Roberts 2002). To enable DNA packing in eukaryotic cells, DNA is wrapped around histone proteins to form nucleosomes, the basic repeating structural unit of chromatin (Figure 1). Each eukaryotic nucleosome contains a histone octamer consisting of two of each of the histones H2A, H2B, H3 and H4, which binds and wraps 1.6 turns of DNA, or about 146 base pairs (Holde, Sahasrabuddhe, and Shaw 1974; Thomas and Kornbergt 1975). The nucleosomes are connected by short stretches of linker DNA to form a more condensed chromatin structure, sometimes described as a 'beads on a string' type structure (Schalch et al. 2005). At the next level of organisation, the chromatin is folded into 30 nm-wide fibres that are further packed into higher-order structures (Song et al. 2014).

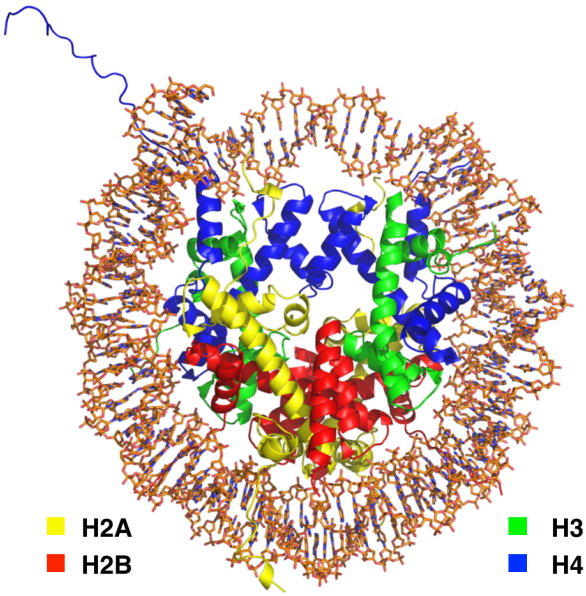


Figure 1 Views from a crystal structure of the nucleosome (PDB 1EQZ). DNA double helix winds around the central histone octamer. Hydrogen bonds and electrostatic interactions with the histones hold the DNA in place.

1.2. Histone modification and relating enzymes

The control of gene expression is a dynamic process. Such control is essential for cells to respond rapidly to physiological stimuli. However, due to the densely packed chromatin structure, cellular responses at the transcriptional level require carefully controlled chromatin remodelling to enable the transcriptional machinery to access specific genes (A. J. Bannister, Schneider, and Kouzarides 2002). One way this is achieved is proposed to be *via* a 'histone code' – a combinatorial pattern of usually small covalent modifications including acetylation, methylation, phosphorylation, ubiquitination on the flexible *N*-terminal tails of the histone proteins (Strahl and Allis 2000). The modifications upon histone proteins are dynamically controlled through addition and removal ('writing' and 'erasing') by various enzymes including histone acetyltransferases (HATs) and histone deacetylases (HDACs) (Berger et al. 2009; Fischle, Wang, and Allis 2003). It is hypothesised that the 'histone code' is recognised, or 'read' by specific proteins, which are recruited to the modification site to alter chromatin structure and regulate transcription (Berger 2002; Jenuwein and Allis 2001).

1.2.1. Histone acetylation

Histone acetylation is catalysed by HAT enzymes, which transfer an acetyl group from acetyl-coenzyme A (acetyl-CoA) to the ε-amino group of certain lysine side chains in histone *N*-terminal tail regions (Allfrey, Faulkner, and Mirsky 1964; Loidl 1994; Sterner and Berger 2000). Crystal structures of nucleosomes reveal that these regions extend out from the globular domains, and bind DNA through charge-charge interactions between the positively charged lysine side chains and the negatively charged DNA backbone (Harp et al. 2000; Richmond et al. 1997). Therefore by

neutralising the positively charged *N*-terminal histone tails *via* acetylation, histone-DNA interactions are weakened, leading to increased access for transcriptional machinery and gene activation (Brownell et al. 1996; Hebbes, Thorne, and Crane-Robinson 1988; Turner 1993). Histone acetylation is a reversible process; the removal of the acetyl group is catalysed by HDAC enzymes (Figure 2a). Deacetylation is often associated with gene repression, and HDACs can be recruited by sequence-specific transcriptional repressors (Pazin and Kadonaga 1997; Yi Zhang et al. 1997).

1.2.2. Histone phosphorylation

Histone phosphorylation occurs on the side chains of serine and threonine residues in the *N*-terminal histone tails (Berger 2002). Histone phosphorylation is associated with transcriptional activation and is involved in the DNA repair process and chromosome condensation during cell division (Banerjee and Chakravarti 2011; Wei et al. 1999). Various kinases catalyse histone phosphorylation, and it is proposed that phosphorylation disrupts the charge interactions between the histone tail and negatively charged DNA backbone, thus increases accessibility of transcriptional machinery (Cheung, Allis, and Sassone-Corsi 2000). Like histone acetylation, phosphorylation is a reversible histone mark, and phosphatases, such as Wip1, have been identified to reverse this modification (Rossetto, Avvakumov, and Côté 2012). There is also evidence suggesting cross-talk between histone phosphorylation and acetylation in the regulation of transcription (Koshibu et al. 2009; Lo et al. 2001).

1.2.3. Histone ubiquitination

Histone ubiquitination is catalysed by E2 and E3 ubiquitin ligases, which conjugate ubiquitin to the core region of histone H2A and H2B (Olson et al. 1975; Weake and Workman 2008). Histone ubiquitination is controlled by early steps in

transcription initiation and elongation processes, and is involved in nucleotide excision repair mechanisms (Bergink et al. 2006; Osley 2006). In general, H2A ubiquitination is considered to be repressive, whereas H2B ubiquitination has roles in both gene silencing and activation (Cao, Tsukada, and Zhang 2005; Kao et al. 2004; Weake and Workman 2008; Wyce et al. 2007). Interestingly, studies have also shown that H2B monoubiquitination is required for H3K4 and H3K79 methylation (Briggs et al. 2002; Sun and Allis 2002).

1.2.4. Histone methylation

Histone methylation occurs on the basic side chains of lysine- and arginine-residues, and is involved in important biological processes including heterochromatin formation and X-chromosome inactivation (Martin and Zhang 2005; Plath et al. 2003). Unlike acetylation, which in general correlates with transcriptional activation, histone methylation can trigger either gene activation or repression, depending on the modification site and status (Berger 2002; Kouzarides 2002).

Arginine residues can be mono-methylated and di-methylated (Figure 2b), both of which are catalysed by protein arginine methyltransferases (PRMTs). PRMTs transfer a methyl group from a *S*-adenosylmethionine (AdoMet) to the side chain of arginine, resulting in a *S*-adenosylhomocysteine (AdoHcy) and a methyl arginine (Di Lorenzo and Bedford 2011). Histone arginine methylation is often associated with gene activation, and PRMTs such as coactivator-associated arginine methyltransferase 1 (CARM1) are recruited to promoter regions as co-activators during the transcriptional activation process (D. Chen et al. 1999; H. Wang et al. 2001). Consistent with the concept that the transcriptional outcomes are tuned by a combination of various histone modifications, there is evidence that suggests cross-talk between arginine

methylation and lysine acetylation; for example, Wang *et al.* have demonstrated that methylation on histone H4R3 facilitates the acetylation on H4 tails as catalysed by the transcriptional co-activator p300 (H. Wang et al. 2001).

In vivo, N^{ϵ}-methylated lysines are found on histone H3 (K4, K9, K27, K36 and K79) and H4 (K20) (a J. Bannister et al. 2001; Bernstein et al. 2002; J. Fang et al. 2002; Feng et al. 2002; Lachner, O'Sullivan, and Jenuwein 2003; Plath et al. 2003; Strahl et al. 2002). Histone lysine methylation is catalysed mainly by the SET-domain-containing proteins, which operate *via* the same general mechanism as the PRMTs (Lachner, O'Sullivan, and Jenuwein 2003). During catalysis, the methyl group is also transfered from AdoMet, which is converted to AdoHcy (Figure 2c) (Feng et al. 2002; Krishnan, Horowitz, and Trievel 2011; Rea et al. 2000). The outcomes of most of the histone lysine methylations are dependent on the presence of other modifications; however, histone H3K4 methylation is generally associated with transcriptional activation (Lachner, O'Sullivan, and Jenuwein 2003; Lacoste et al. 2002; Rice et al. 2003; Strahl et al. 2002; Tachibana et al. 2002). The notion that 'the transcriptional outcome is tuned by a combinatory histone modification pattern' is also supported by the existence of multi-domain proteins such as the chromatin regulator TRIM24, which has a PHD domain and a bromodomain that recognise methylated H3K4 and acetylated H3K23 respectively (Tsai et al. 2010).

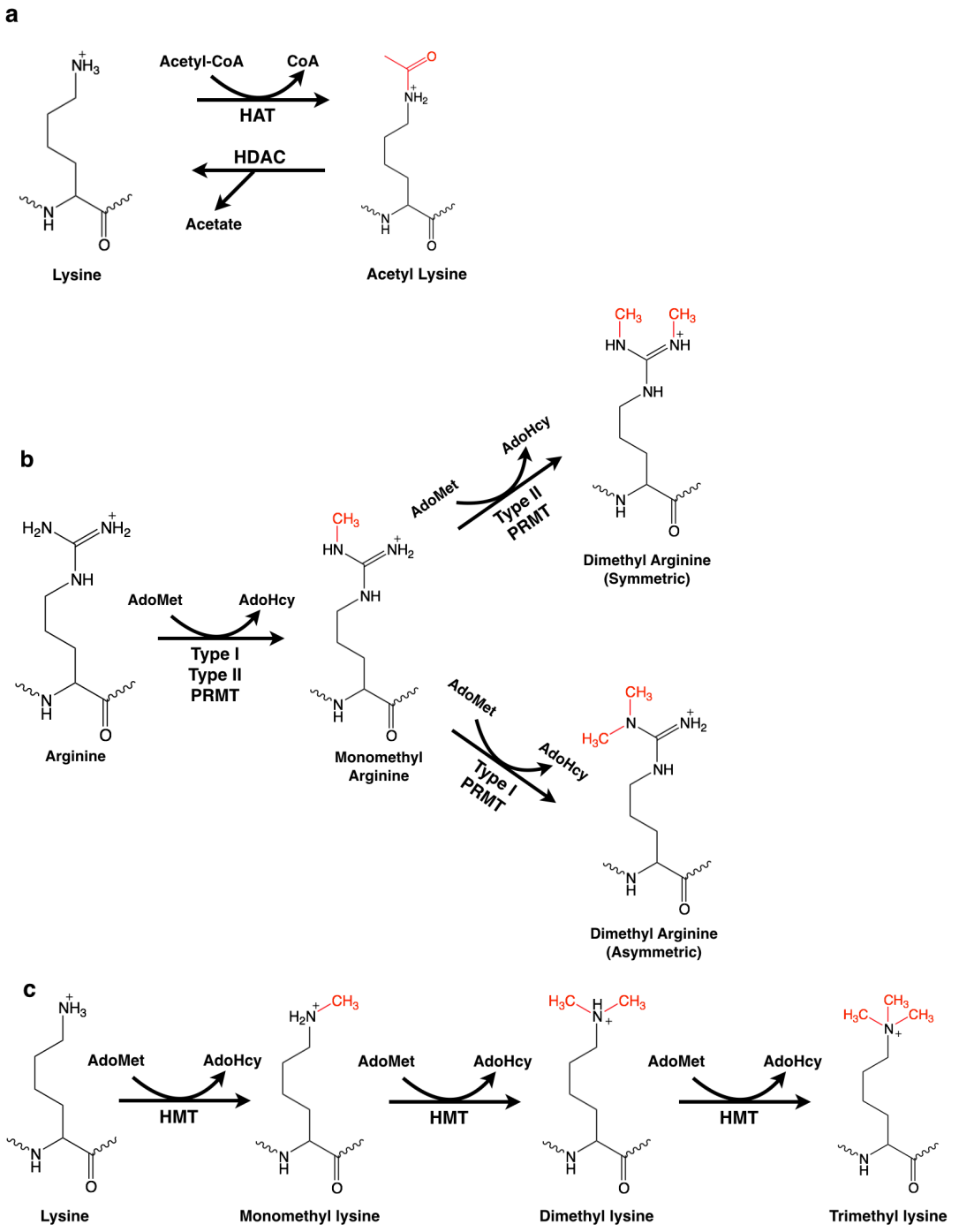


Figure 2 Summary of histone modifications. a) Histone acetylation is catalysed by HAT enzymes, which transfer an acetyl group from acetyl-CoA to the ε-amino group of the lysine side chain. This modification is reversed by HDAC enzymes. **b)** There are three main forms of methylated arginine identified in mammalian cells: monomethyl arginine (MMA), asymmetric dimethyl arginine (ADMA) and symmetric dimethyl arginine (SDMA). Type I and type II PRMTs catalyse the formation of an MMA intermediate, then type I PRMTs further catalyse the production of ADMA, while type II PRMTs catalyse the formation of SDMA. AdoMet is converted to AdoHcy during catalysis. **c)** Lysine can be methylated to monomethyl-, dimethyl- and trimethyl lysine by HMTs. AdoMet is converted to AdoHcy during catalysis.

1.2.5. Histone demethylase

Until recently, histone methylation was thought to be irreversible. However, in 2005, the first *bona fide* histone demethylase, lysine-specific demethylase 1 (LSD1, or KDM1A) was described; LSD1 specifically catalyses demethylation of histone H3K4 and H3K9, and induces transcriptional repression (Metzger et al. 2005; Shi et al. 2004). Subsequently, two distinct families of histone demethylases have emerged. LSD1 was the founding member of the first family, which catalyses oxidative demethylation using flavin as a cofactor (**Figure 3**a) (Culhane and Cole 2007). The other member of this family is LSD2 (KDM1B). LSD2 is also a histone H3K4 demethylase, and studies have shown that it is highly expressed in oocytes and is involved in the gene imprinting process (F. Chen et al. 2013; Ciccone et al. 2009; R. Fang et al. 2012).

The second and the largest demethylase family is the Jumonji C-domain (JmjC)-containing histone demethylases (JHDMs). The JHDM enzymes are members of the superfamily of Fe^{2+} and 2-oxoglutarate (2OG) dependent dioxygenases, which utilise Fe^{2+} as a cofactor, and 2OG and oxygen as co-substrates to catalyse oxidative demethylation (**Figure 3**b). Due to the proposed mechanistic requirement for imine formation, LSD1 can only demethylate mono- and di-methylated lysine, whereas JHDMs are capable of reversing all three lysine-methylation status (Anand and Marmorstein 2007). The first member of this family to be discovered was FBXL11 (JHDM1A, or KDM2A), which is a histone H3K36me2 specific demethylase consisting of a JmjC domain, a zinc finger, a PHD finger, a F-box domain and three leucine-rich repeat (LRR) domains (Tsukada et al. 2006). To date, JHDMs have been shown to demethylate N^{ε}-methylated lysine residues including H3K4, H3K9, H3K27, H3K36 and H4K20 (Agger et al. 2007; Christensen et al. 2007; Klose et al. 2006; Qi

et al. 2010; Tsukada et al. 2006; Whetstine et al. 2006). The JHDMs play roles in many important biological processes including regulation of stem cell pluripotency and cell cycle control (van Haaften et al. 2009; Loh et al. 2007; Mosammaparast and Shi 2010).

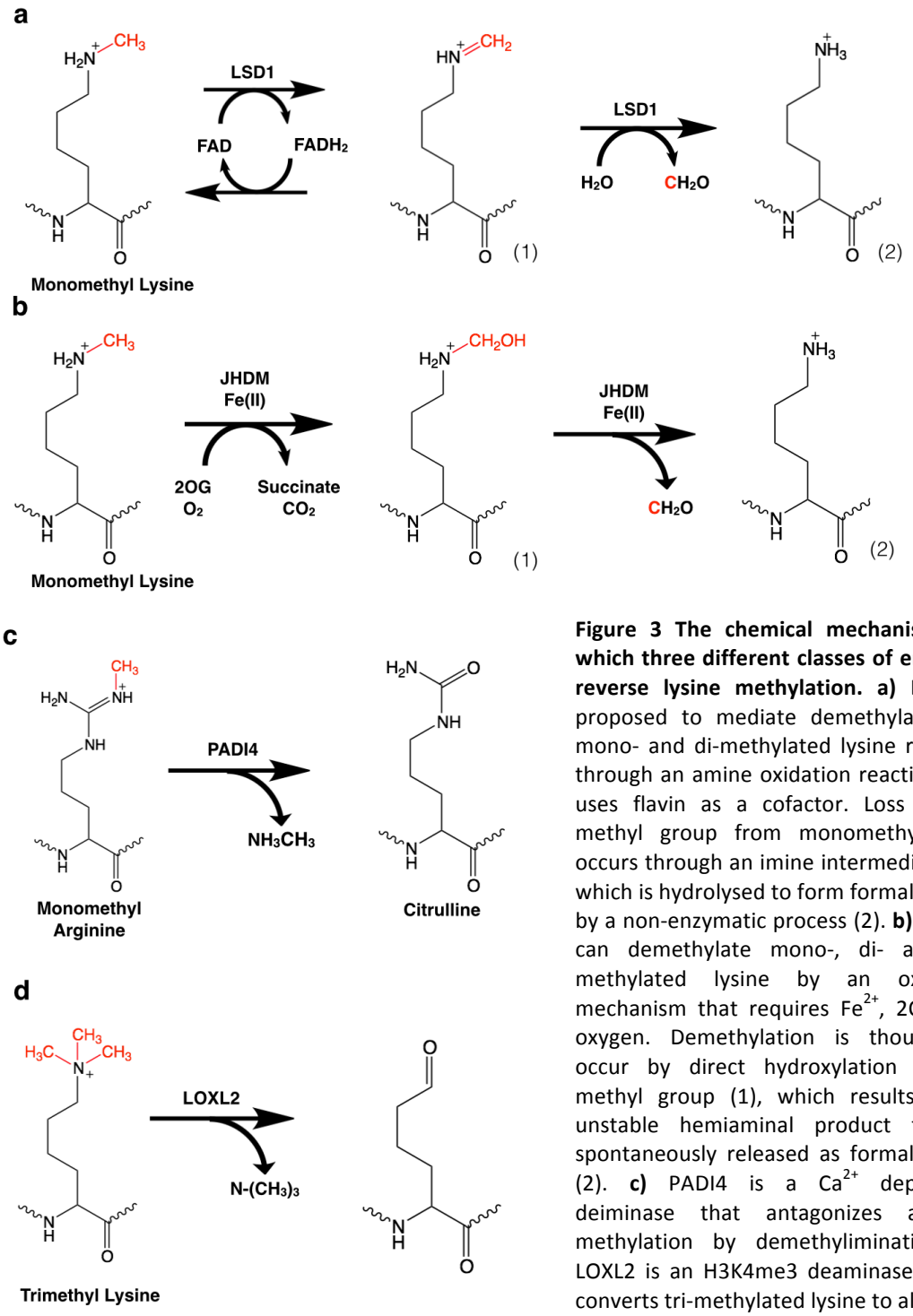
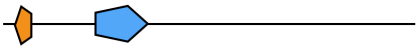
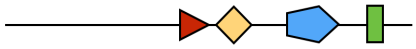
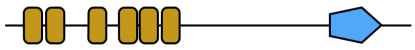
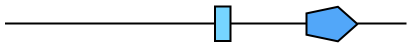
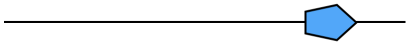


Figure 3 The chemical mechanisms by which three different classes of enzymes reverse lysine methylation. a) LSD1 is proposed to mediate demethylation of mono- and di-methylated lysine residues through an amine oxidation reaction that uses flavin as a cofactor. Loss of the methyl group from monomethyl-lysine occurs through an imine intermediate (1), which is hydrolysed to form formaldehyde by a non-enzymatic process (2). **b)** JHDMs can demethylate mono-, di- and tri-methylated lysine by an oxidative mechanism that requires Fe^{2+}, 2OG and oxygen. Demethylation is thought to occur by direct hydroxylation of the methyl group (1), which results in an unstable hemiaminal product that is spontaneously released as formaldehyde (2). **c)** PADI4 is a Ca^{2+} dependent deiminase that antagonizes arginine methylation by demethylimination. **d)** LOXL2 is an H3K4me3 deaminase, which converts tri-methylated lysine to allysine.

The human JHDMs can be divided into subfamilies based on structure and substrate specificity (**Table 1**), and many of them contain additional domains such as plant homeodomains (PHD finger) and tudor domains, which can contribute to substrate specificity (Klose, Kallin, and Zhang 2006). In the case of PHF8 and KIAA1718 from the KDM7 JHDM subfamily, even the linker region between the two functional domains is involved in determining the substrate specificity (Horton et al. 2010).

Table 1 Summary of KDM subfamilies

Group	Group Member	Domain architecture
KDM2 (JHDM1)	KDM2A (JHDM1A, FBXL11)	
	KDM2B (JHDM1B, FBXL10)	
KDM7 (PHF2/PHF8)	KDM7C (PHF2)	
	KDM7B (PHF8)	
	KDM7A (KIAA1718)	
KDM5 (JARID)	KDM5A (JARID1A)	JARID1 
	KDM5B (JARID1B)	
	KDM5C (JARID1C)	
	KDM5D (JARID1D)	
	JARID2	JARID2 
KDM4 (JMJD2)	KDM4A (JMJD2A)	KDM4A, 4B, 4C 
	KDM4B (JMJD2B)	
	KDM4C (JMJD2C)	KDM4D 
	KDM4D (JMJD2D)	
KDM6 (UTX/UTY)	KDM6A (UTX)	
	KDM6B (JMJD3)*	
	KDM6C (UTY)	
KDM3 (JHDM2)	KDM3A (JHDM2A)	
	KDM3B (JHDM2B)	
	KDM3C (JHDM2C)	
JmjC domain only	MINA53	
	KDM8 (JMJD5)	
	FIH	
	JMJD4	
	NO66	



* KDM6B has TPR-like domains instead of TPR.

There are other histone methylation antagonising enzymes such as peptidyl arginine deiminase 4 (PADI4), which converts methyl-arginine to citrulline (**Figure 3**c) (Cuthbert et al. 2004; Y. Wang et al. 2004). Recently, a histone deaminase, LOXL2 has been identified that catalyses a deamination reaction on histone H3K4me3 (**Figure 3**d) (Herranz et al. 2012).

1.3. 2OG-dependent oxygenases

The JHDM enzymes are members of the superfamily of Fe^{2+} and 2OG dependent dioxygenases (Loenarz and Schofield 2011; Ryle and Hausinger 2002). The 2OG oxygenases are the largest known family of non-haem oxygenases and are conserved in the genomes of most aerobic organisms (Loenarz and Schofield 2011). 2OG dependent oxygenases regulate a variety of biological processes including the hypoxic response, nucleic acid repair, and modification, fatty acid metabolism and histone modification (Bleijlevens et al. 2008; Delaney et al. 2005; Klose, Kallin, and Zhang 2006; Loenarz and Schofield 2009; Loenarz et al. 2008; Mukherji et al. 2003). Some prokaryotes including *Streptomyces clavuligerus* also have 2OG oxygenases such as deacetoxycephalosporin C synthase (DAOCS), which is involved in the biosynthesis of cephalosporin antibiotics (H. J. Lee et al. 2001; Lloyd et al. 1999).

Structural studies have revealed that 2OG oxygenases contain a conserved double-stranded β-helix (DSBH, jelly-roll, cupin or JmjC) core fold. The Fe^{2+} cofactor is usually coordinated by the side chains of a conserved HxD/E…H triad within the fold, and the 2-oxo carboxylate group of the co-substrate 2OG chelates the Fe^{2+} in a bidentate manner (Aik et al. 2012; Z. Chen et al. 2006; McDonough et al. 2010). 2OG oxygenases are able to catalyse hydroxylation or demethylation *via* an initial hydroxylation reaction depending on the particular enzyme involved and

substrate. The cofactor-bound JmjC domain uses oxygen and 2OG to form a highly reactive oxoferryl species that inserts an oxygen atom into a substrate C-H bond, and CO_2 and succinate is released (**Figure 4**a). In the cases of JHDMs, a hemiaminal group is formed on the hydroxylated substrate, and subsequent demethylation is driven by the formation of formaldehyde (**Figure 4**b) (Walport, Hopkinson, and Schofield 2012). Consistent with the proposed mechanism of oxidative demethylation, crystallographic studies on AlkB have captured a structure with a hemiaminal intermediate (Yi et al. 2010).

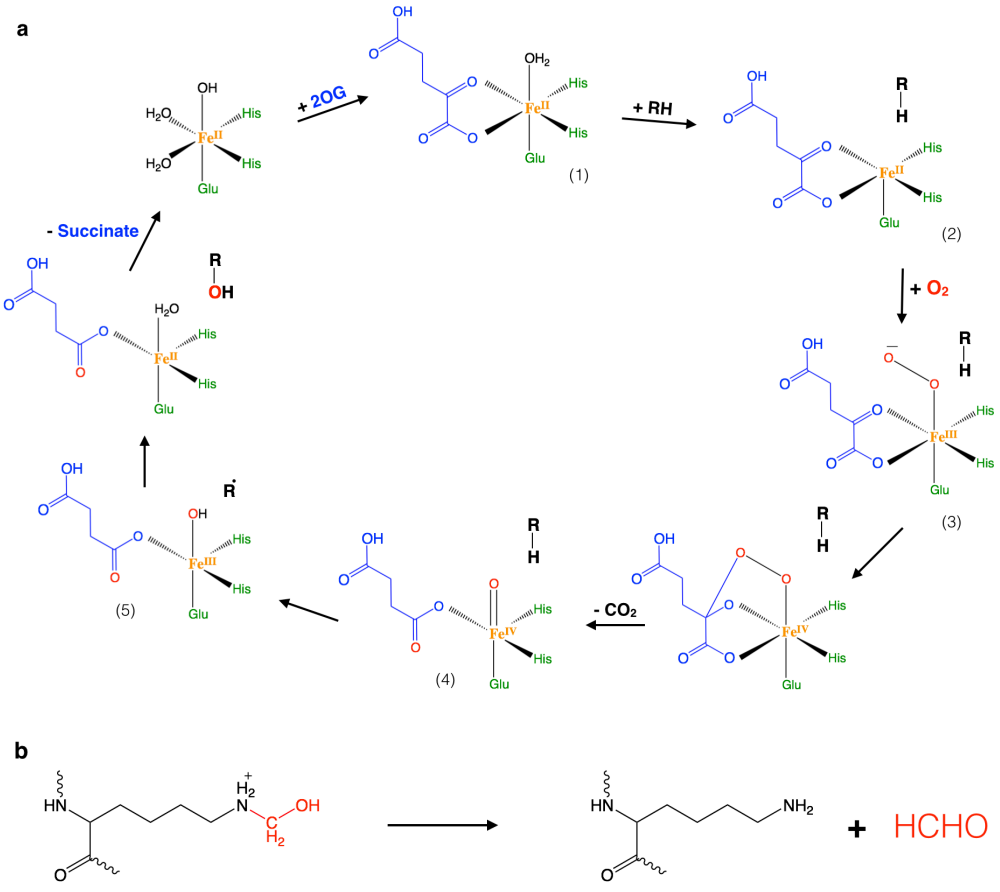


Figure 4 The outline mechanisms of 2OG oxygenases. a) (1) 2OG binds to the iron centre, coordinating via its 1- and 5- carboxylate groups. (2) Binding of the alkyl bond containing "prime" substrate to the Fe-2OG complex is thought to facilitate oxygen binding. Crystallographic data suggests oxygen binds in a site previously occupied by water. (3) Oxidative decarboxylation of 2OG generates a Fe(IV) intermediate, succinate and CO_2. (4) This reactive Fe(IV) species abstracts a hydrogen from the substrate alkyl bond. (5) Hydroxylation of the radical alkyl intermediate occurs. Both oxygen atoms of the dioxygen co-substrate have been transferred into products. This is followed by a release of succinate and the hydroxylated product. The active site is then regenerated. **b)** When the substrate is methylated lysine, a hemiaminal group is formed on the hydroxylated substrate, and subsequent demethylation is driven by the formation of formaldehyde.

1.3.1. Prolyl hydroxylases

Of the post-translational modifications involving addition of atoms or groups, hydroxylation involves one of the smallest changes in size. It is involved in both collagen modifications and cellular oxygen sensing mechanisms (Loenarz and Schofield 2011). Collagen prolyl hydroxylase (CPH) was the first 2OG oxygenase identified in 1967. It catalyses *trans* prolyl-4-hydroxylation of the Xxx-Pro-Gly motifs in collagen, a modification that stabilises the collagen triple helix (**Figure 5**a) (Hutton, Kaplan, and Udenfriend 1967; Loenarz and Schofield 2008). A related enzyme, prolyl-3-hydroxylase was found to catalyse prolyl-3-hydroxylation, which requires prior prolyl-4-hydroxylation (**Figure 5**a). This modification has a destabilising effect on the collagen triple helix, and is thought to facilitate other modification. Studies have also shown that C5 of the lysine residues in collagen can undergo hydroxylation, which can serve as an anchor point for glycosylation (Loenarz and Schofield 2008; Myllyharju and Kivirikko 2004).

The hypoxia-inducible factor (HIF) is a heterodimeric transcriptional factor consisting of HIF-α and HIF-β subunits (Loenarz and Schofield 2008). The prolyl hydroxylase domain (PHD) enzyme catalyses the hydroxylation of the conserved prolyl residues in the *N*- and *C*-terminal oxygen-dependent degradation domain (NODD and CODD) of HIF-α (**Figure 5**a). This modification enables binding of HIF-α to the von Hippel-Lindau tumour suppressor (pVHL), which targets HIF-α for proteasomal degradation *via* the ubiquitin pathway (Kaelin and Ratcliffe 2008; Min et al. 2002). The requirement of oxygen for 2OG oxygenases as co-substrate allows animals to use them in oxygen sensing mechanisms. Under hypoxic conditions, PHD cannot catalyse sufficient hydroxylation reactions, HIF-α is thus stabilised and forms a complex with HIF-β, which activates transcription of more than 100 genes involved

in processes including angiogenesis and glycolysis (Loenarz et al. 2008; Schofield and Ratcliffe 2004; Semenza 1999). Besides PHD, another hydroxylase, factor inhibiting HIF (FIH) has also been reported in the oxygen sensing mechanism. FIH hydroxylates an asparagine residue in the *C*-terminal transcriptional activation domain of HIF-α (**Figure 5**a), which reduces its interaction with the transcriptional co-activator protein p300 (Loenarz et al. 2008; Mahon, Hirota, and Semenza 2001).

1.3.2. DNA demethylase

Studies on DNA repair mechanisms in prokaryotes led to the discovery of *E. coli* DNA demethylase AlkB, a 2OG oxygenase which catalyses the *N*-demethylation of alkylated DNA (Falnes, Johansen, and Seeberg 2002; Trewick et al. 2002). Subsequently, eight human AlkB homologues (ABH 1-8) were identified, of which ABH2 and ABH3 have been reported to have demethylase activity on 1-methyladenine and 3-methylcytosine residues on single- and double-stranded DNA (**Figure 5**b) (Müller, Meek, and Hausinger 2010; Sedgwick et al. 2007; Westbye et al. 2008). To date, substrates for most of the ABHs remain elusive. However, recent studies have shown that ABH8 catalyses a hydroxylation reaction of 5-methoxycarbonylmethyluridine of tRNA, which reveals the breadth in the functionality of ABHs (Fu et al. 2010).

Besides ABHs, other 2OG oxygenases have been shown to catalyse DNA modifications. The ten-eleven translocation (TET) enzymes convert the hydroxylation of 5-methylcytosine to a previously unknown base, 5-hydroxymethylcytosine, and fat mass and obesity-associated protein (FTO) is a DNA/RNA demethylase with a strong preference for 3-methylthymidine in single-stranded DNA and 3-methyluracil in

single-stranded RNA (**Figure 5**b) (Gerken et al. 2007; Han et al. 2010; Hashimoto et al. 2014; Tahiliani et al. 2009).

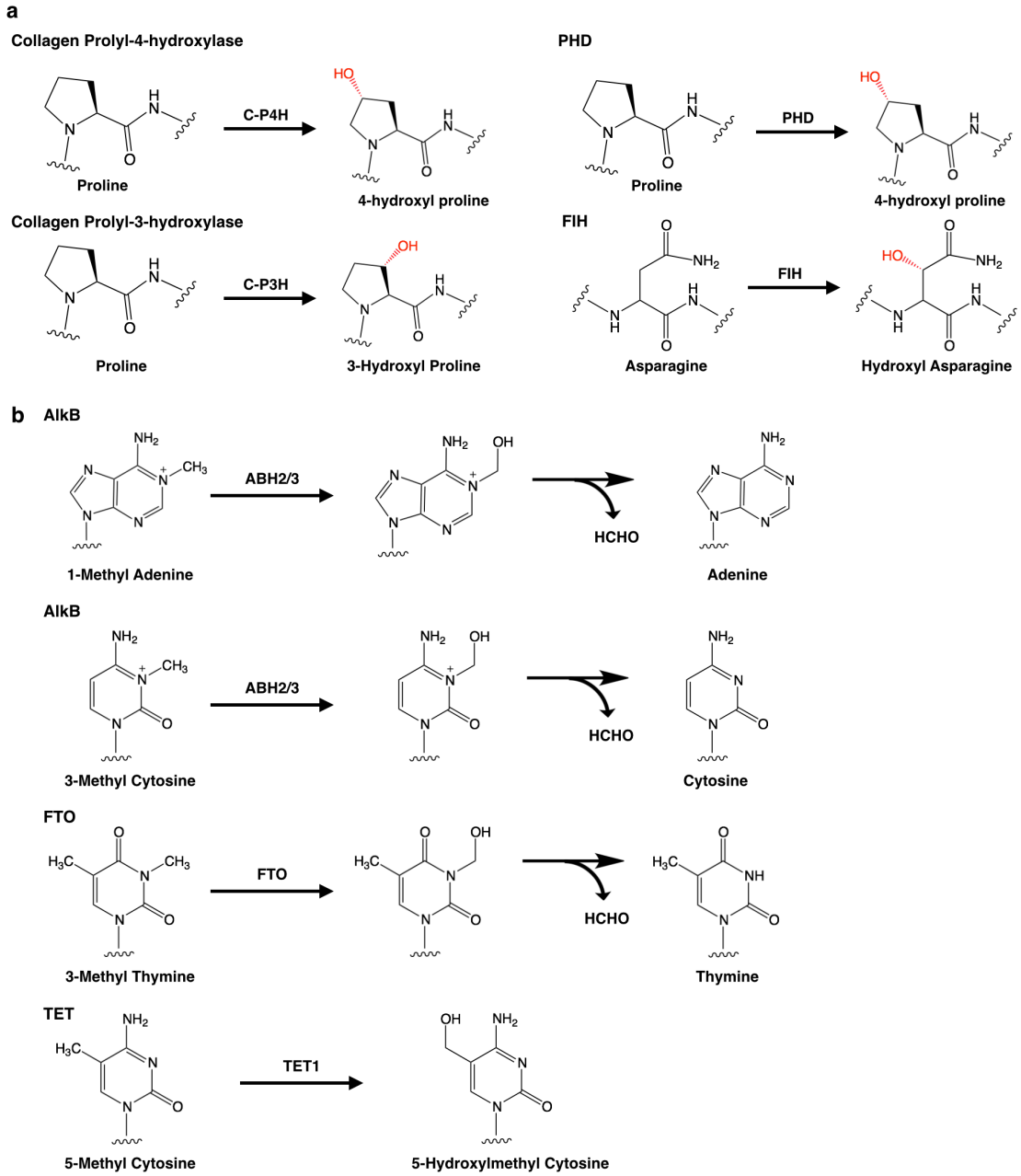


Figure 5 Examples of modifications catalysed by 2OG oxygenases. a) Post-translational modifications catalysed by prolyl hydroxylases. **b)** Post-translational modifications catalyzed by DNA demethylases and hydroxylases.

1.4. JHDM KDM7 subfamily

The KDM7 subfamily of JHDM has three members in humans and mice, PHF2, PHF8 and KIAA1718. Functional studies suggest that PHF8 is involved in cell cycle control and brain development, and PHF2 is involved in chondrogenesis (Hata et al. 2013; Laumonnier et al. 2005; Liu et al. 2010; Loenarz et al. 2010; Yokoyama et al. 2010). Some evidence suggested that KIAA1718 is involved in the early phase of neural differentiation (Huang et al. 2010).

Each of the proteins from the KDM7 subfamily contains a PHD finger and a JmjC domain in their *N*-terminal half: the PHD finger is known to recognise methylated histone H3K4, and the JmjC domain is involved in removing histone methylation (Figure 6a) (Klose, Kallin, and Zhang 2006). Despite the fact that PHF8 and KIAA1718 share 82% identity between their PHDs and ~ 65% identity between their JmjC domains, studies have shown that PHF8 catalyses the demethylation reaction on histone H3K9me2, whereas KIAA1718 catalyses the same reaction on H3K27me2 (Loenarz et al. 2010; Yokoyama et al. 2010). By investigating the structures of these two proteins, an interesting feature has emerged regarding their substrate specificity: the PHF8 PHD finger adopts a bent conformation toward the JmjC domain in the presence of substrate binding, whereas the two corresponding domains of KIAA1718 adopt an extended conformation with an ordered linker between its PHD and JmjC domain. It is proposed that both PHF8 and KIAA1718 utilise their PHD fingers for histone H3K4 binding; however, by having a shorter linker, PHF8 is able to locate its JmjC domain to the site of H3K9 on the substrate peptide, whereas the longer and more rigid linker enables the JmjC of KIAA1718 to catalyse demethylation reaction on histone H3K27 (Horton et al. 2010). Studies have demonstrated that the other human member of this JHDM subfamily, PHF2, catalyses

demethylation on histone H3K9me2 in cells, however, sequence alignment shows that the linker region between its PHD and JmjC domain is more similar to that of KIAA1718 than PHF8 (Supp. Figure 1) (Horton et al. 2011; Wen et al. 2010). Thus it would be interesting to investigate the molecular details of the substrate specificity of PHF2. In addition, in the Fe^{2+} coordinating motif HxD/E…H that is conserved in almost all JHDMs, PHF2 has a tyrosine in the place of the second histidine in its active site. The significance of this variance remains elusive.

1.5. PHD finger protein 2 (PHF2)

PHF2 is a JHDM belonging to the KDM7 subfamily, which contains a PHD finger and a JmjC domain (Figure 6a) (Hasenpusch-Theil et al. 1999). Studies have shown that PHF2 facilitates chondrogenesis and adipogenesis by interacting with AT-rich interactive domain 5b (ARID5B) protein, a co-regulator of Sox9, which acts as a master regulator of chondrogenesis (Baba et al. 2011; Hata et al. 2013; Okuno et al. 2013). Cell-based experiments have demonstrated that PHF2 recognise histone H3K4me3, and as shown by western blot and confocal microscopy, it catalyses demethylation at H3K9me2 site (Horton et al. 2011; Wen et al. 2010).

1.5.1. Domain architecture of PHF2

The PHF2 gene is located on chromosome 9q22 in human genome, and its mouse homologue is mapped on the syntenic region on mouse chromosome 13. The protein contains a PHD finger and a JmjC domain (Hasenpusch-Theil et al. 1999). The PHD finger is a common motif found in all eukaryotic genomes. It was first discovered by Schindler *et al.*, who noticed a stretch of conserved sequence with eight regularly spaced cysteine/histidine residues between two plant homeodomains (Schindler U, Beckmann H 1993). Two years later, it was found that the PHD finger is a *bona fide*

motif that is widely present in eukaryotic genomes, especially in proteins involved in transcriptional regulation (Rein Aasland, Toby J. Gibson 1995). Structural analysis shows that PHD fingers use conserved Cys_4-His-Cys_3 residues to coordinate two Zn^{2+} ions, forming a zinc-binding core with two variable loops that are often involved in ligand binding (Bienz 2006; Pascual et al. 2000). PHD fingers, including the one in PHF2, can read the histone tails (mainly the methylated H3K4) (van Ingen et al. 2008; Peña et al. 2006; Sanchez and Zhou 2011; Taverna et al. 2006; Wen et al. 2010). Studies on PHF2 suggest that it recognises histone H3K4me3 and demethylates at H3K9 methylation site, which is consistent with the fact that it has both a PHD and a JmjC domain similar to PHF8 (Baba et al. 2011; Horton et al. 2011; Wen et al. 2010).

1.5.2. The biological relevance of PHF2

In vivo studies have shown that PHF2 facilitates chondrogenesis and adipogenesis (Baba et al. 2011; Hata et al. 2013; Okuno et al. 2013). Co-immunoprecipitation analysis has confirmed a physical interaction between PHF2 and AT rich interactive domain 5B (ARID5B), and ARID5B also interacts with Sox9 (a transcription factor that acts as a principle regulator of early chondrogenesis) *via* its *C*-terminal region (Akiyama and Lefebvre 2011; Hata et al. 2013). Both *in vivo* studies and cell-based experiments have collectively demonstrated that ARID5B is a co-regulator of Sox9, which promotes chondrogenesis together with Sox9 by recruiting PHF2 to the promoter regions of chondrogenic genes and reversal of the repressive H3K9me2 methylation mark, therefore facilitating the transcription of target genes (Baba et al. 2011; Hata et al. 2013; Okuno et al. 2013). However, there is limited evidence to suggest that PHF2 catalyses H3K9me2 demethylation in *in vitro* biochemical assays (Horton et al. 2011; Wen et al. 2010). In addition, a recent study has identified PHF2 as a tumour suppressor in association with p53 in cancer

development (K. Lee et al. 2014). Another member of the KDM7 subfamily, PHF8 has also been proposed to play a role in cancer development (Björkman et al. 2012).

1.5.3. The structure of PHF2

Structural studies of PHF2 have provided useful insights to its mechanism at the molecular level. A structure of the PHF2 PHD finger with its substrate peptide (Histone $H3_{1-6}K4me3$) has revealed an overall structure that contains two anti-parallel β-sheets and three short α-helices on the side of the β-sheet core. Similar to other PHD modules, the PHF2 PHD contains two zinc finger motifs that coordinate two zinc ions. The binding of the trimethyl-lysine from the histone peptide is stabilised by four aromatic residues (Tyr^7, Tyr^{14}, Met^{20} and Trp^{29}, Figure 6b-c) (Wen et al. 2010).

A structure of PHF2 JmjC domain shows the DSBH fold that is a signature of 2OG oxygenases (Figure 6d). The overall metal binding site of PHF2 closely resembles the Fe^{2+} binding sites of other JHDMs. However, comparison between the PHF2 JmjC domain and the PHF8 JmjC domain reveals a single but potentially important difference. As the histidine in the HxD…H motif that is conserved in almost all 2OG oxygenases is replaced to a tyrosine, the longer side chain of Y321 of PHF2 active site apparently pushes the Fe^{2+} away from the corresponding binding position in PHF8, which might place the metal in a non-reactive mode by decreasing its oxygen binding affinity (Figure 6e) (Horton et al. 2011).

Although the structures of individual domains of PHF2 are available in part, the structure with both functional domains together still remains to be solved. In addition, it is unclear whether the PHF2 JmjC domain contributes to peptide recognition as a structure of histone peptide bound to the JmjC domain of PHF2 has yet to be elucidated.

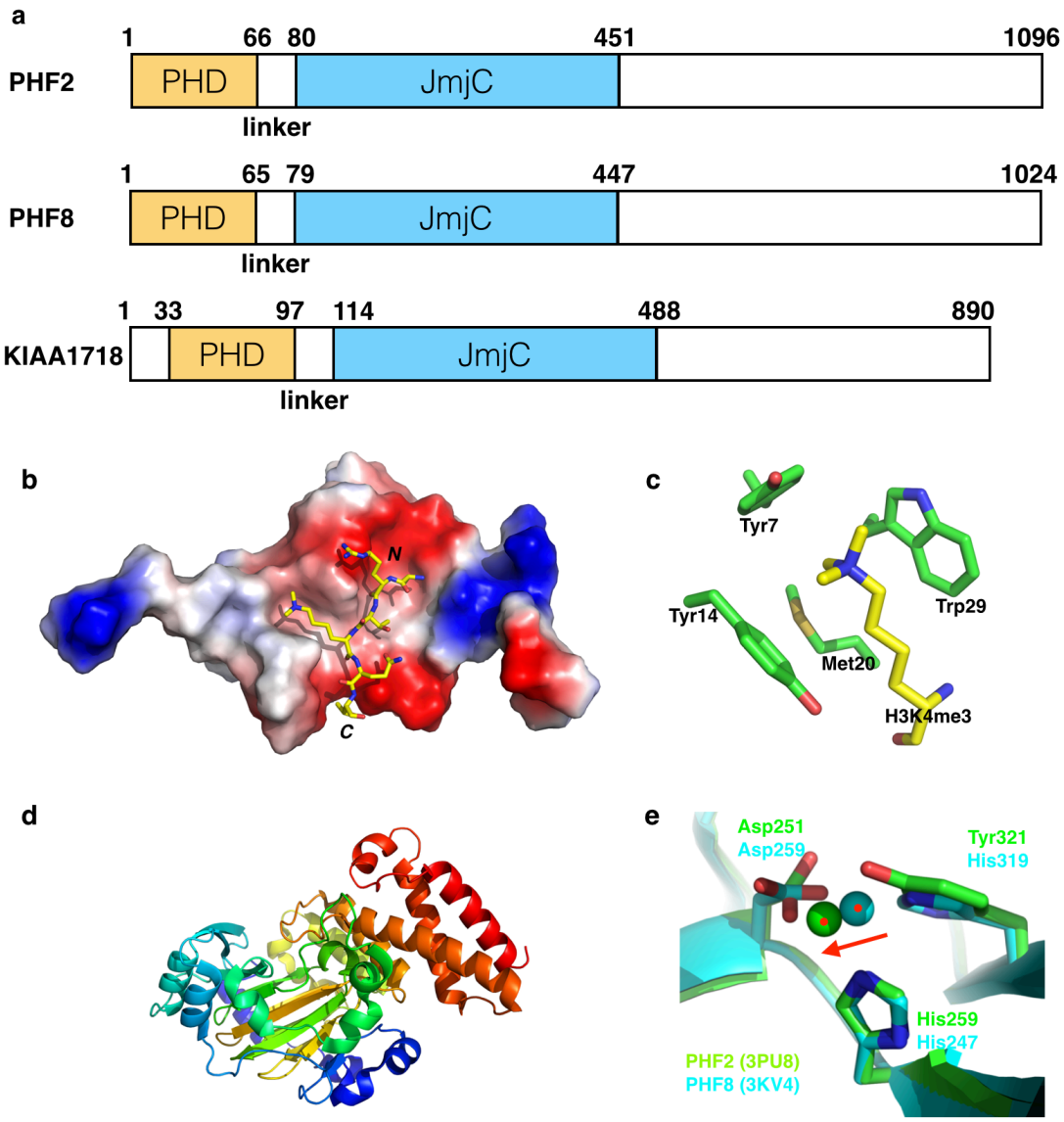


Figure 6 The domain architecture of KDM7 enzymes and the structures of PHF2 PHD and the JmjC domain. a) The domain architecture of PHF2. **b)** The crystal structure of the PHF2 PHD finger in complex with an H3K4me3 peptide (3KQI). The PHD finger is shown as an electrostatic surface, with red as negatively charged surface and blue as positively charged surface, and the histone peptide is shown as a stick, with carbon, oxygen, and nitrogen atoms coloured yellow, red, and blue, respectively. *N* and *C* indicate the *N*-terminus and the *C*-terminus of the peptide. **c)** A stick representation of H3K4me3 (yellow) in the aromatic cage of the PHF2 PHD finger composed of Tyr7, Tyr14, Met20, and Trp29 residues (3KQI). **d)** The overall structure of PHF2 JmjC domain (3PU8). **e)** Overlay of the JmjC domains of PHF2 (3PU8, in green) and that of PHF8 (3KV4, in cyan). By comparing the position of the Fe^{2+} in the catalytic site of PHF8 (cyan), the Fe^{2+} in PHF2 (green) is pushed away by the longer side chain of tyrosine 321.

1.6. Aim of this project

As discussed above, PHF2 has a tyrosine in the place of the second histidine in its conserved Fe^{2+} coordinating motif HxD/E…H. Given the critical role the histidine normally plays in Fe^{2+} binding (Aik et al. 2012), it would be interesting to investigate the mode of Fe^{2+} coordination in PHF2. It is also unclear (i) whether the PHF2 JmjC contributes to substrate recognition as well as the PHD finger, and (ii) if the linker region between the two domains affects the peptide binding in the same way as the ones do in the other two proteins, PHF8 and KIAA1718, from the same subfamily as described above in Section 1.4. The aim of this project was thus to study the structure and function of PHF2 using X-ray crystallography and *in vitro* biophysical/biochemical assays. Both wild-type and Y321H (substituting the tyrosine at the metal binding site for the normally conserved histidine) PHF2 proteins were produced and compared in functional studies.

Chapter 2 Materials and Methods

All materials were supplied by Sigma-Aldrich (MO, USA) unless otherwise stated. Water (dH_2O) was used from Millipore Elix 10 system. Standard sterile techniques were employed throughout. All instruments and pipette tips were sterilised in a TouchClave® II autoclave (LTE Scientific, Lancashire, UK) at 121°C for 20 min.

2.1. Common buffers and recipes

2xTY solution – 1 litre

- 16 g Bacto-tryptone (Oxoid, Cheshire, UK)
- 10 g Yeast extract (Merck Millipore, MA, USA)
- 5 g NaCl (Fisher Scientific, MA, USA)

LB Agar Plate – 200 mL

- 3 g Agar (Oxoid, Cheshire, UK)
- 2 g Bacto-tryptone (Oxoid, Cheshire, UK)
- 1 g Yeast extract (Merck Millipore, MA, USA)
- 2 g NaCl (Fisher Scientific, MA, USA)
- 10 % (w/v) sucrose if it is used for ligation-independent cloning selection

SDS-PAGE loading buffer 5x – 50 mL

- 500 mg Bromophenol Blue
- 17.5 mL Glycerol
- 7.5 g Sodium dodecyl sulfate (SDS)
- 16 mL 1 M Trizma base
- 12.5 mL β-mercaptoethanol

- pH 6.8

Coomassie SDS-PAGE Gel Stain – 1 litre

- 5 g Coomassie brilliant blue
- 100 mL acetic acid
- 500 mL methanol

SDS-PAGE Gel De-stain – 1 litre

- 200 mL acetic acid
- 200 mL methanol

12% SDS-PAGE Running Gel – 2 gels

- 2.6 mL 1.5 M Trizma Base
- 100 µL 10% (w/v) ammonium persulfate
- 4 mL 30% (w/v) acrylamide/Bis solution, 37.5:1
- 100 µL 10% (w/v) SDS
- 10
- µL tetramethylethylenediamine (TEMED)
- pH 8.8

SDS-PAGE Stacking Gel – 2 gels

- 1.25 mL 0.5 M Trizma Base
- 50 µL 10% (w/v) ammonium persulfate
- 670 mL 30% (w/v) acrylamide/Bis solution, 37.5:1
- 50 µL 10% (w/v) SDS
- 5 µL TEMED
- ,pH 6.8

Purification – Resuspension buffer

- 50 mM HEPES free acid (Apollo, Cheshire, UK)
- 500 mM NaCl (Fisher Scientific, MA, USA)
- 20 mM Imidazole
- 1 mM tris(2-carboxyethyl)phosphine (TCEP, Hampton Research, CA, USA)
- 1 mM Ethylenediaminetetraacetic acid (EDTA, Apollo, Cheshire, UK)
- 0.1 mM PMSF
- DNAase and RNAse
- pH 8.0

Purification – Histrap buffer A

- 50 mM HEPES free acid (Apollo, Cheshire, UK)
- 500 mM NaCl (Fisher Scientific, MA, USA)
- 20 mM Imidazole
- 1 mM TCEP (Hampton Research, CA, USA)
- pH 8.0

Purification – Histrap buffer B

- 50 mM HEPES free acid (Apollo, Cheshire, UK)
- 500 mM NaCl (Fisher Scientific, MA, USA)
- 1 M Imidazole
- 1 mM TCEP (Hampton Research, CA, USA)
- pH 8.0

Purification – Size exclusion chromatography (SEC) buffer

- 20 mM HEPES free acid (Apollo, Cheshire, UK)

- 200 mM NaCl (Fisher Scientific, MA, USA), or 500 mM for Y321H variant
- 1 mM TCEP (Hampton Research, CA, USA)
- pH 8.0

Purification – IEX buffer A

- 50 mM HEPES free acid (Apollo, Cheshire, UK)
- 50 mM NaCl (Fisher Scientific, MA, USA)
- 1 mM TCEP (Hampton Research, CA, USA)
- pH 8.0

Purification – IEX buffer B

- 50 mM HEPES free acid (Apollo, Cheshire, UK)
- 1 M NaCl (Fisher Scientific, MA, USA)
- 1 mM TCEP (Hampton Research, CA, USA)
- pH 8.0

2OG Turnover assay buffer

- 50 mM Trizma base
- 200 mM NaCl (Fisher Scientific, MA, USA)
- pH 8.0

In vitro demethylase assay buffer

- 50 mM HEPES free acid (Apollo, Cheshire, UK)
- 200 mM NaCl (Fisher Scientific, MA, USA)
- pH 8.0

Tryptophan fluorescence assay buffer:

- 50 mM HEPES free acid (Apollo, Cheshire, UK)

- 500 mM NaCl
- pH 8.0

Fluorescence polarisation assay buffer:

- 100 mM HEPES free acid (Apollo, Cheshire, UK)
- 500 mM NaCl (Fisher Scientific, MA, USA)
- 0.1% v/v Tween-20
- pH 8.0

Differential Scanning Fluorimetry buffer:

- 100 mM HEPES free acid (Apollo, Cheshire, UK)
- 200 mM NaCl (Fisher Scientific, MA, USA)
- pH 8.0

Buffers were made by dissolving all components in water followed by adjusting pH using hydrochloric acid or sodium hydroxide solution. All buffers were made fresh prior to relevant experiments.

2.2. Cloning

A total of six constructs of PHF2 were made during this project. The wild-type constructs were cloned using Ligase-independent cloning (LIC) method (Blanusa et al. 2010), and the corresponding Y321H variant was generate by site-directed mutagenesis (SDM) (Shortle, DiMaio, and Nathans 1981). The constructs were:

1. pNIC28-Bsa4-PHF2 (1-449)
2. pNIC28-Bsa4-PHF2 (1-449) Y321H
3. pcDNA3-N-Flag-PHF2 (1-1099)

4. pcDNA3-N-GFP-PHF2 (1-1099)
5. pNIC28-Bsa4-PHF2 (60-449)
6. pNIC28-Bsa4-PHF2 (60-449) Y321H

The following protocol uses construct No. 1 as an example. The rest of the constructs from above list were made using the same protocol. The polymerase chain reaction (PCR) was used as the first step of cloning to generate fragments of PHF2 (1-449) flanked by complementary overhang sequences to pNIC28-Bsa4 vector (Saiki et al. 1988). The template was the plasmid containing the cDNA of PHF2 obtained from Dr L. Walport. The primers are listed in (Supp. Table 1). The reaction was set up using Q5 Hot Start High-Fidelity DNA Polymerase (New England Biolabs, MA, USA), and contained:

- 1x Q5 reaction buffer
- 200 μM dNTPs (each)
- 0.5 μM forward primer
- 0.5 μM reverse primer
- 100 ng template DNA
- 0.1 U (0.02 U/μL) Q5 Hot Start High-Fidelity DNA Polymerase
- Nuclease-free water to 50 μL of final volume

The reaction was heated in MiniOpticon Real-time PCR System (Bio-rad, CA, USA):

1. 98 °C, 30 seconds
2. 98 °C, 10 seconds

3. 62 °C, 30 seconds
4. 72 °C, 90 seconds (30 seconds/kb)
5. Repeat 2-5 30 cycles
6. 72 °C, 2 minutes
7. 4 °C, forever

Reaction was loaded on 1% (w/v) agarose gel at 100 V for 20 minutes. The band with the PCR fragments was purified using GeneJET Gel Extraction Kit (Thermo, MA, USA) according to manufacturer's protocol.

The vectors pNIC28-Bsa4 was digested using restriction enzyme BsaI (New England Biolabs, MA, USA). The digestion reaction contained:

- 1x NEBuffer 3
- 1 µg plasmid
- 100 µg/mL BSA
- 10 U BsaI
- Nuclease-free water to a volume of 50 µL

The digestion was incubated at 37 °C for 1 hour before cleaning up using GeneJET PCR Purification Kit (Thermo, MA, USA) according to manufacturer's protocol. Ligation-independent cloning treatments were carried out for both insert and the vector using T4 polymerase (New England Biolabs, MA, USA). The reactions contained:

- 1x NEBuffer 2
- 5 mM Dithiothreitol (DTT)
- 100 µg/mL BSA
- 2.5 mM dGTP (dCTP for the insert)

- 600 ng BsaI-digested LIC vector (or 0.2 pmol insert)
- 400 U (or 40 U for insert, 4 U/μL) T4 DNA polymerase
- Nuclease-free water to a volume of 100 μL (10 μL for insert)

The reactions were incubated at 22 °C for 30 minutes before heat inactivation at 75 °C for 20 minutes. Then the LIC-treated vector and insert were mixed at a 1:2 ratios. The mixture was transformed in 50 μL *E. coli* XL-10 Gold ultracompetent cells (Agilent, CA, USA) and plated on LB Agar plate with 50 μg/mL Kanamycin sulfate (Apollo, Cheshire, UK) (Green and Sambrook 2012). The transformation protocol is shown below:

- 1 μL of reaction or plasmid was added to 50 μL *E. coli* XL-10 Gold competent cells and incubated for 10 minutes on ice.
- The mixture was heat-shocked at 42 °C for 45 seconds, and recovered on ice for 2 minutes.
- 150 μL of 2xTY medium was added to the cells and incubated at 220 rpm, 37 °C for 1 hour (INNOVA® 44, Hamburg, Germany).
- The cells were plated out on LB agar plate with appropriate selection marker. The plates were incubated at 37 °C overnight and moved to 4 °C afterwards.

Individual colonies on each the plate were picked and grown in 2xTY media (10 mL) at 220 rpm, 37 °C overnight (INNOVA® 44, Hamburg, Germany), and mini-preped using GeneJET Plasmid Miniprep Kit (Thermo, MA, USA) according to manufacture's protocol. The concentration of plasmid was analysed using Nanodrop 1000 spectrophotometer (Thermo, MA, USA). The plasmids obtained were sequenced using T7 forward, T7 reverse and PHF2 sequence specific primers (Source Bioscience, Cambridgeshire, UK).

PHF2 (1-449) Y321H was generated by SDM using its wild-type construct (construct No. 1, PHF2 [1-449]) as a template (Shortle, DiMaio, and Nathans 1981). The reaction was set up using Q5 Hot Start High-Fidelity DNA Polymerase (New England Biolabs, MA, USA), it contained:

- 1x Q5 reaction buffer
- 200 μM dNTPs (each)
- 0.5 μM forward primer
- 0.5 μM reverse primer
- 1000 ng template DNA
- 0.1 U (0.02 U/μL) Q5 Hot Start High-Fidelity DNA Polymerase
- Nuclease-free water to 50 μL of final volume

The reaction was heated in MiniOpticon Real-time PCR System (Bio-rad, CA, USA):

1. 98 °C, 30 seconds
2. 98 °C, 10 seconds
3. 62 °C, 30 seconds
4. 72 °C, 5 minutes (30 seconds/kb)
5. Repeat 2-5 30 cycles
6. 72 °C, 2 minutes
7. 4 °C, forever

The relevant plasmid was transformed in 50 μL *E. coli* XL10-Gold Ultracompetent cells (Agilent, CA, USA) and plated on LB Agar plate with kanamycin sulfate (50 μg/mL). Individual colonies on each the plate were picked and grown in 2xTY media (10 mL) at 220 rpm, 37 °C overnight (INNOVA® 44, Hamburg, Germany), and mini-preped using GeneJET Plasmid Miniprep Kit (Thermo, MA,

USA) according to manufacture's protocol. The concentration of plasmid was analysed using Nanodrop 1000 spectrophotometer (Thermo, MA, USA). The plasmids obtained were sequenced using T7 forward, T7 reverse and PHF2 sequence specific primers (Source Bioscience, Cambridgeshire, UK).

2.3. Protein Production

2.3.1. Expression Optimisation

Expression trials for production of PHF2 (1-449) were carried out with various induction temperatures and IPTG concentrations for optimisation. The plasmid was transformed into *E. coli* BL21 (DE3) cells (see Section 2.2 for protocol), 2xTY medium (10 mL) supplemented with kanamycin sulfate was inoculated with a single colony from the plate, and was grown at 220 rpm, 37 °C overnight (INNOVA® 44, Hamburg, Germany). The culture (1 mL) was added into 2xTY culture (100 mL) for test expression and was grown at 220 rpm, 37 °C until the $OD_{600\ nm}$ reached 0.7 (INNOVA® 44, Hamburg, Germany). The cultures were then induced with IPTG (1 mM) for 3 hours at 37 °C and IPTG (0.1 mM) for overnight at 18 °C. All cultures were shaken at 220 rpm (INNOVA® 44, Hamburg, Germany). The $OD_{600\ nm}$ values of each condition were recorded prior to harvesting by centrifugation (Beckman JA-10, 4000 g, 10 minutes). Each pellet was weighed and stored at -80 °C. To analyse the expression conditions, resuspension buffer was added to each pellet according to their weight (8ml/g). The suspension was sonicated on ice for five rounds of 1 minute with 1-minute interval (Sonics & Materials, CT, USA, model VCX-600). A sample (200 µL) was taken from each suspension for SDS-PAGE analysis. The lysate was centrifuged at 58387 g, 4 °C for 20 minutes. A sample (200 µL) was taken from each supernatant for SDS-PAGE analysis, and the rest of the supernatant was filtered using

0.45 μm filter (Waters, MA, USA) before being applied to a HisTrap™ 1 mL Crude FF affinity chromatography column (GE Healthcare, Bucks, UK) manually. The protein was washed using HisTrap buffer A (50 mL) before elution using 10% v/v and 20% v/v HisTrap buffer B. A sample (200 μL) was taken from the flow through, wash, and elution fractions for SDS-PAGE analysis. All the SDS-PAGE analysis samples were mixed with SDS loading buffer (200 μL) and analysed by SDS-PAGE (220 V, 100 mA and 45 minutes). All the polyacrylamide gels used in this project were 12% polyacrylamide unless otherwise specified. The condition with most protein of interest expressed in the soluble fractions was selected for large-scale expression.

2.3.2. Large Scale Protein Expression

The wild-type PHF2 (1-449) and the Y321H variant encoding plasmids were used to transform *E. coli* BL21 (DE3) cells. 2xTY media (100 mL) supplemented with kanamycin sulfate was inoculated with a single colony from each plate, and was grown at 220 rpm, 37 °C overnight (INNOVA® 44, Hamburg, Germany). This culture (6 mL) was added into 2xTY media (600 mL) with kanamycin sulfate and was grown at 220 rpm, 37 °C until $OD_{600\ nm}$ reached 0.7 (INNOVA® 44, Hamburg, Germany). At this point the temperature was reduced to 18 °C and expression was induced by addition of IPTG (0.1 mM). The cultures were harvested after 16 hours and $OD_{600\ nm}$ was recorded. The pellets were obtained by centrifugation (Beckman JA-10, 4000 g, 10 minutes) and stored at -80 °C.

2.4. Protein Purification

In the purification optimisation process, a two-step purification method consisting of affinity chromatography and ion-exchange chromatography was used

and compared with a two-step purification method with affinity chromatography and size exclusion chromatography. The two-step method with affinity chromatography followed by size exclusion chromatography was used in large-scale purifications. The whole purification process was carried out at 4 °C. All elution was collected in 5 mL fractions.

2.4.1. Affinity Chromatography

The Resuspension buffer (see Section 2.1) was added to each pellet according to their weight (8ml/g). The suspension was sonicated on ice for five rounds of 1 minute with 1-minute interval (Sonics & Materials, CT, USA, model VCX-600). A sample (200 µL) was taken from each suspension for SDS-PAGE analysis. The lysate was centrifuged at 58000 g, 4 °C for 20 minutes (Beckman JA25.50). A sample (200 µL) was taken from each supernatant for SDS-PAGE analysis. The remaining supernatant was filtered using 0.45 µm filter (Waters, MA, USA) before applied on HisTrap^{TM} 5 mL Crude FF affinity chromatography column pre-equilibrated with Histrap Buffer A (GE Healthcare, Bucks, UK) using ÄKTA FPLC (GE Healthcare, Bucks, UK). The proteins was washed using buffer (100 mL) containing 5% v/v HisTrap Buffer B before being eluted using 10% v/v HisTrap buffer B. A sample (200 µL) was taken from the flow through, wash and elution fractions for SDS-PAGE analysis. All the SDS-PAGE analysis samples were mixed with 2x SDS loading buffer (200 µL) and analysed by SDS-PAGE (220 V, 100 mA and 45 minutes). The fractions containing the purest protein of interest were pooled and concentrated to 2 mL using an Amicon Ultra-15 30 kDa MWCO Centrifugal Filter device (Millipore, MA, USA).

2.4.2. Ion-exchange Chromatography

The protein from the affinity chromatography step was buffer exchanged into IEX buffer A using a Micro Bio-Spin Chromatography Column (Bio-rad, CA, USA) before being applied onto a Resource Q 6 mL ion-exchange chromatography column pre-equilibrated with IEX buffer A. The protein was washed with IEX buffer A (30 mL) before being eluted using IEX buffer B gradient (1% - 50% over 10 column volumes). The eluted fractions were analysed using SDS-PAGE. The fractions containing the purest protein of interest were pooled and concentrated to 2 mL using an Amicon Ultra-15 30 kDa MWCO Centrifugal Filter device (Millipore, MA, USA). Protein concentrations were determined using a Nanodrop 1000 spectrophotometer (Thermo, MA, USA) calculated based on the extinction coefficient and the molecular weight of the protein (values obtained by using ExPASy ProtParam), and the protein was stored at -80 °C.

2.4.3. Size exclusion chromatography

The protein from affinity chromatography step was loaded on a HiLoad 26/60 Superdex 75 prep grade column pre-equilibrated with SEC buffer using a 2 mL injection loop. The protein was eluted with 1.2 column volumes SEC buffer at a flow rate of 1 mL/min. Peak fractions were collected and analysed by SDS-PAGE. The purest fractions were pooled and concentrated to 10 mg/mL using Amicon Ultra-15 30 kDa MWCO Centrifugal Filter devices (Millipore, MA, USA). Protein concentrations were determined using a Nanodrop 1000 spectrophotometer (Thermo, MA, USA) calculated based on the extinction coefficient and the molecular weight of the protein (values obtained by using ExPASy ProtParam), and the protein was stored at -80 °C.

2.5. 2OG Turnover Assays using NMR

2OG conversion rates of PHF2 (1-449) wild-type and Y321H were measured by nuclear magnetic resonance spectroscopy (NMR) (Hopkinson et al. 2010). PHF2 was buffer exchanged into the NMR assay buffer using a Micro Bio-Spin Chromatography Column (Bio-rad, CA, USA) prior to the experiments. Each reaction contained:

- 1 mM 2OG disodium salt hydrate
- 500 μM sodium ascorbate
- 100 μM ammonium Fe^{2+} sulfate hexahydrate
- 20 μM enzyme
- NMR assay buffer to final volume of 75 μL

All reagents were freshly made prior to the experiments. The control reaction contained protein buffer instead of PHF2 where all other reagents remained the same. The reaction was transferred to a Bruker Avance III 700 MHz NMR spectrometer (Bruker, MA, USA), and the 2OG turnover rate was assessed using ^{1}H-NMR with an automated routine of 20 measurements. Each measurement contained 16 transients consisting of 89 seconds total acquisition time. The solvent (HDO) signal was suppressed using excitation sculpting. If succinate were produced by uncoupled 2OG turnover, a singlet peak at ~ 2.4 ppm should be observed in the NMR spectrum indicating the presence of succinate.

2.6. *In vitro* Demethylase Assays using MALDI

In vitro demethylase activity of PHF2 (1-449) wild-type and the Y321H variant was measured using Matrix-assisted laser desorption/ionisation mass spectrometry (MALDI) using a MicroMass MALDI mass spectrometer (Waters, MA, USA) with α-

cyano-4-hydroxycinnamic acid (CHCA) as the matrix (Beavis, Chaudhary, and Chait 1992; Tsukada et al. 2006). Each reaction contained:

- 2 μM enzyme
- 50 μM 2OG disodium salt hydrate
- 100 μM sodium ascorbate
- 10 μM ammonium Fe^{2+} sulfate hexahydrate
- 10 μM histone peptide
- MALDI buffer to a final volume of 20 μL

A variety of histone peptides were tested using MALDI containing different methylation marks (**Table 2**). The reactions were incubated at 37 °C for 1 hour before mixed with CHCA matrix (5 mg/mL) and analysed using MALDI Mass Spectrometry. A positive control containing PHF8 and peptide $H3_{1-14}$K4me3H9me2 was also tested. All reagents were freshly made prior to the experiments.

Table 2 Peptide substrate tested in the MALDI assay

Peptide	Sequence
H3K4me1	ARTK(Me1)QTARKSTGGKAPRKQLATKA
H3K4me2	ARTK(Me2)QTARKSTGGKAPRKQLATKA
H3K4me3	ARTK(Me3)QTARKSTGGKAPRKQLATKA
H3K9me1	ARTKQTARK(Me1)STGGKAPRKQ
H3K9me2	ARTKQTARK(Me2)STGGKAPRKQ
H3K9me3	ARTKQTARK(Me3)STGGKAPRKQ
H3K27me1	LATKAARK(Me1)SAPSTGGVKK
H3K27me2	LATKAARK(Me2)SAPSTGGVKK
H3K27me3	LATKAARK(Me3)SAPSTGGVKK
H3K36me1	KSAPSTGGVK(Me1)KPHRYRPGTVALRE
H3K36me2	KSAPSTGGVK(Me2)KPHRYRPGTVALRE
H3K36me3	KSAPSTGGVK(Me3)KPHRYRPGTVALRE
H4K20me1	KGGAKRHRK(Me1)VLRDNIQ
H4K20me2	KGGAKRHRK(Me2)VLRDNIQ
H4K20me3	KGGAKRHRK(Me3)VLRDNIQ
H3K4me3K9me2	ARTK(Me3)QTARK(Me2)STG
ARID5B	ALYKYMKERK(Me2)TPIERIP

2.7. Non-denaturing ESI-MS Analyses

Non-denaturing ESI-MS was used to characterise the non-covalent interaction between PHF2 and its cofactors/co-substrates (Sanglier et al. 2008; Tarhonskaya et al. 2014). Prior to the non-denaturing ESI-MS experiments, PHF2 protein was desalted into 200 mM ammonium acetate (pH 8.2) using a Micro Bio-Spin Chromatography Column (Bio-rad, CA, USA). Data were acquired on a Q-TOF mass spectrometer (Q-TOF micro, Waters, MA, USA) linked to a Nanomate (Advion Biosciences, NY, USA) with a chip voltage of 1.80 kV and a delivery pressure 0.5 psi (1 psi = 6.81 kPa). The sample cone voltage was typically 80 V or 120 V with a source temperature of 40 °C and an acquisition/scan time of 10 s/1 s. The pressure at the interface between the atmospheric source and the high vacuum region was fixed at 6.60 mbar. Data were processed with MASSLYNX 4.0 (Waters, MA, USA). Data were acquired for the following samples:

- 10 μM PHF2
- 20 μM PHF2 and 20 μM $MnCl_2$
- 20 μM PHF2 and 10 or 20 μM $NiCl_2$
- 20 μM PHF2 and 20, 40 or 80 μM ammonium Fe^{2+} sulfate hexahydrate
- 10 μM PHF2 and 10 μM ammonium Fe^{2+} sulfate hexahydrate
- 10 μM PHF2, 10 μM $NiCl_2$ and 15 μM 2OG

2.8. Tryptophan Fluorescence Analyses

Tryptophan fluorescence binding experiments were used to investigate the metal binding abilities of wild-type PHF2 and the Y321H variant (van Ingen et al. 2008; Vivian and Callis 2001). The assay was carried out in 384-well Special Optics Clear Bottom Plates (Corning, NY, USA), and the tryptophan fluorescence was measured

using PHERAstar FS microplate reader (BMG Labtech, Bucks, UK). Each assay contained:

- 10 μM enzyme
- A range of concentration of Mn^{2+}, Fe^{2+} or Ni^{2+} (2-fold serial dilution starting from 15 mM across the plate to 0.015 mM)
- Buffer to a final volume of 30 μL

The assay was incubated at room temperature for 5 minutes in dark before the tryptophan fluorescence (280 nm and 350 nm for excitation and emission wavelength, respectively) was measured. The wells containing buffer only were subtracted from the assay as background. Each measurement was subtracted from the protein-only measurement before the determination of binding curves and K_ds using Prism 6 (Graphpad, CA, USA). The data was fitted to the equation of $Y=B_{max}*X/(K_d+X)$ + NS*X + Background, where B_{max} refers to the maximum binding in the same units as Y, K_d refers to the equilibrium dissociation constant in the same units as X, NS refers to the slope of the non-linear regression in Y units divided by X units, and background refers to measured binding with no ligand added (valued obtained from the control experiments). The reactions were performed in triplicate and standard deviation was calculated and presented as error bars on the fitted curve.

2.9. Fluorescence Polarisation Analyses

The binding of the wild-type PHF2 (1-449) and the Y321H vairant to FITC labelled histone peptide $H3_{1-14}$K4me3K9me2 (ARTK[me3]QTARK[me2]STGGK, the proposed substrate peptide of PHF2) was determined using fluorescence polarisation (Perrin 1926; Xu et al. 2013). The assay was carried out in 96-well Special Optics Clear Bottom Plates (Corning, NY, USA), and the fluorescence

polarisation was measured using PHERAstar FS microplate reader (BMG Labtech, Bucks, UK). Each assay contained:

- 50 nM FITC-$H3_{1-14}$K4me3K9me2 peptide
- Enzyme at a range of concentrations (2 fold serial dilution from 10 μM enzyme across the plate to 0.01 μM)
- FP buffer to a final volume of 100 μL per well.

This assay was also used to investigate the effects of metal ions on peptide binding. Each reaction contained:

- 50 nM FITC-$H3_{1-14}$K4me3K9me2 peptide
- 0, 10, 20, 50 and 100 μM Ni^{2+} or ammonium Fe^{2+} sulfate hexahydrate
- Enzyme at a range of concentrations (2 fold serial dilution from 20 μM enzyme across the plate to 0.01 μM)
- FP buffer to a final volume of 100 μL per well.

This assay was also used to investigate the effects of 2OG and NOG on peptide binding. Each reaction contained:

- 50 nM FITC-$H3_{1-14}$K4me3K9me2 peptide
- 10 μM $NiCl_2$
- Enzyme at a range of concentrations (2 fold serial dilution from 20 μM enzyme across the plate to 0.01 μM)
- 0, 5, 10, 20, 50 and 200 μM NOG or 2OG
- FP buffer to a final volume of 100 μL per well.

The assays were incubated at room temperature for 20 minutes in the dark before fluorescence polarisation (492 nm and 517 nm for excitation and emission wavelength respectively) was measured. The wells containing protein only were subtracted from

the assay as background. Binding curves and K_ds were determined using Prism 6 (Graphpad, CA, USA). The data was fitted to the equation of $Y=B_{max}*X/(K_d+X) + NS*X + Background$, where B_{max} refers to the maximum binding in the same units as Y, K_d refers to the equilibrium dissociation constant in the same units as X, NS refers to the slope of the non-linear regression in Y units divided by X units, and background refers to measured binding with no ligand added (valued obtained from the control experiments). The reactions were performed in triplicate and standard deviation was calculated and presented as error bars on the fitted curve.

2.10. Differential Scanning Fluorimetry (DSF, or T_m shift) Analyses

Differential scanning fluorimetry (DSF) was used as a semi-quantitative method to determine the stability of PHF2 under different conditions (Niesen, Berglund, and Vedadi 2007a). The assay was carried out in a white 96-well Non-skirted Low Profile PCR plate (Thermo, MA, USA) in a MiniOpticon Real-time PCR System (Bio-rad, CA, USA). In the experiments determining the effect of NaCl concentration on protein stability, each reaction contained:

- 1 x SYPRO Orange dye (Invitrogen, CA, USA)
- 2 μM enzyme
- T_m shift buffer to a final volume of 50 μL

The DSF assay was also used to select the best stabilising metal for PHF2. Each reaction contained:

- 1 x SYPRO Orange dye (Invitrogen, CA, USA)
- 2 μM enzyme
- 50 μM Fe^{2+}, Mg^{2+}, Ni^{2+}, Mn^{2+}, Co^{2+}, Cu^{2+} or Zn^{2+}
- T_m shift buffer to a final volume of 50 μL

The DSF assay was also used to screen inhibitors for PHF2. Each reaction contained:

- 1 x SYPRO Orange dye (Invitrogen, CA, USA)
- 2 μM enzyme
- 4 μM Ni^{2+}
- 1 mM inhibitors
- T_m shift buffer to a final volume of 50 μL

The plate was sealed securely. Melting curves were obtained using a MiniOpticon Real-time PCR System (Bio-rad, CA, USA) from 25 – 80 °C. The excitation and emission wavelength of SYPRO orange is 492 and 610 nm, respectively. The melting curves and melting temperatures were determined using Prism 6 (Graphpad, CA, USA). Except for the initial inhibitor screen, each reaction was repeated three times.

2.11. X-ray crystallography

The PHF2 (1-449) protein used in crystallographic studies was at a concentration of 11 mg/mL. Purified PHF2 protein, PHF2 with $MnCl_2$ (500 μM), and PHF2 with $MnCl_2$ (500 μM) and NOG (1 mM) were used to set up crystallisation trials. Commercial screens including JCSG+ (Molecular Dimensions, Suffolk, UK), PACT Premier (Molecular Dimensions, Suffolk, UK) and PEG/Ion (Hampton Research, CA, USA) were used in initial screening. The proteins were mixed with mother liquor at 1:2, 1:1 and 2:1 ratios using a Phoenix crystallisation robot (Rigaku, Tokyo, Japan). Hits from initial screening were optimized using a range of concentrations of the components from the hit conditions (**Table 3**). The sitting-drop vapour diffusion

method and 20 °C incubation temperature (except one plate using JCSG+ screen that was incubated at 4 °C) were used in the work.

Table 3 Optimisation conditions of PHF2

Proteins	Conditions
PHF2, $MnCl_2$ (500 µM) and NOG (1 mM)	0.1 M HEPES, 5% – 16% PEG 8000 (w/v), 2% – 16% ethylene glycol (w/v), pH 7.5
PHF2 apo protein	0.1 M – 0.296 M sodium malonate, 11% – 22% PEG 3350 (w/v), pH 7.0
PHF2 and $MnCl_2$ (500 µM)	0.04 M – 0.18 M succinic acid, 9% – 20% PEG 3350 (w/v), pH 7.0
PHF2, $MnCl_2$ (500 µM) and NOG (1 mM)	0.14 M – 0.28 M sodium malonate, 10% – 21% PEG 3350 (w/v)

The crystals were transferred to a cryobuffer (reservoir buffer supplemented with 25% v/v glycerol) and flash frozen in liquid nitrogen. The crystallographic data were collected at the Diamond Light Source (DLS) beamline I04-1. To process the crystallographic datasets, molecular replacement program CCP4 was used to obtain crystallographic phases. The model was built manually using COOT and refinement was carried out with Phenix Refine. MacPyMol (DeLano Scientific, CA, USA) was used to generate structural figures.

Chapter 3 Cloning, Expression, and Protein Purification

The full length PHF2 has over 1000 residues with a PHD and a JmjC domain at its *N*-terminus. Domain searches suggested a lack of other identifiable domains present throughout the rest of the protein using NCBI's Conserved Domain Database (Marchler-Bauer et al. 2011). A total of six constructs of PHF2 were made during this project. The constructs were:

1. pNIC28-Bsa4-PHF2 (1-449)
2. pNIC28-Bsa4-PHF2 (1-449) Y321H
3. pcDNA3-N-Flag-PHF2 (1-1099)
4. pcDNA3-N-GFP-PHF2 (1-1099)
5. pNIC28-Bsa4-PHF2 (60-449)
6. pNIC28-Bsa4-PHF2 (60-449) Y321H

In order to facilitate production of soluble PHF2 protein, the full length PHF2 was truncated at position 449 to include only the PHD and the JmjC domains. The plasmid containing the gene for PHF2 (60-449) was made to include only the JmjC domain, in order to investigate the binding properties of PHF2. The gene encoding the full length PHF2 was also cloned into mammalian expression vectors with an N-terminal FLAG tag or an N-terminal green fluorescent protein (GFP) tag for future cell-based experiments. A plasmid encoding the gene for PHF2 Y321H variant was made for construct No. 1 and 5 in order to study the significance of the tyrosine in the active site of PHF2. All the constructs were made using ligation-independent cloning method, and the Y321H variant constructs were made by site-directed mutagenesis from their corresponding wild type constructs. The identity of each construct was

confirmed by sequencing using T7 forward, T7 reverse and PHF2 specific primers (see Supp. Table 1 for primer sequences, the sequencing service was performed by Source Bioscience, Cambridgeshire, UK).

Initially, the expression conditions were optimised (Figure 7). Based on the results, the recombinant proteins were produced in *E. coli* BL21 (DE3) cells at 18 °C, and induced with isopropyl β-D-thiogalactoside (IPTG, 0.1 mM) in 2xTY media overnight.

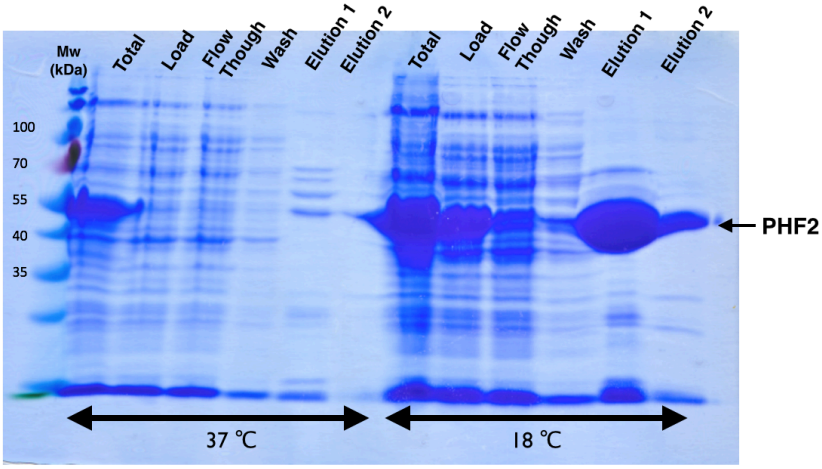


Figure 7 Expression trial of wild-type PHF2 protein under 37 °C, 1 mM IPTG, 3 hours and 18 °C, 0.1 mM IPTG, overnight. The lysate was manually loaded on a 1 mL Histrap FF column (GE Healthcare, Bucks, UK) followed by manual wash and elution. The fractions were analysed by SDS-PAGE. The second condition (18 °C, 0.1 mM IPTG, overnight) was selected for large-scale expression of PHF2 due to the increased amount of soluble protein present.

Protein purification processes were then optimised; metal-chelate affinity chromatography followed by size exclusion chromatography, or metal-chelate affinity chromatography followed by ion exchange chromatography were employed. Visible precipitation was observed for Y321H variant protein during metal-chelate affinity chromatography process in the absence of EDTA in the lysis buffer. Therefore EDTA (1 mM) was added in the lysis buffer in all purification procedures afterwards. SDS-PAGE analysis revealed no significant difference in purity between the protein

extracted from size exclusion chromatography and that from ion exchange chromatography (Figure 8a-b). However, there was a considerable amount of visible precipitation observed during the ion exchange chromatography due to the instability of PHF2 protein in buffers with low NaCl concentration (protein needs to be buffer exchanged into a no salt or low salt buffer prior to ion exchange chromatography to stimulate column binding). Therefore the desired proteins were purified by affinity chromatography and size exclusion chromatography. The proteins were then stored in 20 mM HEPES, pH 8.0, 200 mM NaCl (500 mM NaCl for Y321H) and 1 mM TCEP (Figure 8d-h) at - 80 °C. With that, degradation was observed if the purification process was carried out over more than one day (Figure 8c).

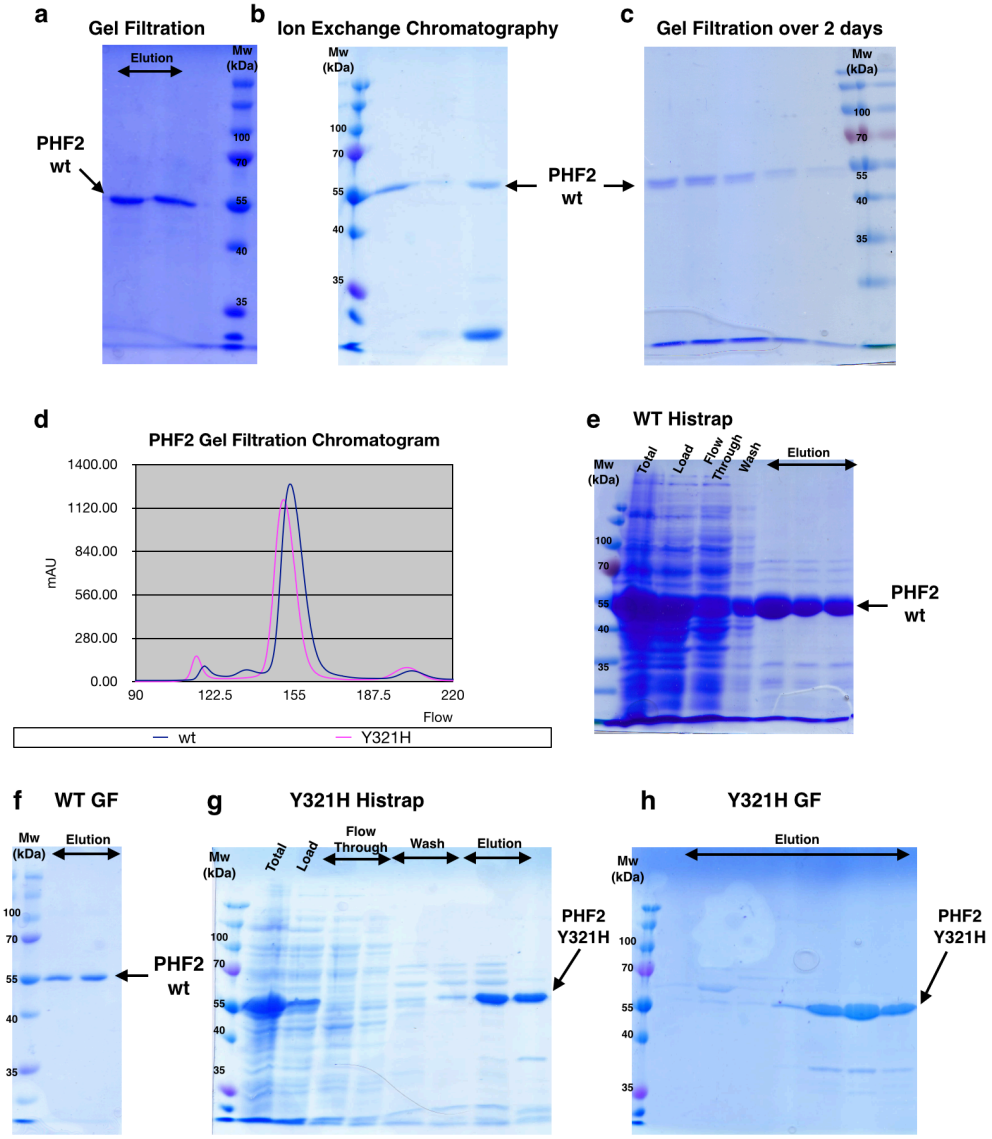


Figure 8 Purification of wild-type PHF2 and the Y321H variant proteins. a) SDS-PAGE analysis of wild-type PHF2 purified using size exclusion chromatography chromatography (SEC) during purification optimisation. **b)** SDS-PAGE analysis of wild-type PHF2 purified using ion exchange chromatography (IEX) during purification optimisation. The contaminant band at the bottom of the gel can be easily separated by SEC. **c)** SDS-PAGE analysis of initial wild-type PHF2 purification over the course of two days. Note the small contaminating band below the main PHF2 band indicated by the arrow. **d)** Final SEC chromatograms for wild-type PHF2 and the Y321H variant proteins. **e)** SDS-PAGE analysis of fractions from affinity chromatography (IMAC) of wild-type PHF2 using 5 mL HisTrap^{TM} ff Crude column. The eluted fractions were collected and were further purified using S75 26/60 SEC column. **f)** SDS-PAGE analysis of fractions from SEC of wild-type PHF2. **g)** SDS-PAGE analysis of fractions from IMAC of PHF2 Y321H variant using 5 mL HisTrap^{TM} ff Crude column. The eluted fractions were collected and were further purified using S75 26/60 SEC column. **h)** SDS-PAGE analysis of fractions from the SEC of PHF2 Y321H variant.

Chapter 4 Biochemical Characterisation of PHD Finger Protein 2 (PHF2)

4.1. 2OG Turnover Assays using NMR

Having obtained the purified PHF2 protein, various biochemical assays were performed to characterise PHF2. 2OG is often converted to succinate by JHDMs in the absence of the prime substrate (uncoupled turnover), which can be used as one of the indications of an active and correctly folded protein (Hewitson et al. 2005). Therefore the 2OG turnover rate of PHF2 was first studied using Nuclear Magnetic Resonance (NMR). The enzyme (20 μM), 2OG (1 mM), sodium ascorbate (500 μM) and Fe^{2+} (100 μM) were mixed, and the reaction was analysed in 'real-time' using NMR. If succinate were produced by uncoupled 2OG turnover, a singlet peak at ~ 2.4 ppm should be observed in the NMR spectrum indicating the presence of succinate. However, no 2OG turnover was observed for either wild-type PHF2 or the Y321H variant whereas a clear succinate singlet peak was observed for the positive control using PHF8 protein (obtained from Dr. L. Walport).

No uncoupled 2OG turnover was observed for either wild-type PHF2 or the Y321H variant, however, this result does not conclusively demonstrated that PHF2 is inactive as there are some 2OG oxygenases that do not catalyse substrate uncoupled 2OG turnover such as hypoxia-inducible factor prolyl hydroxylase 2 (PHD2) (Flashman et al. 2010). Further, the unusual composition of the active site of PHF2 may affect the binding affinities for its co-substrates and cofactor, which might reduce or completely abolish uncoupled 2OG turnover. The negative results could also be a consequence of non-optimised experimental conditions. As observed during protein purification, the stability of PHF2 was greatly reduced with a decrease in NaCl

concentration. However, a high NaCl concentration was not used in this assay in order to avoid damage to the cryo-probe of the instrument. Therefore more assays were needed to characterise PHF2.

4.2. *In vitro* demethylation assays using MALDI

The demethylation activity of PHF2 was then investigated by *in vitro* peptide demethylation assays using Matrix-assisted Laser Desorption/Ionisation (MALDI). The MALDI *in vitro* peptide demethylation assay is a widely used method for studying the activity of 2OG oxygenases, and a range of histone peptides with different methylation status were tested in this project (R. Fang et al. 2012; Kruidenier et al. 2012; Lacoste et al. 2002; Shi et al. 2004; Taverna et al. 2006).

A variety of peptides were tested as PHF2 substrates using MALDI; no demethylation reaction by PHF2 was detected with any peptides. Demethylation was observed in a positive control reaction containing PHF8 and its substrate peptide histone $H3_{1\text{-}14}$ K4me3K9me2 (**Table 4** and Figure 9a-b). The Y321H variant of PHF2 was also tested using peptide H3K4me3K9me2, as this peptide was the proposed substrate of PHF2 (Figure 9c). Once again no demethylation activity was detected. Literature reports state that PHF2 mediated demethylation on histone H3K9me2 occurred in cells transfected with PHF2, however, no demethylation reaction was detected on either H3K9me2 or H3K4me3K9me2 peptides (Baba et al. 2011; Horton et al. 2011; Wen et al. 2010). These results are consistent with the literature reports with purified recombinant PHF2(Baba et al. 2011; Horton et al. 2011).

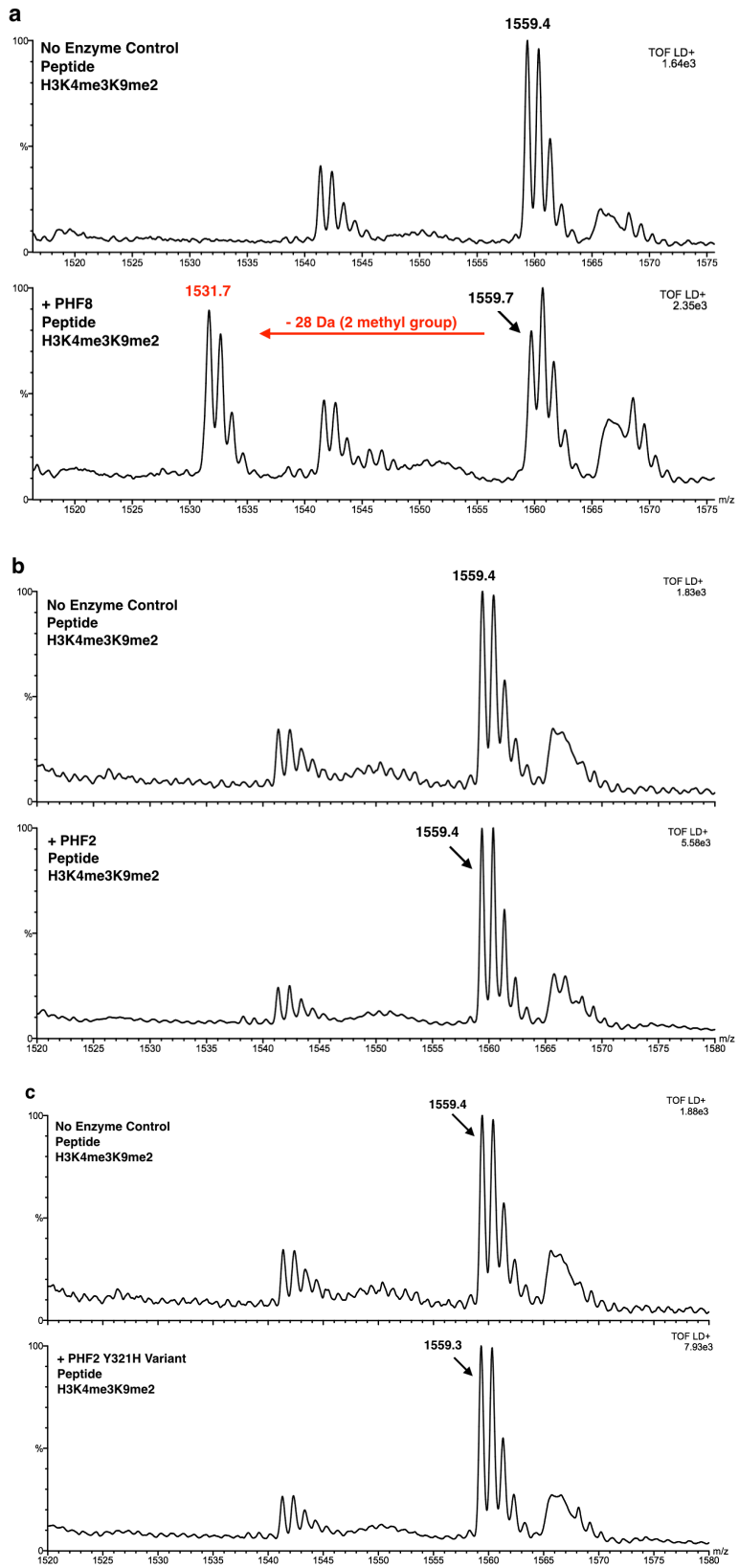


Figure 9 MALDI *In vitro* demethylation assay. Example spectra showing a) PHF8 as a positive control and histone peptide $H3_{1-14}$K4me3K9me2 (expected mass 1560 Da). **b)** PHF2 and histone peptide $H3_{1-14}$K4me3K9me2 (expected mass 1560 Da). **c)** PHF2 Y321H variant and histone peptide $H3_{1-14}$K4me3K9me2 (expected mass 1560 Da). The sequence of the $H3_{1-14}$K4me3K9me2 peptide used was ARTK(me3)QTARK(me2)STG.

Table 4 Peptide substrate tested in the MALDI assay		
Peptide	**Sequence**	**Demethylation Observed?**
H3K4me1	ARTK(Me1)QTARKSTGGKAPRKQLATKA	No
H3K4me2	ARTK(Me2)QTARKSTGGKAPRKQLATKA	No
H3K4me3	ARTK(Me3)QTARKSTGGKAPRKQLATKA	No
H3K9me1	ARTKQTARK(Me1)STGGKAPRKQ	No
H3K9me2	ARTKQTARK(Me2)STGGKAPRKQ	No
H3K9me3	ARTKQTARK(Me3)STGGKAPRKQ	No
H3K27me1	LATKAARK(Me1)SAPSTGGVKK	No
H3K27me2	LATKAARK(Me2)SAPSTGGVKK	No
H3K27me3	LATKAARK(Me3)SAPSTGGVKK	No
H3K36me1	KSAPSTGGVK(Me1)KPHRYRPGTVALRE	No
H3K36me2	KSAPSTGGVK(Me2)KPHRYRPGTVALRE	No
H3K36me3	KSAPSTGGVK(Me3)KPHRYRPGTVALRE	No
H4K20me1	KGGAKRHRK(Me1)VLRDNIQ	No
H4K20me2	KGGAKRHRK(Me2)VLRDNIQ	No
H4K20me3	KGGAKRHRK(Me3)VLRDNIQ	No
H3K4me3K9me2	ARTK(Me3)QTARK(Me2)STG	No
ARID5B	ALYKYMKERK(Me2)TPIERIP	No
H3K4me3K9me2 + Y321H variant PHF2	ARTK(Me3)QTARK(Me2)STG	No

There are several possible explanations for the lack of demethylation activity of PHF2 *in vitro* compare to that detected in cells (Baba et al. 2011). The demethylation activity detected in cells could be a result of series of signalling cascade initiated by the overexpression of PHF2 rather than the reactions catalysed directly by PHF2. *In vitro*, PHF2 itself may lack demethylation activity due to the unusual composition of its active site. This might affect its binding affinity for its co-substrates/cofactors, subsequently reduced or abolished demethylation activity. Thus the lack of *in vitro* demethylation activity may occur with peptides containing the histone H3K9 methylation marks. In addition, it was previously reported that PHF2 forms a complex with another protein, AT-rich interactive domain 5b (ARID5B), in cells (Baba et al. 2011). Hence, another possible explanation for the data obtained using MALDI is that PHF2 requires post-translational modifications or formation of a complex with other

proteins such as ARID5B to catalyse histone demethylation, which were missing in the *in vitro* assays.

Due to the limited time available for this project, it was decided that the binding affinity of PHF2 for its cofactor/co-substrates would be the main focus of the reminder of the project; the potential binding partners of PHF2 and the possible signalling pathways initiated by PHF2 or its complex were not investigated.

4.3. Non-denaturing ESI-MS Analyses

The results detailed in the previous sections suggested a lack of uncoupled 2OG turnover and a lack of *in vitro* demethylation activity for PHF2 (see Sections 4.1 and 4.2). Due to the unusual composition of the active site of PHF2, the metal binding ability of PHF2 was next investigated. The coordination of Fe^{2+} to the catalytic site of 2OG oxygenase is required for catalysis, which enables the binding of co-substrates including 2OG and oxygen and subsequent reaction (see Section 1.3). Non-denaturing ESI-MS was used to characterise the non-covalent interaction between PHF2 and its cofactors and, its co-substrates (Sanglier et al. 2008; Tarhonskaya et al. 2014).

Initially, the mass spectrum of wild-type PHF2 protein alone was determined and revealed a prominent peak at 53810 Da. This is consistent with the mass of PHF2 (expected 53685 Da) containing a PHD finger with two Zn^{2+} ions (2 x 65 Da) coordinated and an apo JmjC (i.e. no Fe^{2+}) domain (Figure 10a). The apparent lack of Fe^{2+} may be due to the purification procedure because EDTA (1 mM) was present in the lysis buffer, which might be sufficient to remove the endogenous ions in the JmjC active site but not the PHD finger (the two Zn^{2+} ions are required for structural stability of the PHD finger). This observation is interesting given the non-canonical

composition of the JmjC domain of PHF2, which may reduce its metal binding affinity.

Next, the metal binding ability of PHF2 was investigated using Ni^{2+}, Fe^{2+} and Mn^{2+}. Fe^{2+} is the natural co-factor of 2OG oxygenases; Ni^{2+} and Mn^{2+} are often used as substitutes in biochemical studies and crystallography (Aik et al. 2012, 2013; Loenarz and Schofield 2009). Experiments with a 1:1 molar ratio of wild-type PHF2 and Ni^{2+} resulted in the observation of predominately a single peak, at 53870 Da, likely corresponding to purified PHF2 (53810 Da) bound to a Ni^{2+} ion (+ 59 Da, Figure 10b). In contrast, experiments with a 1:1 molar ratio of wild-type PHF2 and Fe^{2+} resulted in the observation of two peaks, a prominent one corresponding to the purified PHF2 (53810 Da), and a smaller one at 53910 Da, which was ascribed to be PHF2 (53810 Da) with an Fe^{2+} ion (+ 55 Da) and a K^{+} ion (+ 39 Da, likely arising from impurities in the Fe^{2+}, Figure 10c). No peak at 53860 Da (PHF2 and a Mn^{2+} ion) was observed for experiment with a 1:1 molar ratio of wild-type PHF2 and Mn^{2+}, and the spectrum for this experiment was more noisy than the previous ones. The above results suggest that (i) wild-type PHF2 binds to both Fe^{2+} and Ni^{2+}, but may not bind Mn^{2+} so well (due to the noise of that particular spectrum it is not conclusive that PHF2 does not bind Mn^{2+}), and (ii) that the wild-type PHF2 might have stronger affinity for Ni^{2+} than Fe^{2+}, as PHF2 seemed to be fully saturated when mixed with equal molar of Ni^{2+} ions, whereas a significant amount of PHF2 with apo JmjC domain (53810 Da) was detected in the PHF2 + Fe^{2+} experiment. However, due to the propensity of Fe^{2+} to oxidise, it is difficult to determine the actual Fe^{2+} concentration during the experiment. No interpretable spectra were obtained for the experiments with PHF2 with more than an equimolar amount of metal ions.

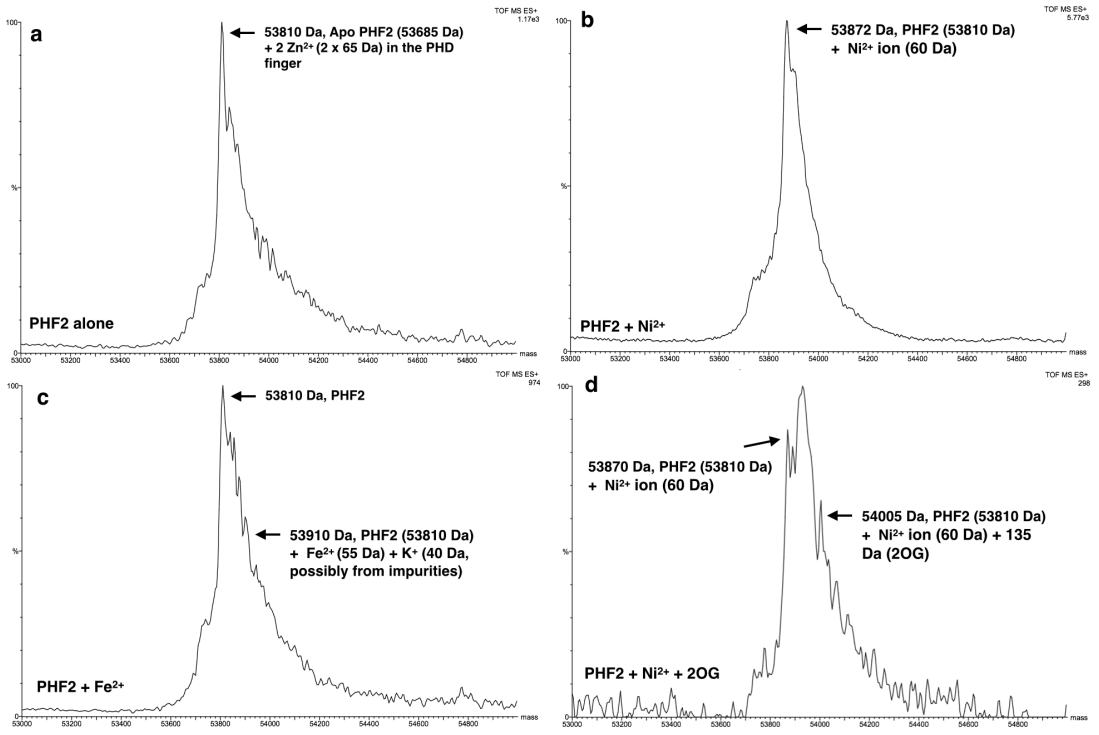


Figure 10 The use of non-denaturing ESI-MS to investigate the interactions between metal ions, 2OG/NOG and wild-type PHF2. a) Non-denaturing ESI-MS analysis of purified wild-type PHF2. **b)** Non-denaturing ESI-MS analysis of PHF2 with equal molar amount of Ni^{2+} added. **c)** Non-denaturing ESI-MS analysis of PHF2 with equal molar amount of Fe^{2+} added. **d)** Non-denaturing ESI-MS analysis of samples containing PHF2, Ni^{2+} and 2OG mixed at a 1:1:1.5 ratios.

Next, a sample containing PHF2, Ni^{2+} and 2OG mixed at a 1:1:1.5 ratios was analysed; the results revealed a peak (54005 Da) possibly due to purified PHF2 (53810 Da), one Ni^{2+} (+ 59 Da) and one 2OG (+ 135 Da, Figure 10d). This observation suggested that the purified wild-type PHF2 is capable of forming a complex with Ni^{2+} and 2OG that is detectable by non-denaturing ESI-MS. However, spectra from experiments with PHF2, Fe^{2+} and *N*-oxalylglycine (NOG, a close 2OG analogue (Hamada et al. 2009)) mixed at a 1:1:1 ratio, and PHF2, Ni^{2+} and NOG mixed at a 1:1:1 ratios were difficult to interpret due to the high level of noise. In addition, the Y321H variant PHF2 was analysed by non-denaturing ESI-MS. However, no interpretable spectra were obtained, possibly due to the instability of this protein.

4.4. Tryptophan Fluorescence Analyses

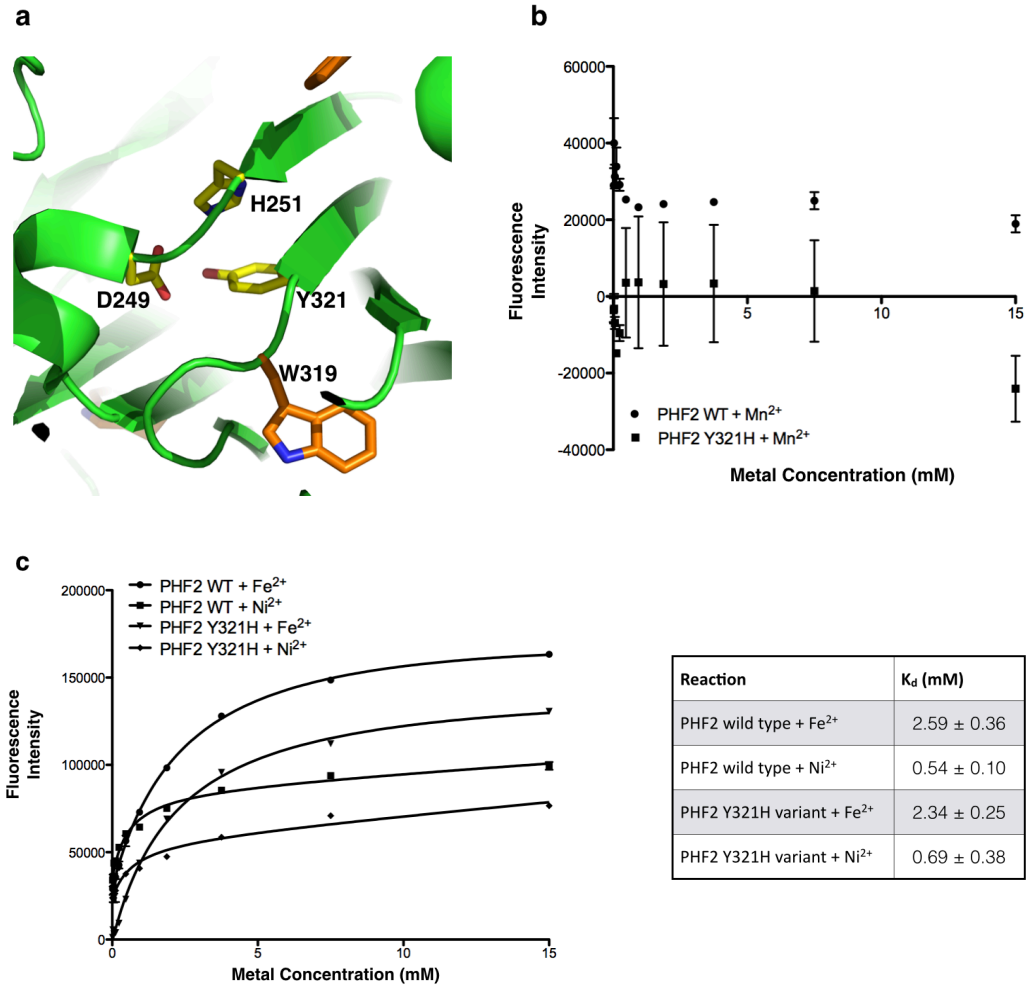
The results from non-denaturing ESI-MS analyses described in Section 4.2 suggested that wild-type PHF2 binds to Ni^{2+} and Fe^{2+} but not Mn^{2+}. Further wild-type PHF2 seemed to have a stronger affinity for Ni^{2+} than Fe^{2+} as PHF2 was fully saturated when mixed with equimolar of Ni^{2+}. Thus, the next step was to validate these observations and more quantitatively determine the metal binding affinities of PHF2.

There are limited reliable and robust assays currently available to determine the binding constants (K_ds) of proteins for metal binding, as most of the kinetic tools require either labeled ligands or a significant change in size in proteins upon ligand binding (Xu et al. 2013; Y Zhang and Reinberg 2001; Yi Zhang et al. 1997). Tryptophan fluorescence can be an efficient and relatively easy technique, which is widely used as a tool to monitor changes in proteins and investigate protein-ligand interactions (Vivian and Callis 2001). Tryptophan residues have long been known to be intrinsically fluorescent (280 nm and 350 nm for excitation and emission wavelengths, respectively); the tryptophan fluorescence can be quenched by changes in the surrounding environment including as a result of conformational changes occurring on ligand binding (Burstein, Vedenkina, and Ivkova 1973). This technique has been exploited in other K_d determination studies such as the ones with ING PHD finger, Yng1 PHD finger and TAF3 PHD finger (van Ingen et al. 2008; Li et al. 2006; Taverna et al. 2006).

The PHF2 construct used in this project (1-449) contains nine tryptophan residues, including one (W319) adjacent to the catalytic triad (Figure 11a). Thus, it was considered that tryptophan fluorescence maybe a suitable assay to measure the metal

binding affinity of PHF2, assuming that the fluorescence associated with W319 is quenched upon metal binding.

Various concentrations of Ni^{2+}, Mn^{2+} and Fe^{2+} ions (0.015 mM – 15 mM) were titrated against a fixed concentration of wild-type PHF2 and the Y321H variant (10 μM), and the fluorescence intensity was measured (280 nm and 350 nm for excitation and emission wavelength, respectively). In the Fe^{2+} binding experiment, the resultants K_ds were 2.59 ± 0.36 mM and 2.34 ± 0.25 mM, for wild-type PHF2 and the Y321H variant, respectively (Figure 11c). In the Ni^{2+} binding experiment, the K_ds were 0.54 ± 0.10 mM and 0.69 ± 0.38 mM, for wild-type PHF2 and the Y321H variant, respectively (Figure 11c). No binding could be fitted for the Mn^{2+} binding experiment, suggesting that PHF2 has a very low or no bind affinity for Mn^{2+} ions, which is consistent with the noisy data obtained using non-denaturing ESI-MS (Figure 11b). It was noticed that the K_d value for the Y321H variant to Ni^{2+} had a relatively large standard deviation, indicating reduced accuracy of this particular data set. This may be due to the general instability of the Y321H variant protein and the destabilising effects of Ni^{2+} ions; it was observed that the Y321H variant protein was more prone to precipitation than the wild-type PHF2 protein, especially in the presence of Ni^{2+} ions.



Reaction	K_d (mM)
PHF2 wild type + Fe^{2+}	2.59 ± 0.36
PHF2 wild type + Ni^{2+}	0.54 ± 0.10
PHF2 Y321H variant + Fe^{2+}	2.34 ± 0.25
PHF2 Y321H variant + Ni^{2+}	0.69 ± 0.38

Figure 11 View from a crystal structure of PHF2 showing its active site and the tryptophan fluorescence studies on the metal binding affinities of PHF2. a) The crystal structure of the PHF2 active site; note the tryptophan (W319) close to the metal binding site. **b-c)** The binding affinities of wild-type PHF2 and the Y321H variant to metal ions determined using tryptophan fluorescence. The experiments were carried out in triplicate and the error bars indicate standard deviation.

The results from tryptophan fluorescence assays indicated that (i) there was no significant difference in the Fe^{2+} binding affinities between the wild-type PHF2 and the Y321H variant, (ii) in consistent with the data obtained using non-denaturing ESI-MS (see Section 4.3), PHF2 has stronger affinities for Ni^{2+} than Fe^{2+}, and Mn^{2+} did not seem to bind PHF2. Despite the general trends observed in the experiments, it was noticed that the K_ds determined using tryptophan fluorescence were in the millimolar range, which may not represent the true binding affinities of the enzymes since an equimolar of Ni^{2+} ions were able to saturate wild-type PHF2 as observed in the non-

denaturing ESI-MS experiments (see Section 4.3). Given that there are nine tryptophans in the PHF2 construct used in this section, the unusually high K_ds may be likely due to the interference of the other tryptophans with the assay. To determine the accurate K_ds using tryptophan fluorescence assay, all the tryptophans except W319 (the one near the catalytic site) would have to be replaced by non-fluorescent residues. However, this may induce structural changes of the protein and significant decrease in the structural stability of PHF2. Due to the limited time available for this project, these substitutions were not carried out and hence the accurate K_ds of PHF2 in metal binding were not determined. However, the general conclusions (no significant difference in metal binding affinities between wild-type PHF2 and the Y321H variant, and PHF2 binds tighter to Ni^{2+} than Fe^{2+}) may be of biological relevance.

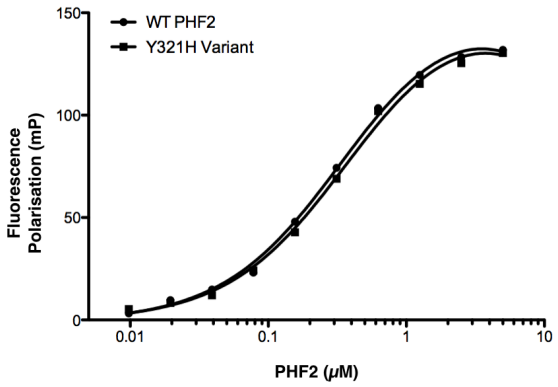
4.5. Fluorescence Polarisation Analyses

The data obtained from the *in vitro* demethylation assay showed no demethylation activity for PHF2 on its reported substrate peptide histone H3K4me3K9me2 (see Section 2.6), which raised questions on the binding ability of PHF2 to its cofactors and co-substrates. The results of the metal binding studies using non-denaturing ESI-MS (see Section 4.3) and tryptophan fluorescence (see Section 4.4) collectively suggested that PHF2 binds to Ni^{2+} and Fe^{2+} but not Mn^{2+}, and a complex possibly containing PHF2, Ni^{2+} and 2OG was observed in non-denaturing ESI-MS experiments. Having investigated the metal binding ability of PHF2, it was decided that the next step was to investigate the substrate peptide binding properties using a fluorescence polarisation assay.

Fluorescence polarisation measures the fluorescence intensities parallel and perpendicular to the plane of polarised excitation light, and the result is expressed as

the ratios of these two intensities, which is termed as fluorescence polarisation or anisotropy (Perrin 1926). Fluorescently labelled small molecules rotate rapidly in solution. As such, initial polarised excitation light is emitted in random directions, which results in low fluorescence polarisation. However, binding of this small molecule to a large protein greatly reduces its rate of rotation, and hence can result in increased fluorescence polarisation (Perrin 1926; Xu et al. 2013).

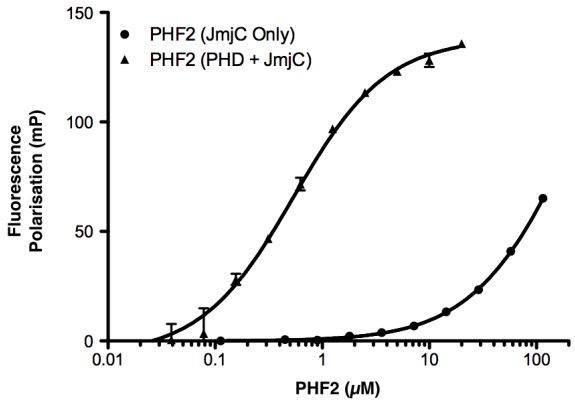
Various groups have reported histone H3K4me3K9me2 as the peptide substrate for PHF2 in cell-based studies (Baba et al. 2011; Horton et al. 2011; Wen et al. 2010). Therefore this peptide (labelled with fluorophore FITC) was chosen as the ligand used in fluorescence polarisation assays. To investigate whether the Y321H variant affects the peptide recognition process, 50 nM FITC-labelled peptide $H3_{1-14}$K4me3K9me2 was titrated against both wild-type PHF2 and the Y321H protein at a range of concentrations (0 – 20 μM). The results showed that the K_ds were 0.35 ± 0.04 μM (wild-type) and 0.38 ± 0.05 μM (Y321H variant), indicating no significant difference in the binding affinities between the two PHF2 proteins (Figure 12). This raised questions whether the peptide binding affinity of PHF2 may be predominately determined by its PHD finger.



Protein	K_d (μM)
PHF2 wild type	0.35 ± 0.04
PHF2 Y321H varian	0.38 ± 0.05

Figure 12 The peptide binding affinity of wild-type PHF2 and the Y321H variant determined by fluorescence polarisation assays. The experiments were carried out in triplicate and the error bars indicate standard deviation. The peptides used in this was histone $H3_{1-14}$K4me3K9me2 (ARTK[me3] QTARK[me2]STGGK).

Since PHF2 has two domains, i.e. its PHD finger and its JmjC domain, the next experiments tested the peptide binding affinity using PHF2 (1-449) containing both domains and the JmjC only protein to investigate the contribution of each domain to substrate recognition (Figure 13). The results showed that the K_d of PHF2 (PHD + JmjC) for the histone $H3_{1-14}$K4me3K9me2 was 0.54 ± 0.07 μM, whereas in the case for PHF2 (JmjC only), hardly any binding was observed to the substrate peptide (~95.14 ± 30.19 μM). This suggested that the substrate recognition was mainly determined by the PHD finger of PHF2, which also explains the fact that no significant difference was observed in peptide binding affinity between the wild-type PHF2 and the Y321H variant.

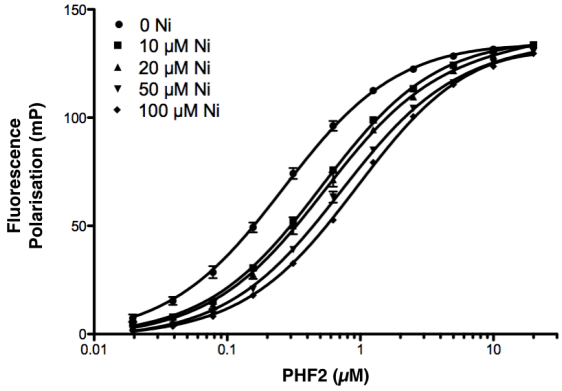


Protein	K_d (μM)
PHF2 (PHD + JmjC)	0.54 ± 0.07
PHF2 (JmjC only)	~ 95.14 ± 30.19

Figure 13 The peptide binding affinity of wild-type PHF2 (JmjC only) and wild-type PHF2 (PHD finger + JmjC) determined by fluorescence polarisation assays. The experiments were carried out in triplicates and the error bars indicate standard deviation. The peptides used in this section were histone $H3_{1-14}$K4me3K9me2 (ARTK[me3]QTARK[me2]STGGK).

To further investigate the peptide binding mechanism of PHF2, the effect of Ni^{2+} ions, 2OG and NOG on peptide binding was next investigated. It is possible that the JmjC domain of PHF2 requires a specific conformational change induced by initial cofactor/co-substrate binding in order to bind its substrate peptide. Various concentration of Ni^{2+} ions (0 – 100 μM) were added to the assay to investigate their effect on the peptide binding, as the coordination of metal ions at the active site is

essential for subsequent co-substrate binding, and it may help stabilise the protein as well (Figure 14). However, the results showed a slight decrease in the peptide binding affinities of PHF2 as the concentration of Ni^{2+} increased (the K_d decreased from 0.26 μM to 0.96 μM as the concentration of Ni^{2+} increased from 0 μM to 100 μM). It was noticed that during the process of protein purification and sample preparation for biochemical assays, PHF2 was sensitive to Ni^{2+} ions, as visible precipitation was often observed when high concentration of Ni^{2+} was added. Therefore the slight decrease in K_d with increased Ni^{2+} concentration was likely due to the destabilising effect of Ni^{2+} to PHF2.



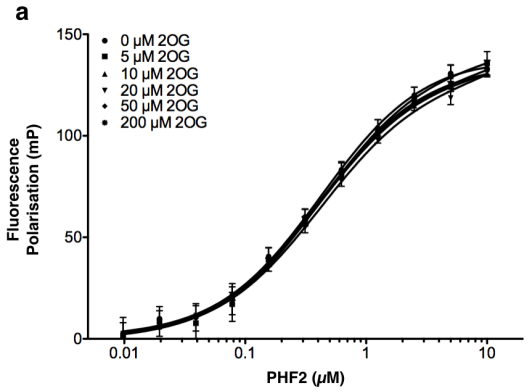
Sample	K_d (μM)
PHF2	0.26 ± 0.008
PHF2 + 10 μM Ni^{2+}	0.51 ± 0.02
PHF2 + 20 μM Ni^{2+}	0.54 ± 0.03
PHF2 + 50 μM Ni^{2+}	0.71 ± 0.04
PHF2 + 100 μM Ni^{2+}	0.96 ± 0.04

Figure 14 The effect of Ni^{2+} ions on the peptide binding affinity of wild-type PHF2 determined by fluorescence polarisation assays. The experiments were carried out in triplicates and the error bars indicate standard deviation. The peptides used in this section were histone $H3_{1-14}$K4me3K9me2 (ARTK[me3]QTARK[me2]STGGK).

Various studies on 2OG oxygenases have shown that the substrate binding of 2OG oxygenases are often enhanced by the binding of its co-substrate 2OG and 2OG mimics such as NOG, as the binding of 2OG or similar inhibitors increases the general stability of the protein (Chowdhury et al. 2011; Rose et al. 2012). Next, the effect of 2OG (co-substrate of 2OG oxygenases) and NOG (an 2OG oxygenase inhibitor which mimics the structure of 2OG) on peptide binding was investigated (**Figure 15**a and b). In this experiment, 50 nM FITC-labelled peptide $H3_{1-}$

$_{14}$K4me3K9me2 supplemented with of Ni^{2+} (10 μM, to allow 2OG/NOG coordination) was titrated against PHF2 protein at a range of concentrations (0 – 10 μM), and 2OG/NOG (0, 10, 20, 50 and 200 μM) was supplemented into each binding experiment to investigate if the 2OG/NOG affect peptide binding affinities of PHF2. The K_ds were determined subsequently. This experiment was also repeated with the JmjC domain from PHF2 using 2OG and NOG (500 μM) to investigate whether cofactor/co-substrate coordination at the JmjC domain has any effect on peptide recognition. Interestingly, the results showed no significant difference in the peptide binding affinities of PHF2 when various concentrations of 2OG or NOG were added, and no peptide binding was observed for the JmjC domain in the presence of 2OG/NOG, suggesting that the JmjC domain is probably not involved in substrate peptide binding. A structure of PHF8-peptide complex (a close relative of PHF2, and the only structure of KDM7 subfamily JHDM solved that contains a peptide-bound complex, PDB 3KV4) revealed that the dimethyl group (K9me2) of the substrate peptide is mainly stabilised by the hydrophobic cage containing aromatic and non-polar residues on PHF8, except an electrostatic interaction between the $O^{\delta-}$ on NOG and the $N^{\delta+}$ from K9me2 on the histone peptide (Horton et al. 2010). Therefore if PHF2 bind to its substrate peptide in a similar fashion, it is plausible that the presence of metal ions, co-substrates or 2OG mimics might have little effect on substrate recognition. Additionally, the substrate specificities of other members in this JHDM subfamily are mainly determined by the PHD finger and possibly the linker region between two domains (see Section 1.4). However, compared to PHF8, the linker region between the two domains is much longer in PHF2, which may not be able to maintain the rigid 'bend-over' conformation as in PHF8 that keeps the PHD finger and the JmjC domain at K4 and K9 position of the peptide respectively (Horton et al.

2010). Thus it raises questions whether the JmjC domain of PHF2 is involved in the binding of the substrate K9me2 site at all, which could be the reason that changes at the JmjC domain (changing in the catalytic triad itself or the binding of 2OG/NOG) did not affect the peptide binding, and no *in vitro* demethylation activity was observed. It is plausible that the cellular demethylation activity reported previously may be the result of some modifications or binding of other protein, which induces a conformational change in PHF2, such that it could adopt a similar rigid structure of PHF8, or the cellular demethylation activity was a consequence of series of signalling cascade initiated by PHF2 upon a binding, or demethylation of a unknown substrate.



Sample	K_d (μM)
PHF2	0.42 ± 0.03
PHF2 + 5 μM 2OG	0.43 ± 0.04
PHF2 + 10 μM 2OG	0.41 ± 0.01
PHF2 + 20 μM 2OG	0.42 ± 0.03
PHF2 + 50 μM 2OG	0.41 ± 0.01
PHF2 + 100 μM 2OG	0.39 ± 0.01

Sample	K_d (μM)
PHF2	0.27 ± 0.01
PHF2 + 10 μM NOG	0.29 ± 0.01
PHF2 + 20 μM NOG	0.27 ± 0.03
PHF2 + 50 μM NOG	0.31 ± 0.01
PHF2 + 200 μM NOG	0.26 ± 0.03

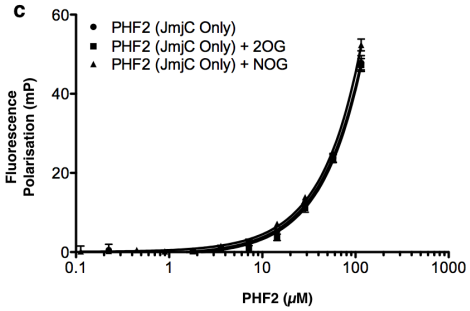


Figure 15 The peptide binding affinity of PHF2 determined by fluorescence polarisation assays. a) – b) The effect of 2OG/NOG on the peptide binding of PHF2. **c)** The effect of 2OG/NOG on the peptide binding of PHF2 (JmjC only). The K_ds could not be determined for PHF2 (JmjC only). The experiments were carried out in triplicate and the error bars indicate standard deviation. All the peptides used in this section were FITC-histone H3K4me3K9me2 (ARTK[me3]QTARK[me2] STGGK).

4.6. Differential Scanning Fluorimetry (DSF, or T_m shift) Analysis

Studies have shown that PHF2 facilitates chondrogenesis and adipogenesis by interacting with AT-rich interactive domain 5b (ARID5B) protein, a co-regulator of Sox9, which acts as a master regulator of chondrogenesis (Baba et al. 2011; Hata et al. 2013; Okuno et al. 2013). In addition, a recent study has identified PHF2 as a tumour suppressor in association with p53 in cancer development (K. Lee et al. 2014). Therefore it was decided to screen inhibitors for PHF2, not only to identify a tool for probing its biological functions, but also to help characterise this enzyme, as the studies on the mode of inhibition might provide insights into its catalytic or substrate-binding mechanisms. A PHF2 specific inhibitor may also be useful to study the function of this protein in cells. Moreover, an inhibitor with strong binding affinity to PHF2 could facilitate crystallographic studies as tight-binding inhibitors often help stabilise the protein.

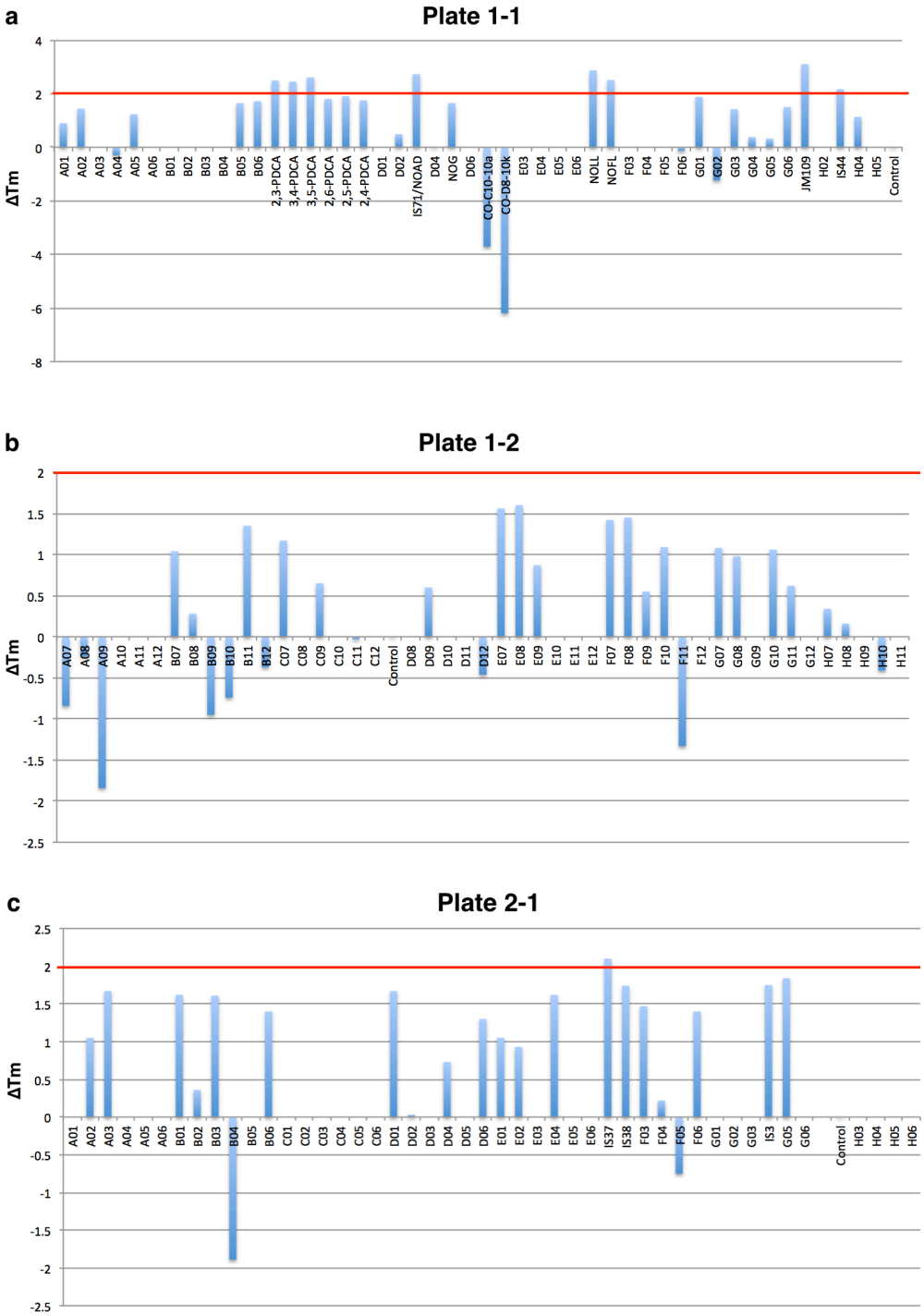
A differential scanning fluorimetry (DSF) assay was used in the initial screen of inhibitors for PHF2, as it is relatively quick and easy to perform. This technique is a semi-quantitative method to determine the stability of proteins under different conditions. Protein stability is related to its Gibbs free energy of unfolding (ΔG_u), which is temperature dependent. In general, protein stability decreases as the temperature increases. The melting temperature (T_m) is defined as the temperature where the concentrations of folded and unfolded protein are equal (when ΔG_u reaches zero). The DSF assay employs a dye, SYPRO Orange (Invitrogen, CA, USA), which is highly fluorescent in non-polar environments such as the hydrophobic core of protein that is often only exposed when the protein is unfolded (Aik et al. 2013; Niesen, Berglund, and Vedadi 2007b). Thus, as more protein becomes unfolded with increasing temperature, the fluorescence level is also increased due to the binding of

the dye to the exposed hydrophobic protein core. Therefore by continuously monitoring the fluorescence level of a given sample as it is gradually heated, a T_m can be obtained by locating the temperature where the fluorescence level is half of the maximum. The results obtained using the DSF assay do not necessarily indicate compound binding, however, the increase in stability is generally associated with the formation of protein-inhibitor complex as most of the ligand binding events are exothermic.

In the DSF assay, wild-type PHF2 (2 μM) was mixed with Ni^{2+} ions (4 μM) and inhibitor (1 mM). The temperature was increased from 25 °C to 80 °C, and the fluorescence level at each degree was recorded. Approximately 200 compounds (2OG mimics) were screened in this project (2 x 96 well plates obtained from Dr. Akane Kawamura, Figure 16a-d). The T_m for each compound was subtracted from the T_m of the control experiment (no inhibitor added). Inhibitors that increased the T_m by more than 2 °C were selected as hits (Figure 16e1-14). Among the hits, IS70, IS71, IS37 and IS38 (Figure 16e10-13) closely resemble the structure of 2OG (Figure 16e15), and compounds 1, 2, 5, 6 and 7 are very similar to compound 4 (2,4-PDCA), which is a generic 2OG oxygenases inhibitor that is often used as a probe in biochemical studies and crystallography (Kristensen et al. 2012). It was noticed that compound CO-D8-10k and CO-C10-10a (Figure 16e 16 and 17) exhibited great destabilising effects on PHF2, suggesting that PHF2 has low tolerance for 2OG mimics with bulky addition at the C-2 position.

The initial hit list provided valuable insight for future inhibitor development, as they could serve as a template for derivative compounds. Given more time and resources, the binding affinities of each one could be determined using the fluorescence polarisation assay in competition assays against a labelled generic

inhibitor such as FITC-NOG. PHF8, KIAA1718 or JHDMs from other subfamilies could be also used to select the PHF2 specific or KDM7 subfamily specific inhibitors. Then, the cell-permeability of each compound could be tested, and the inhibitor with both selectivity and cell permeability could be used in cell-based assays as a probe to investigate the biological funciton of PHF2.



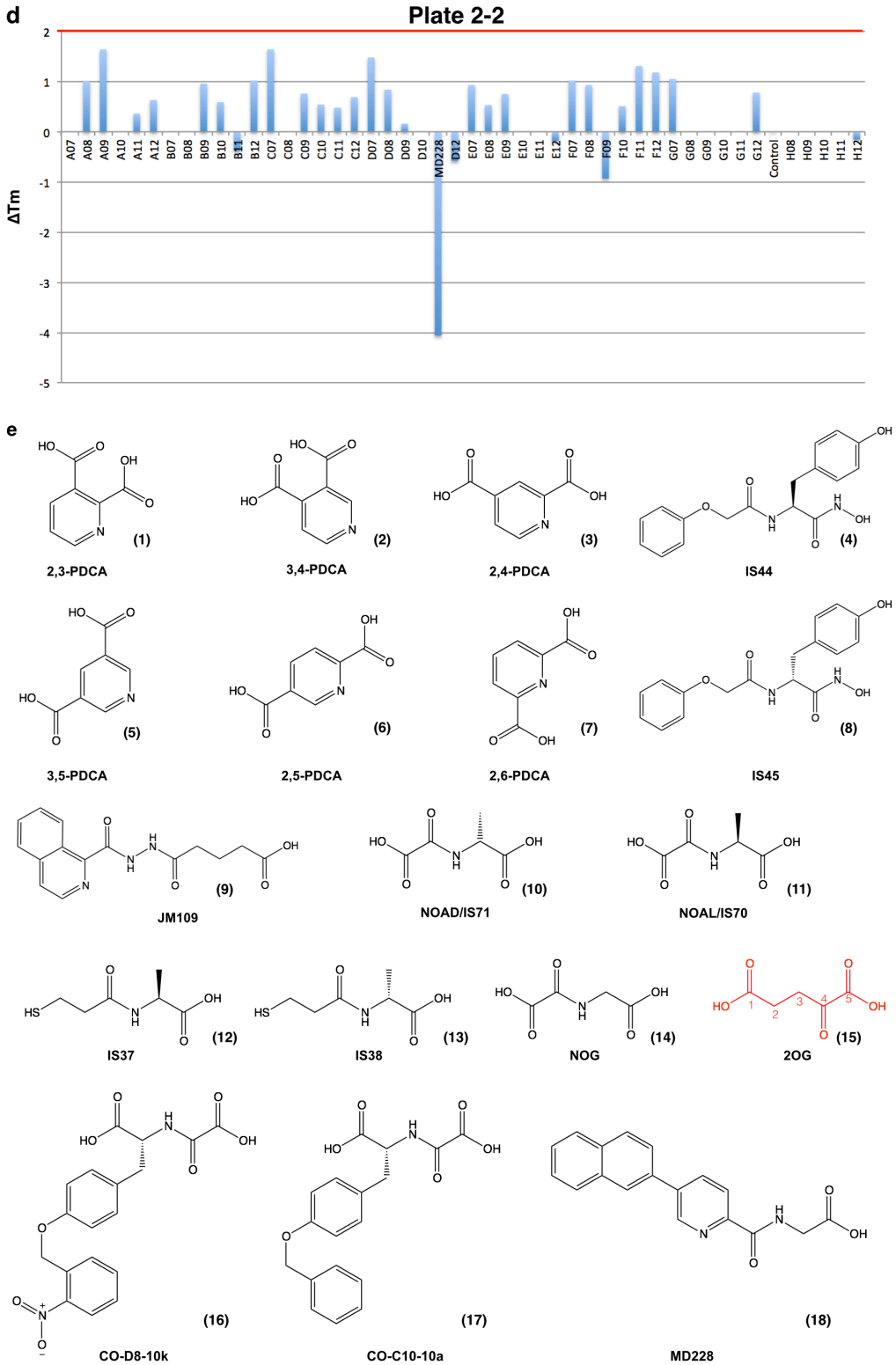


Figure 16 Inhibitor screening for PHF2 using differential scanning fluorimetry (DSF) assay and the chemical structures of initial hits and 2OG. a) – d) The results of the inhibitor screening for PHF2 using DSF assay, the T_m for each compound was subtracted from the control. The inhibitors that increased the T_m for more than 2 °C (indicated by the red line) were selected as hits and were evaluated further. **e)** Structures of selected inhibitors from the inhibitor screen.

Chapter 5 X-ray crystallography

Structural approaches such as X-ray crystallography are often used to reveal information on protein structures and enzymatic mechanisms at the molecular level. The individual structures of the PHD finger (PDB 3KQI) and the JmjC domain (PDB 3PUA) of PHF2 have been solved with substrate peptide and NOG, respectively (Horton et al. 2011; Wen et al. 2010). However, a structure containing both the PHD finger and the JmjC domain remains to be elucidated, and would reveal, (i) whether the PHF2 binds the proposed substrate peptide in a similar way as PHF8, (ii) whether the PHF2 linker region between the two domains affects the peptide binding in the same way as in either PHF8 or KIAA1718, from the same JHDM subfamily (discussed in Section 1.4) and (iii) whether the JmjC domain of PHF2 contribute to peptide recognition. Due to the limited time available for this project, crystallographic studies were carried out before the completion of relevant biochemical studies such as metal binding assays. The metal ion added in crystallisation trials was selected based on the result of a screening of the most stabilising metal ion for PHF2 by a T_m shift assay.

5.1. Screening of the most stabilising conditions for PHF2 by DSF assay

To serve as guidance for crystallography, metal ions were screened in order to select the most stabilising one for the protein. Hence a DSF assay was used before conducting crystallographic studies as an efficient semi-quantitative method to characterise the changes in stability of the protein under different conditions (see Section 2.10 and 4.6 for details on DSF assay) (Niesen, Berglund, and Vedadi 2007a).

During the purification process, it was noticed that the PHF2 Y321H variant was more prone to precipitation than the wild-type. Therefore the stability of PHF2 was

tested using a HEPES based buffer with different NaCl concentrations (200 mM, 400 mM and 600 mM). It was observed that wild-type PHF2 was in general more stable than the Y321H variant, as demonstrated by the higher T_m, and that increases in salt concentration increased protein stability dramatically (by an increase of 4.3 °C and 3.0 °C for the wild-type and Y321H variant respectively, see Figure 17). Therefore all *in vitro* functional studies were carried out in buffer containing 500 mM NaCl unless high-salt concentration interfered with the specific assay, such as for NMR (the experiments in this section were conducted prior to the biochemical assays).

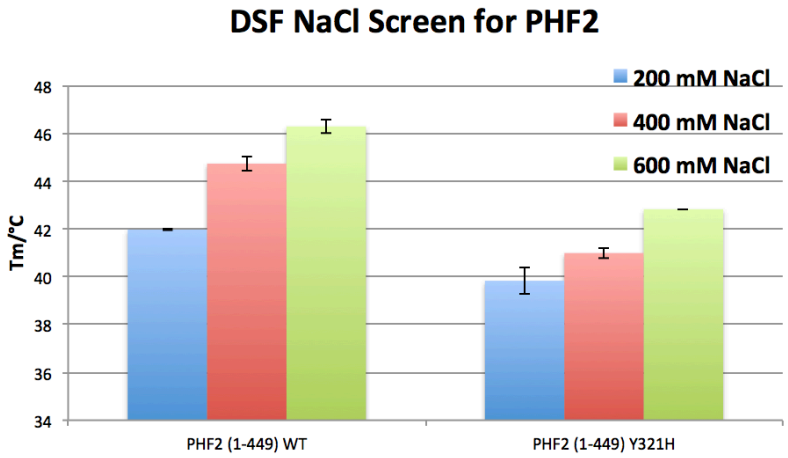


Figure 17 NaCl concentrations screen for PHF2 using DSF assay. a) DSF screen of NaCl concentrations (200 mM, 400 mM and 600 mM) for wild-type PHF2 and PHF2 Y321H. The experiments were carried out in triplicates and the error bars indicate standard deviation.

Fe^{2+} ion is the natural co-factor of all JHDMs, which is essential for 2OG coordination and subsequent catalysis (see Section 1.3). Therefore structures of metal-bound complex, or metal-2OG/NOG-bound complex are more desired. To serve as guide for crystallography, metal ions were screened in order to select the most stabilising one for the protein using DSF assays (see Section 2.10 and 4.6 for details on DSF assay) (Niesen, Berglund, and Vedadi 2007a).

EDTA was used to chelate metal ions present originally in the JmjC domain of PHF2 by incubating the protein in storage buffer (see Section 2.4 for recipe) supplemented with 1 mM or 3 mM EDTA overnight. The protein was buffer exchanged into an EDTA-free buffer (see Section 4.6 for recipe) prior to the initiation of a T_m shift assay for metal screening. Metal ions screening included Fe^{2+}, Mg^{2+}, Ni^{2+}, Mn^{2+}, Co^{2+}, Cu^{2+} and Zn^{2+}, which were tested using 1 mM EDTA-treated PHF2 initially in T_m shift (Figure 18a). The assay was repeated using 1 mM and 3 mM EDTA-treated enzymes (Figure 18b). Each reaction contained enzyme (2 μM) and metal ions (50 μM). No melting curves were obtained on addition of Co^{2+}, Cu^{2+} or Zn^{2+} suggesting that these ions have deleterious effects on the PHF2 protein stability. Among the ions that generated data, Ni^{2+} had a significant destabilising effect on wild-type PHF2 (no melting curves were observed with the variant), which might explain the high levels of precipitation observed for Y321H after its elution from the HisTrap™ column when EDTA was not present in the lysis buffer. Combining with the non-denaturing ESI-MS data (see Section 4.3, which was not obtained as all experiments in this section were performed before the relevant biochemical assays due to the limited time available for this project) where wild-type PHF2 was fully saturated with Ni^{2+} when mixed with at a equimolar ratios, the results collectively suggested that PHF2 has a relatively strong affinity for Ni^{2+} ions, however, high concentration of Ni^{2+} ions may induce a destabilising effect on PHF2 and result in protein precipitation. From the results of this DSF assay, Fe^{2+} and Mn^{2+} both stabilised wild-type PHF2, and Fe^{2+} is the natural cofactor for most of the JHDMs. However, Fe^{2+} has the propensity to oxidise. Therefore, Mn^{2+} was used in crystallographic studies, due to its stabilising effects on the proteins and its general stability with respect to oxidation (see Sections 4.3 and 4.4, which suggested that

PHF2 does not bind Mn^{2+} were not obtained when experiments in this section was performed). It was noted that the results of DSF assay do not necessarily correlate with the binding affinity between the metal ions and the protein.

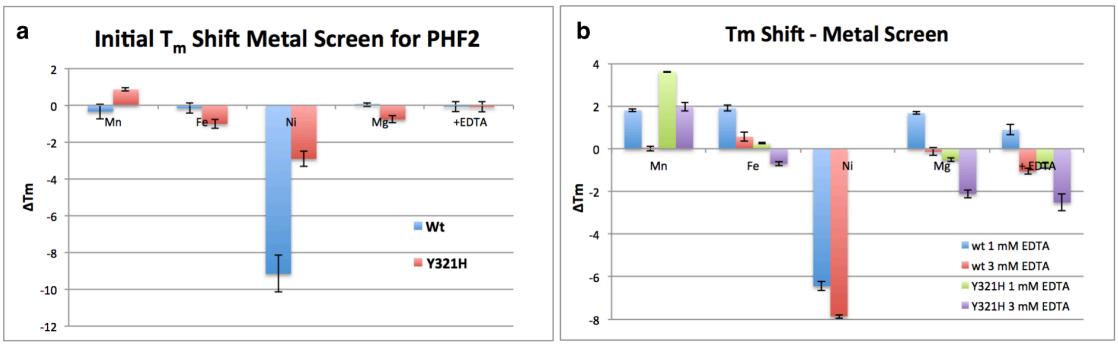


Figure 18 T_m shift screen of various metal ions. a) Initial T_m Shift screen of metal ions using 1 mM EDTA-treated PHF2. Each sample mixture contained 2 µM enzyme and 50 µM metal ions. Proteins without EDTA added were used as controls. **b)** Repeat of the T_m shift screen of various metal ions using 1 mM EDTA- and 3 mM EDTA-treated PHF2. Each sample mixture contained 2 µM enzyme and 50 µM metal ions. No melting curves were observed for Y321H protein with Ni^{2+}. Proteins without EDTA added were used as controls. The experiments were carried out in triplicates and the error bars indicate standard deviation.

5.2. X-ray crystallography

Based on the results obtained in Section 5.1, Mn^{2+} ions (500 µM) were added to the crystallisation trials as Mn^{2+} seemed to have the most stabilising effect on PHF2. A decreased NaCl concentration (200 mM) was used as high NaCl concentration (such as 500 mM) may shield the effects of other ions or salt present in the crystallisation screens. NOG (1 mM) was also added to some of the crystallisation trials. Commercial screens including JCSG+ (Molecular Dimensions, Suffolk, UK), PACT Premier (Molecular Dimensions, Suffolk, UK) and PEG/Ion (Hampton Research, CA, USA) were used in initial screening. Crystals were observed in a variety of conditions, with the largest found in wells containing 0.2 M sodium tartrate dibasic dihydrate, pH 7.4, 20% (w/v) polyethylene glycol 3350 with a protein-to-mother liquor ratio of 1:2 using the sitting-drop vapour diffusion method at 20 °C.

Two datasets to a resolution of 1.9 Å (PHF2 without NOG) and 2.1 Å (PHF2 with NOG added) were collected at the Diamond Light Source beamline I04-1 (**Figure 19**). Both structures were solved by molecular replacement using the PHASER subroutine of PHENIX with the published PHF2 JmjC domain structure (3PUA, 100% sequence similarity) (Borbulevych et al. 2014). The refinement was carried out using PHENIX and the model was built manually using COOT (Emsley and Cowtan 2004).

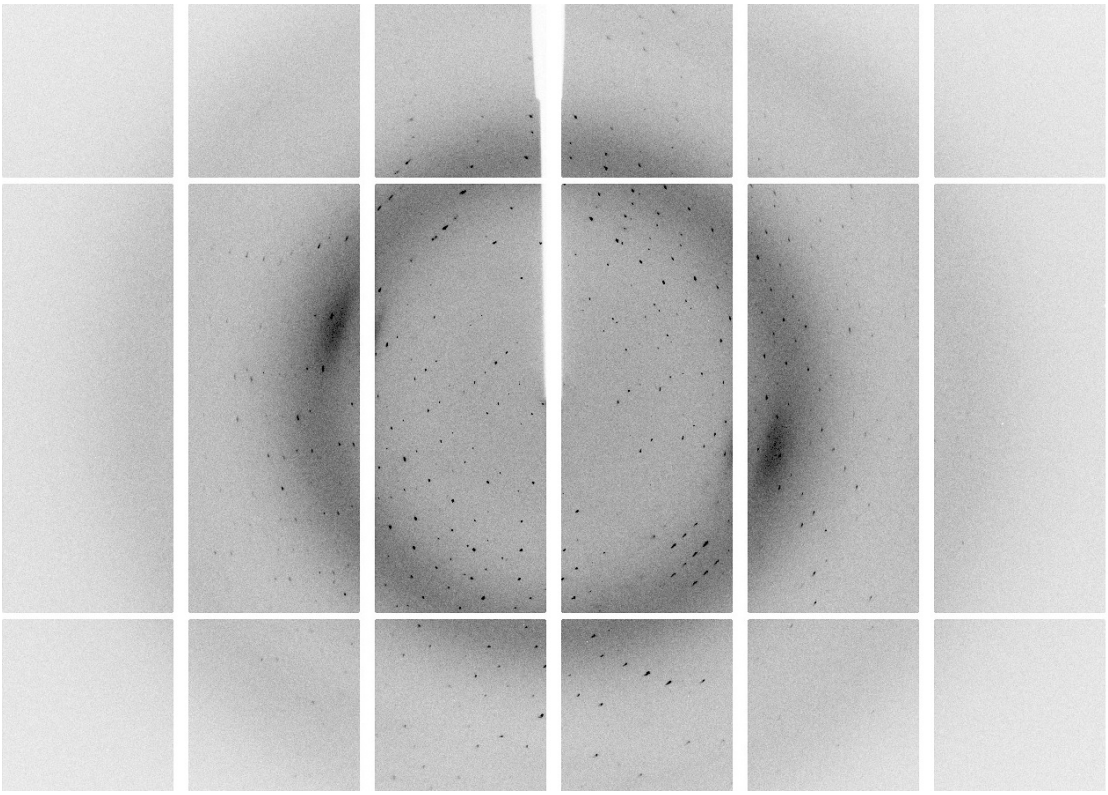


Figure 19 Diffraction image of a PHF2 crystal taken at Diamond Light Source beamline I04-1.

Interestingly, both PHF2 structures solved in this project revealed only an apo JmjC domain fragment, rather than the intact PHD and JmjC construct have been used for crystallisation. The structures obtained in this section were nearly identical to the reported structure used for molecular replacement (PDB 3PTR, Figure 20a, sequence dentity 100%; rmsd value of 0.212 Å). SDS-PAGE analysis of the crystallisation drops PHF2 revealed two distinct bands, which suggested the cleavage of PHF2

occurred during crystallisation trials possibly due to residual protease present after protein purification (Figure 20e). The 1.9 Å dataset was refined in space group C 1 2 1 (**Table 5**). The catalytic site of PHF2 JmjC (apo) contains the HxD…Y metal coordination motif as well as a tyrosine (Y259) that points towards the catalytic site (Figure 20b). Comparison between the PHF2 and the published PHF2 JmjC-Ni(II)-NOG (3PUA) structures reveal an interesting conformational change of the Y259 side chain, which suggested that upon binding, NOG pushes the side Y259 chain away to coordinate to the Ni^{2+} (Figure 20c). This conformational change (Y257) was also observed in the PHF8 structures (Figure 20d) (Horton et al. 2010). Although Mn^{2+} ions and NOG were added during crystallisation, no structures of a metal- or metal-NOG-bound PHF2 complex were obtained. Experiments investigating the metal binding ability of PHF2 (see Section 4.3 and 4.4, performed after crystallography) suggested that PHF2 does not at least efficiently bind Mn^{2+} ions at its active site. Therefore a PHF2-NOG complex could not be obtained, as metal binding is required first to complete NOG interaction in the active site.

Table 5 Crystallographic data and refinement statistics

Data Collection	**PHF2**
X-ray Source	Diamond Light Source beamline I04
Wavelength (Å)	0.9795
Resolution (Å)	1.90 (1.97 - 1.90)[§]
Space group	C 1 2 1
Unit Cell Dimensions a, b, c (Å)	(α = γ = 90°) 110.39 65.98 66.98
Molecules per a.u.	1
Total Number of Reflections Observed	72009
Number of Unique Reflections	36454 (3632)[§]
Redundancy	2.0 (2.0)[§]
Completeness (%)	98.2 (99.1)[§]
I/σ	14 (2.5)[§]
R_{merge}	0.031 (0.289)
R_{work}/R_{free}	0.1778/0.2110
RMS deviation	0.0079 (1.049°)
Average B factors (Å^2)	37.89
Number of water molecules	198

§ Parentheses indicate high resolution shell

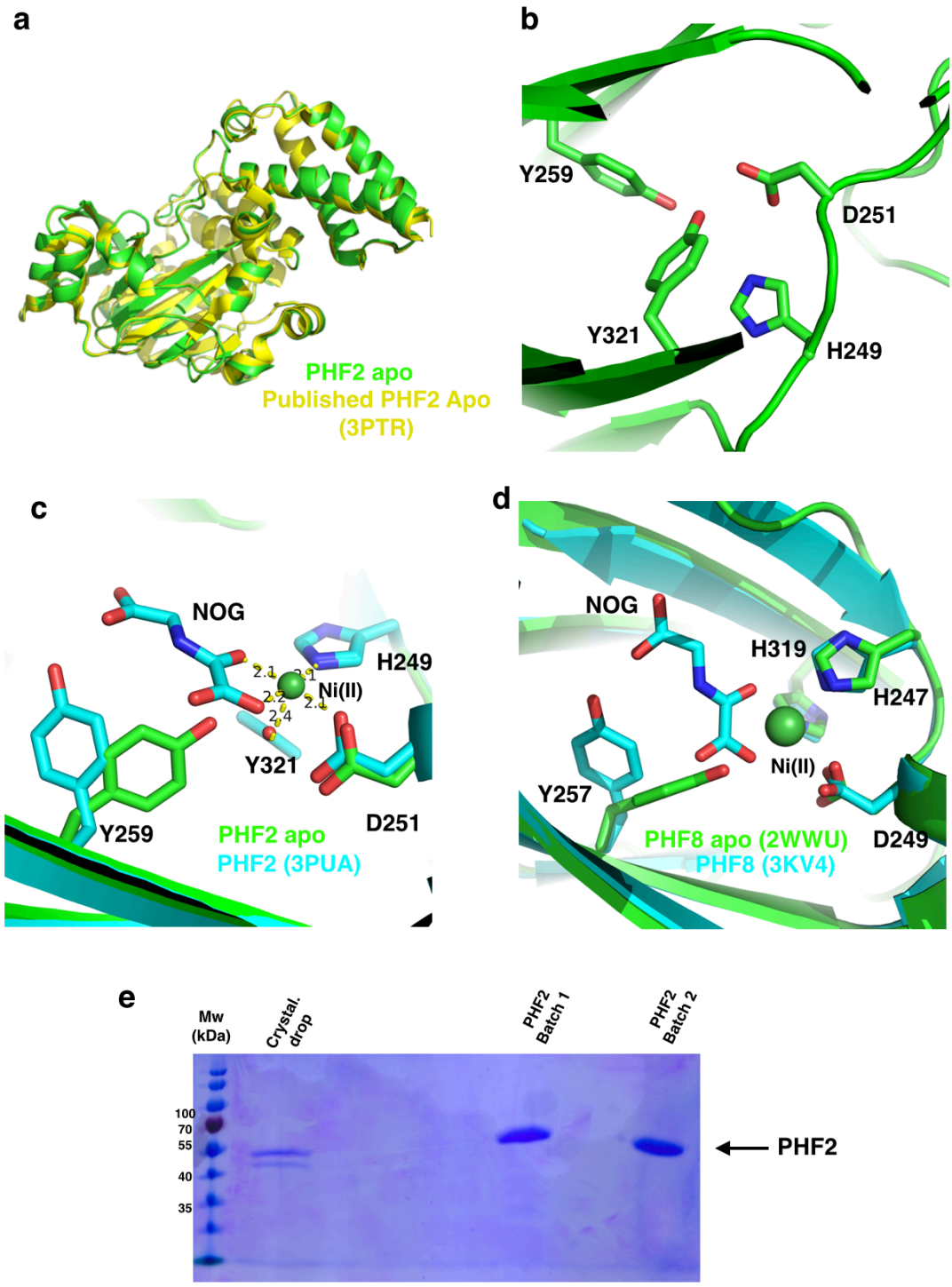


Figure 20 Structures of PHF2 JmjC domain and SDS-PAGE analysis. a) View of the overall structure of PHF2 JmjC domain overlayed with the published PHF2 JmjC domain structure (3PTR) (Horton et al. 2011). **b)** View of the active site of PHF2. **c)** Superimposition of active sites of PHF2 apo (green) and PHF2-Ni(II)-NOG (3PUA, blue) (Horton et al. 2011). **d)** Superimposition of active sites of PHF8 apo (2WWU, green) and PHF8-Ni(II)-NOG (3KV4, blue) (Horton et al. 2010). Notice that the flip of Y259 upon NOG coordination in PHF2 was also observed in PHF8 (Y257). **e)** SDS-PAGE analysis of the crystallisation drop and two different batches of PHF2 protein stored at -80 °C.

Conclusions

The project objectives of this dissertation, as outlined in the introduction section, were to:

- Characterise PHF2 biochemically
- Structurally characterise PHF2 using X-ray crystallography.

In summary, the following achievements have been made:

(i) An expression and purification protocol for PHF2 has been successfully developed, and large amount of purified PHF2 was obtained without visible precipitations.

(ii) Insights were gained into the cofactor, co-substrates and peptide binding mechanism of PHF2 using NMR, MALDI mass spectrometry, non-denaturing ESI-MS, tryptophan fluorescence assays, and fluorescence polarisation assays.

(iii) About 200 inhibitors were screened for PHF2 and a list of hits were obtained.

(iv) PHF2 protein was successfully crystallised and an apo structure of the JmjC domain from PHF2 was solved at a resolution of 1.90 Å.

The following conclusions can be made based on the results obtained from the above experiments.

1. PHF2 had a stronger binding affinity for Ni^{2+} than Fe^{2+}, although a high concentration of Ni^{2+} seemed to exhibit a destabilising effect on PHF2. This could be due to the unusual composition of the metal binding triad of PHF2. It is possible that the larger side chain of the tyrosine (compared to

the conserved histidine) somehow locks the Ni^{2+} ion, whereas the smaller metal ions such as Fe^{2+} or Mn^{2+} exhibited a weaker binding affinity (Fe^{2+}) or no binding affinity (Mn^{2+}).

2. Although no uncoupled 2OG turnover was observed using NMR, the results from non-denaturing ESI-MS and tryptophan fluorescence indicate that PHF2 is able to bind its cofactor and co-substrates (the binding affinity for oxygen has yet to be determined).
3. It was reported that demethylation at the histone H3K9me2 site was observed in cells over-expressing the gene encoding PHF2. However, no *in vitro* demethylation activity was observed (consistent with the literature reports) (Baba et al. 2011; Horton et al. 2011). Data from the peptide binding assays using fluorescence polarisation suggested that the binding of the proposed substrate peptide histone H3K4me3K9me2 was mainly determined by the PHD finger of PHF2 (binding assays using H3K9me2 peptide could be used to confirm this). As it was confirmed that PHF2 had the ability to coordinate its cofactor and co-substrates, it was expected that the addition of Ni^{2+} and NOG/2OG would increase the peptide binding affinity of PHF2 due to the stabilisation effect of cofactor/co-substrate coordination. However, no difference was observed in the peptide binding affinity of PHF2 by the addition of 2OG and NOG. It raised doubt that the JmjC domain from PHF2 may not be involved in binding of K9me2 site at all. If this hypothesis were true, it would explain the fact that changes in the JmjC domain induced no effect on the peptide recognition of PHF2, and no *in vitro* demethylation activity was observed. Therefore the K9me2 demethylation activity observed in cells are more likely to be due to (i)

series of signalling cascade initiated by PHF2, (ii) the stoichiometric binding of PHF2 to the histone peptide site, hence allows no access of methyltransferase to the K9me2 methylation site, or (iii) that the activity of PHF2 activated or modified by other proteins in the cell.

The work suggested several further lines of investigation could be made to follow up this project:

1. One major issue encountered in this project was the lack of a functional assay for PHF2, as no 2OG conversion and no *in vitro* demethylation activity were observed. Therefore it was difficult to study the significance of the unusual tyrosine in the catalytic site. In future studies, UV-Vis spectroscopy can be exploited to measure the O_2 binding affinities of PHF2, and cell-based demethylation studies could be used to investigate the significance of the tyrosine by comparing the level of methylation at various histone modification sites between cells overexpressing wild-type PHF2 and cells overexpressing the Y321H variant PHF2. In addition, immunoprecipitation of PHF2 could be performed in order to identify binding partners of PHF2, which might reveal a different substrate interaction partner that might stimulate the *in vitro* demethylation activity of PHF2.
2. The initial hits from the inhibitors screen using DSF could be further investigated. The binding affinities of each one for PHF2 could be determined using fluorescence polarization in competition assays against a fluorescently labelled known inhibitor such as FITC-NOG. Other JHDMs could also be used in the binding assays in order to select a PHF2 specific

inhibitor, as a cell-permeable PHF2 specific inhibitor would be useful in cell-based functional studies.

3. A structure of peptide-bound PHF2 containing both PHD finger and the JmjC domain should reveal valuable molecular details about the substrate recognition mechanism of PHF2. The cleavage problem experienced in this project might be solved by the addition of protease inhibitors.

References

Agger, Karl, Paul a C Cloos, Jesper Christensen, Diego Pasini, Simon Rose, Juri Rappsilber, Irina Issaeva, Eli Canaani, Anna Elisabetta Salcini, and Kristian Helin. 2007. "UTX and JMJD3 Are Histone H3K27 Demethylases Involved in HOX Gene Regulation and Development." *Nature* 449(7163): 731–34. http://www.ncbi.nlm.nih.gov/pubmed/17713478 (May 25, 2014).

Aik, WeiShen, Marina Demetriades, Muhammad K K Hamdan, Eleanor A L Bagg, Kar Kheng Yeoh, Clarisse Lejeune, Zhihong Zhang, Michael A McDonough, and Christopher J Schofield. 2013. "Structural Basis for Inhibition of the Fat Mass and Obesity Associated Protein (FTO)." *Journal of medicinal chemistry* 56(9): 3680–88. http://www.ncbi.nlm.nih.gov/pubmed/23547775 (August 21, 2014).

Aik, WeiShen, Michael a McDonough, Armin Thalhammer, Rasheduzzaman Chowdhury, and Christopher J Schofield. 2012. "Role of the Jelly-Roll Fold in Substrate Binding by 2-Oxoglutarate Oxygenases." *Current opinion in structural biology* 22(6): 691–700. http://www.ncbi.nlm.nih.gov/pubmed/23142576 (February 12, 2014).

Akiyama, Haruhiko, and Véronique Lefebvre. 2011. "Unraveling the Transcriptional Regulatory Machinery in Chondrogenesis." *Journal of bone and mineral metabolism* 29(4): 390–95. http://www.pubmedcentral.nih.gov/articlerender.fcgi?artid=3354916&tool=pmcentrez&rendertype=abstract (August 8, 2014).

Alberts, Bruce, Alexander Johnson, and Keith Roberts. 2002. *Molecular Biology of the Cell*.

Allfrey, G, R Faulkner, and A E Mirsky. 1964. "Acetylation and Methylation of Histones and Their Possible Role in the Regulation of RNA Synthesis." *Proceedings of the National Academy of Sciences of the United States of America* 315(1938): 786–94.

Anand, Ruchi, and Ronen Marmorstein. 2007. "Structure and Mechanism of Lysine-Specific Demethylase Enzymes." *The Journal of biological chemistry* 282(49): 35425–29. http://www.ncbi.nlm.nih.gov/pubmed/17897944 (May 27, 2014).

Baba, Atsushi, Fumiaki Ohtake, Yosuke Okuno, Kenichi Yokota, Maiko Okada, Yuuki Imai, Min Ni, Clifford a Meyer, Katsuhide Igarashi, Jun Kanno, Myles Brown, and Shigeaki Kato. 2011. "PKA-Dependent Regulation of the Histone Lysine Demethylase Complex PHF2-ARID5B." *Nature cell biology* 13(6): 668–75. http://www.ncbi.nlm.nih.gov/pubmed/21532585 (October 7, 2013).

Banerjee, Taraswi, and Debabrata Chakravarti. 2011. "A Peek into the Complex Realm of Histone Phosphorylation." *Molecular and cellular biology* 31(24): 4858–73. http://www.pubmedcentral.nih.gov/articlerender.fcgi?artid=3233023&tool=pmcentrez&rendertype=abstract (August 4, 2014).

Bannister, a J, P Zegerman, J F Partridge, E a Miska, J O Thomas, R C Allshire, and T Kouzarides. 2001. "Selective Recognition of Methylated Lysine 9 on Histone H3 by the HP1 Chromo Domain." *Nature* 410(6824): 120–24. http://www.ncbi.nlm.nih.gov/pubmed/11242054.

Bannister, Andrew J, Robert Schneider, and Tony Kouzarides. 2002. "Histone Methylation: Dynamic or Static?" *Cell* 109(7): 801–6. http://www.ncbi.nlm.nih.gov/pubmed/12110177.

Beavis, R. C., T. Chaudhary, and B. T. Chait. 1992. "A-Cyano-4-Hydroxycinnamic Acid as a Matrix for Matrixassisted Laser Desorption Mass Spectromtry." *Organic Mass Spectrometry* 27(2): 156–58. http://doi.wiley.com/10.1002/oms.1210270217 (August 14, 2014).

Berger, Shelley L. 2002. “Histone Modifications in Transcriptional Regulation.” *Current opinion in genetics & development* 12(2): 142–48. http://www.ncbi.nlm.nih.gov/pubmed/11893486.

Berger, Shelley L, Tony Kouzarides, Ramin Shiekhattar, and Ali Shilatifard. 2009. “An Operational Definition of Epigenetics.” *Genes & development* 23(7): 781–83. http://www.pubmedcentral.nih.gov/articlerender.fcgi?artid=3959995&tool=pmcentrez&rendertype=abstract (July 11, 2014).

Bergink, Steven, Florian a Salomons, Deborah Hoogstraten, Tom a M Groothuis, Harm de Waard, Junxin Wu, Li Yuan, Elisabetta Citterio, Adriaan B Houtsmuller, Jacques Neefjes, Jan H J Hoeijmakers, Wim Vermeulen, and Nico P Dantuma. 2006. “DNA Damage Triggers Nucleotide Excision Repair-Dependent Monoubiquitylation of Histone H2A.” *Genes & development* 20(10): 1343–52. http://www.pubmedcentral.nih.gov/articlerender.fcgi?artid=1472908&tool=pmcentrez&rendertype=abstract (July 21, 2014).

Bernstein, Bradley E, Emily L Humphrey, Rachel L Erlich, Robert Schneider, Peter Bouman, Jun S Liu, Tony Kouzarides, and Stuart L Schreiber. 2002. “Methylation of Histone H3 Lys 4 in Coding Regions of Active Genes.” *Proceedings of the National Academy of Sciences of the United States of America* 99(13): 8695–8700. http://www.pubmedcentral.nih.gov/articlerender.fcgi?artid=124361&tool=pmcentrez&rendertype=abstract.

Bienz, Mariann. 2006. “The PHD Finger, a Nuclear Protein-Interaction Domain.” *Trends in biochemical sciences* 31(1): 35–40. http://www.ncbi.nlm.nih.gov/pubmed/16297627 (February 12, 2014).

Björkman, M, P Östling, V Härmä, J Virtanen, J-P Mpindi, J Rantala, T Mirtti, T Vesterinen, M Lundin, a Sankila, a Rannikko, E Kaivanto, P Kohonen, O Kallioniemi, and M Nees. 2012. “Systematic Knockdown of Epigenetic Enzymes Identifies a Novel Histone Demethylase PHF8 Overexpressed in Prostate Cancer with an Impact on Cell Proliferation, Migration and Invasion.” *Oncogene* 31(29): 3444–56. http://www.ncbi.nlm.nih.gov/pubmed/22120715 (August 12, 2014).

Blanusa, Milan, Alexander Schenk, Hengameh Sadeghi, Jan Marienhagen, and Ulrich Schwaneberg. 2010. “Phosphorothioate-Based Ligase-Independent Gene Cloning (PLICing): An Enzyme-Free and Sequence-Independent Cloning Method.” *Analytical biochemistry* 406(2): 141–46. http://www.ncbi.nlm.nih.gov/pubmed/20646988 (July 15, 2014).

Bleijlevens, Boris, Tara Shivarattan, Emily Flashman, Yi Yang, Pete J Simpson, Pertti Koivisto, Barbara Sedgwick, Christopher J Schofield, and Steve J Matthews. 2008. “Dynamic States of the DNA Repair Enzyme AlkB Regulate Product Release.” *EMBO reports* 9(9): 872–77. http://www.pubmedcentral.nih.gov/articlerender.fcgi?artid=2529343&tool=pmcentrez&rendertype=abstract (August 8, 2014).

Borbulevych, Oleg Y, Joshua A Plumley, Roger I Martin, Kenneth M Merz, and Lance M Westerhoff. 2014. “Accurate Macromolecular Crystallographic Refinement: Incorporation of the Linear Scaling, Semiempirical Quantum-Mechanics Program DivCon into the PHENIX Refinement Package.” *Acta crystallographica. Section D, Biological crystallography* 70(Pt 5): 1233–47. http://www.ncbi.nlm.nih.gov/pubmed/24816093 (August 12, 2014).

Briggs, Scott D, Tiaojiang Xiao, Zu-Wen Sun, Jennifer a Caldwell, Jeffrey Shabanowitz, Donald F Hunt, C David Allis, and Brian D Strahl. 2002. “Gene Silencing: Trans-Histone Regulatory Pathway in Chromatin.” *Nature* 418(6897): 498. http://www.ncbi.nlm.nih.gov/pubmed/12152067 (July 21, 2014).

Brownell, J E, J Zhou, T Ranalli, R Kobayashi, D G Edmondson, S Y Roth, and C D Allis. 1996. “*Tetrahymena* Histone Acetyltransferase A: A Homolog to Yeast Gcn5p Linking Histone

Acetylation to Gene Activation." *Cell* 84(6): 843–51. http://www.ncbi.nlm.nih.gov/pubmed/8601308.

Burstein, E A, N S Vedenkina, and M N Ivkova. 1973. "Fluorescence and the Location of Tryptophan Residues in Protein Molecules." *Photochemistry and photobiology* 18(4): 263–79. http://www.ncbi.nlm.nih.gov/pubmed/4583619 (August 21, 2014).

Cao, Ru, Yu-Ichi Tsukada, and Yi Zhang. 2005. "Role of Bmi-1 and Ring1A in H2A Ubiquitylation and Hox Gene Silencing." *Molecular cell* 20(6): 845–54. http://www.ncbi.nlm.nih.gov/pubmed/16359901 (July 15, 2014).

Chen, D., Han Ma, Heng Hong, Stephen S. Koh, Shih-Ming Huang, and Michael R. Stallcup. 1999. "Regulation of Transcription by a Protein Methyltransferase." *Science* 284(5423): 2174–77. http://www.sciencemag.org/cgi/doi/10.1126/science.284.5423.2174 (July 12, 2014).

Chen, Fei, Huirong Yang, Zhenghong Dong, Jian Fang, Ping Wang, Tingting Zhu, Wei Gong, Rui Fang, Yujiang Geno Shi, Ze Li, and Yanhui Xu. 2013. "Structural Insight into Substrate Recognition by Histone Demethylase LSD2/KDM1b." *Cell research* 23(2): 306–9. http://www.pubmedcentral.nih.gov/articlerender.fcgi?artid=3567815&tool=pmcentrez&rendertype=abstract (May 30, 2014).

Chen, Zhongzhou, Jianye Zang, Johnathan Whetstine, Xia Hong, Foteini Davrazou, Tatiana G Kutateladze, Michael Simpson, Qilong Mao, Cheol-Ho Pan, Shaodong Dai, James Hagman, Kirk Hansen, Yang Shi, and Gongyi Zhang. 2006. "Structural Insights into Histone Demethylation by JMJD2 Family Members." *Cell* 125(4): 691–702. http://www.ncbi.nlm.nih.gov/pubmed/16677698 (May 27, 2014).

Cheung, P, C D Allis, and P Sassone-Corsi. 2000. "Signaling to Chromatin through Histone Modifications." *Cell* 103(2): 263–71. http://www.pubmedcentral.nih.gov/articlerender.fcgi?artid=419859&tool=pmcentrez&rendertype=abstract.

Chowdhury, Rasheduzzaman, Kar Kheng Yeoh, Ya-Min Tian, Lars Hillringhaus, Eleanor a Bagg, Nathan R Rose, Ivanhoe K H Leung, Xuan S Li, Esther C Y Woon, Ming Yang, Michael a McDonough, Oliver N King, Ian J Clifton, Robert J Klose, Timothy D W Claridge, Peter J Ratcliffe, Christopher J Schofield, and Akane Kawamura. 2011. "The Oncometabolite 2-Hydroxyglutarate Inhibits Histone Lysine Demethylases." *EMBO reports* 12(5): 463–69. http://www.pubmedcentral.nih.gov/articlerender.fcgi?artid=3090014&tool=pmcentrez&rendertype=abstract (August 13, 2014).

Christensen, Jesper, Karl Agger, Paul a C Cloos, Diego Pasini, Simon Rose, Lau Sennels, Juri Rappsilber, Klaus H Hansen, Anna Elisabetta Salcini, and Kristian Helin. 2007. "RBP2 Belongs to a Family of Demethylases, Specific for Tri-and Dimethylated Lysine 4 on Histone 3." *Cell* 128(6): 1063–76. http://www.ncbi.nlm.nih.gov/pubmed/17320161 (May 27, 2014).

Ciccone, David N, Hui Su, Sarah Hevi, Frédérique Gay, Hong Lei, Jeffrey Bajko, Guoliang Xu, En Li, and Taiping Chen. 2009. "KDM1B Is a Histone H3K4 Demethylase Required to Establish Maternal Genomic Imprints." *Nature* 461(7262): 415–18. http://www.ncbi.nlm.nih.gov/pubmed/19727073 (August 5, 2014).

Culhane, Jeffrey C, and Philip A Cole. 2007. "LSD1 and the Chemistry of Histone Demethylation." *Current opinion in chemical biology* 11(5): 561–68. http://www.pubmedcentral.nih.gov/articlerender.fcgi?artid=2112775&tool=pmcentrez&rendertype=abstract (May 27, 2014).

Cuthbert, Graeme L, Sylvain Daujat, Andrew W Snowden, Hediye Erdjument-bromage, Teruki Hagiwara, Michiyuki Yamada, Robert Schneider, Philip D Gregory, Paul Tempst, Andrew J

Bannister, and Tony Kouzarides. 2004. “Histone Deimination Antagonizes Arginine Methylation.” *Cell* 118: 545–53.

Delaney, James C, Lisa Smeester, Cintyu Wong, Lauren E Frick, Koli Taghizadeh, John S Wishnok, Catherine L Drennan, Leona D Samson, and John M Essigmann. 2005. “AlkB Reverses Etheno DNA Lesions Caused by Lipid Oxidation *in vitro* and *in vivo*.” *Nature structural & molecular biology* 12(10): 855–60. http://www.ncbi.nlm.nih.gov/pubmed/16200073 (August 8, 2014).

Emsley, Paul, and Kevin Cowtan. 2004. “Coot: Model-Building Tools for Molecular Graphics.” *Acta crystallographica. Section D, Biological crystallography* 60(Pt 12 Pt 1): 2126–32. http://www.ncbi.nlm.nih.gov/pubmed/15572765 (July 10, 2014).

Falnes, Pål Ø, Rune F Johansen, and Erling Seeberg. 2002. “AlkB-Mediated Oxidative Demethylation Reverses DNA Damage in *Escherichia coli*.” *Nature* 419(6903): 178–82. http://www.ncbi.nlm.nih.gov/pubmed/12226668.

Fang, Jia, Qin Feng, Carrie S Ketel, Hengbin Wang, Ru Cao, Li Xia, Hediye Erdjument-bromage, Paul Tempst, Jeffrey A Simon, Yi Zhang, Chapel Hill, and North Carolina. 2002. “Purification and Functional Characterization of SET8 , a Nucleosomal Histone H4- Lysine 20-Specific Methyltransferase.” *Current Biology* 12(02): 1086–99.

Fang, Rui, Andrew Barbera, Yufei Xu, Michael Rutenberg, Thiago Leonor, Qing Bi, Fei Lan, Pinchao Mei, Guo-cheng Yuan, Christine Lian, and Junmin Peng. 2012. “Human LSD2/KDM1b/AOF1 Regulates Gene Transcription by Modulating Intragenic H3K4me2 Methylation.” *Molecular cell* 39(2): 222–33.

Feng, Qin, Hengbin Wang, Huck Hui Ng, Hediye Erdjument-bromage, Paul Tempst, Kevin Struhl, Yi Zhang, Chapel Hill, and North Carolina. 2002. “Methylation of H3-Lysine 79 Is Mediated by a New Family of HMTases without a SET Domain.” *Current Biology* 12(02): 1052–58.

Fischle, Wolfgang, Yanming Wang, and C David Allis. 2003. “Histone and Chromatin Cross-Talk.” *Current Opinion in Cell Biology* 15(2): 172–83. http://linkinghub.elsevier.com/retrieve/pii/S0955067403000139 (July 15, 2014).

Flashman, Emily, Lee M Hoffart, Refaat B Hamed, J Martin Bollinger, Carsten Krebs, and Christopher J Schofield. 2010. “Evidence for the Slow Reaction of Hypoxia-Inducible Factor Prolyl Hydroxylase 2 with Oxygen.” *The FEBS journal* 277(19): 4089–99. http://www.ncbi.nlm.nih.gov/pubmed/20840591 (August 27, 2014).

Fu, Ye, Qing Dai, Wen Zhang, Jin Ren, Tao Pan, and Chuan He. 2010. “The AlkB Domain of Mammalian ABH8 Catalyzes Hydroxylation of 5-Methoxycarbonylmethyluridine at the Wobble Position of tRNA.” *Angewandte Chemie (International ed. in English)* 49(47): 8885–88. http://www.pubmedcentral.nih.gov/articlerender.fcgi?artid=3134247&tool=pmcentrez&rendertype=abstract (August 12, 2014).

Gerken, Thomas, Christophe a Girard, Yi-Chun Loraine Tung, Celia J Webby, Vladimir Saudek, Kirsty S Hewitson, Giles S H Yeo, Michael a McDonough, Sharon Cunliffe, Luke a McNeill, Juris Galvanovskis, Patrik Rorsman, Peter Robins, Xavier Prieur, Anthony P Coll, Marcella Ma, Zorica Jovanovic, I Sadaf Farooqi, Barbara Sedgwick, Inês Barroso, Tomas Lindahl, Chris P Ponting, Frances M Ashcroft, Stephen O’Rahilly, and Christopher J Schofield. 2007. “The Obesity-Associated FTO Gene Encodes a 2-Oxoglutarate-Dependent Nucleic Acid Demethylase.” *Science (New York, N.Y.)* 318(5855): 1469–72. http://www.pubmedcentral.nih.gov/articlerender.fcgi?artid=2668859&tool=pmcentrez&rendertype=abstract (July 14, 2014).

Green, Michael R., and Joseph Sambrook. 2012. *Molecular Cloning: A Laboratory Manual*. Cold Spring Harbor Laboratory Press.

Van Haaften, Gijs, Gillian L Dalgliesh, Helen Davies, Lina Chen, Graham Bignell, Chris Greenman, Sarah Edkins, Claire Hardy, Sarah O'Meara, Jon Teague, Adam Butler, Jonathan Hinton, Calli Latimer, Jenny Andrews, Syd Barthorpe, Dave Beare, Gemma Buck, Peter J Campbell, Jennifer Cole, Simon Forbes, Mingming Jia, David Jones, Chai Yin Kok, Catherine Leroy, Meng-Lay Lin, David J McBride, Mark Maddison, Simon Maquire, Kirsten McLay, Andrew Menzies, Tatiana Mironenko, Lee Mulderrig, Laura Mudie, Erin Pleasance, Rebecca Shepherd, Raffaella Smith, Lucy Stebbings, Philip Stephens, Gurpreet Tang, Patrick S Tarpey, Rachel Turner, Kelly Turrell, Jennifer Varian, Sofie West, Sara Widaa, Paul Wray, V Peter Collins, Koichi Ichimura, Simon Law, John Wong, Siu Tsan Yuen, Suet Yi Leung, Giovanni Tonon, Ronald a DePinho, Yu-Tzu Tai, Kenneth C Anderson, Richard J Kahnoski, Aaron Massie, Sok Kean Khoo, Bin Tean Teh, Michael R Stratton, and P Andrew Futreal. 2009. "Somatic Mutations of the Histone H3K27 Demethylase Gene UTX in Human Cancer." *Nature genetics* 41(5): 521–23. http://www.pubmedcentral.nih.gov/articlerender.fcgi?artid=2873835&tool=pmcentrez&rendertype=abstract (July 17, 2014).

Hamada, Shohei, Tae-Dong Kim, Takayoshi Suzuki, Yukihiro Itoh, Hiroki Tsumoto, Hidehiko Nakagawa, Ralf Janknecht, and Naoki Miyata. 2009. "Synthesis and Activity of N-Oxalylglycine and Its Derivatives as Jumonji C-Domain-Containing Histone Lysine Demethylase Inhibitors." *Bioorganic & medicinal chemistry letters* 19(10): 2852–55. http://www.ncbi.nlm.nih.gov/pubmed/19359167 (September 5, 2014).

Han, Zhifu, Tianhui Niu, Junbiao Chang, Xiaoguang Lei, Mingyan Zhao, Qiang Wang, Wei Cheng, Jinjing Wang, Yi Feng, and Jijie Chai. 2010. "Crystal Structure of the FTO Protein Reveals Basis for Its Substrate Specificity." *Nature* 464(7292): 1205–9. http://www.ncbi.nlm.nih.gov/pubmed/20376003 (August 12, 2014).

Harp, Joel M., B. Leif Hanson, David E. Timm, and Gerard J. Bunick. 2000. "Asymmetries in the Nucleosome Core Particle at 2.5 Å Resolution." *Acta Crystallographica Section D Biological Crystallography* 56(12): 1513–34. http://scripts.iucr.org/cgi-bin/paper?S0907444900011847 (August 3, 2014).

Hasenpusch-Theil, K, B P Chadwick, T Theil, S K Heath, D G Wilkinson, and a M Frischauf. 1999. "PHF2, a Novel PHD Finger Gene Located on Human Chromosome 9q22." *Mammalian genome : official journal of the International Mammalian Genome Society* 10(3): 294–98. http://www.ncbi.nlm.nih.gov/pubmed/10051327.

Hashimoto, Hideharu, June E Pais, Xing Zhang, Lana Saleh, Zheng-Qing Fu, Nan Dai, Ivan R Corrêa, Yu Zheng, and Xiaodong Cheng. 2014. "Structure of a Naegleria Tet-like Dioxygenase in Complex with 5-Methylcytosine DNA." *Nature* 506(7488): 391–95. http://www.ncbi.nlm.nih.gov/pubmed/24390346 (July 14, 2014).

Hata, Kenji, Rikako Takashima, Katsuhiko Amano, Koichiro Ono, Masako Nakanishi, Michiko Yoshida, Makoto Wakabayashi, Akio Matsuda, Yoshinobu Maeda, Yutaka Suzuki, Sumio Sugano, Robert H Whitson, Riko Nishimura, and Toshiyuki Yoneda. 2013. "Arid5b Facilitates Chondrogenesis by Recruiting the Histone Demethylase Phf2 to Sox9-Regulated Genes." *Nature communications* 4: 2850. http://www.ncbi.nlm.nih.gov/pubmed/24276541 (May 14, 2014).

Hebbes, Tim R, Alan W Thorne, and C Crane-Robinson. 1988. "A Direct Link between Core Histone Acetylation and Transcriptionally Active Chromatin." *EMBO Journal* 7(5): 1395–1402.

Herranz, Nicolás, Natàlia Dave, Alba Millanes-Romero, Lluis Morey, Víctor M Díaz, Víctor Lórenz-Fonfría, Ricardo Gutierrez-Gallego, Celia Jerónimo, Luciano Di Croce, Antonio García de Herreros, and Sandra Peiró. 2012. "Lysyl Oxidase-like 2 Deaminates Lysine 4 in Histone H3." *Molecular cell* 46(3): 369–76. http://www.ncbi.nlm.nih.gov/pubmed/22483618 (August 15, 2014).

Hewitson, K S, N Granatino, R W D Welford, M A McDonough, and C J Schofield. 2005. "Oxidation by 2-Oxoglutarate Oxygenases: Non-Haem Iron Systems in Catalysis and Signalling."

Philosophical transactions. Series A, Mathematical, physical, and engineering sciences 363(1829): 807–28; discussion 1035–40. http://rsta.royalsocietypublishing.org/content/363/1829/807.long (August 23, 2014).

Holde, K E Van, C G Sahasrabuddhe, and Barbara Ramsay Shaw. 1974. "A Model for Particulate Structure in Chromatin." *Nucleic Acids Research* 1(11): 1579–86.

Hopkinson, Richard J., Refaat B. Hamed, Nathan R. Rose, Timothy D. W. Claridge, and Christopher J. Schofield. 2010. "Monitoring the Activity of 2-Oxoglutarate Dependent Histone Demethylases by NMR Spectroscopy: Direct Observation of Formaldehyde." *ChemBioChem* 11(4): 506–10. http://doi.wiley.com/10.1002/cbic.200900713 (August 14, 2014).

Horton, John R, Anup K Upadhyay, Hideharu Hashimoto, Xing Zhang, and Xiaodong Cheng. 2011. "Structural Basis for Human PHF2 Jumonji Domain Interaction with Metal Ions." *Journal of molecular biology* 406(1): 1–8. http://www.pubmedcentral.nih.gov/articlerender.fcgi?artid=3030633&tool=pmcentrez&rendertype=abstract (October 7, 2013).

Horton, John R, Anup K Upadhyay, Hank H Qi, Xing Zhang, Yang Shi, and Xiaodong Cheng. 2010. "Enzymatic and Structural Insights for Substrate Specificity of a Family of Jumonji Histone Lysine Demethylases." *Nature structural & molecular biology* 17(1): 38–43. http://www.pubmedcentral.nih.gov/articlerender.fcgi?artid=2849977&tool=pmcentrez&rendertype=abstract (February 8, 2014).

Huang, Chengyang, Yang Xiang, Yanru Wang, Xia Li, Longyong Xu, Ziqi Zhu, Ting Zhang, Qingqing Zhu, Kejing Zhang, Naihe Jing, and Charlie Degui Chen. 2010. "Dual-Specificity Histone Demethylase KIAA1718 (KDM7A) Regulates Neural Differentiation through FGF4." *Cell research* 20(2): 154–65. http://dx.doi.org/10.1038/cr.2010.5 (September 3, 2014).

Hutton, J, Arnold Kaplan, and Sidney Udenfriend. 1967. "Conversion of the Amino Acid Sequence Proline Gly-Pro-Pro Hydroxylase in Protein to Gly-Pro-Hyp by Collagen Proline Hydroxylase." *Biochemistry and Biophysics* 121: 384–91.

Van Ingen, Hugo, Frederik M a van Schaik, Hans Wienk, Joost Ballering, Holger Rehmann, Annemarie C Dechesne, John a W Kruijzer, Rob M J Liskamp, H Th Marc Timmers, and Rolf Boelens. 2008. "Structural Insight into the Recognition of the H3K4me3 Mark by the TFIID Subunit TAF3." *Structure (London, England : 1993)* 16(8): 1245–56. http://www.ncbi.nlm.nih.gov/pubmed/18682226 (May 28, 2014).

Jenuwein, T, and C D Allis. 2001. "Translating the Histone Code." *Science (New York, N.Y.)* 293(5532): 1074–80. http://www.ncbi.nlm.nih.gov/pubmed/11498575 (April 29, 2014).

Kaelin, William G, and Peter J Ratcliffe. 2008. "Oxygen Sensing by Metazoans: The Central Role of the HIF Hydroxylase Pathway." *Molecular cell* 30(4): 393–402. http://www.ncbi.nlm.nih.gov/pubmed/18498744 (August 1, 2014).

Kao, Cheng-Fu, Cory Hillyer, Toyoko Tsukuda, Karl Henry, Shelley Berger, and Mary Ann Osley. 2004. "Rad6 Plays a Role in Transcriptional Activation through Ubiquitylation of Histone H2B." *Genes & development* 18(2): 184–95. http://www.pubmedcentral.nih.gov/articlerender.fcgi?artid=324424&tool=pmcentrez&rendertype=abstract (August 4, 2014).

Klose, Robert J, Eric M Kallin, and Yi Zhang. 2006. "JmjC-Domain-Containing Proteins and Histone Demethylation." *Nature reviews. Genetics* 7(9): 715–27. http://www.ncbi.nlm.nih.gov/pubmed/16983801 (September 17, 2013).

Klose, Robert J, Kenichi Yamane, Yangjin Bae, Dianzheng Zhang, Hediye Erdjument-Bromage, Paul Tempst, Jiemin Wong, and Yi Zhang. 2006. "The Transcriptional Repressor JHDM3A

Demethylates Trimethyl Histone H3 Lysine 9 and Lysine 36." *Nature* 442(7100): 312–16. http://www.ncbi.nlm.nih.gov/pubmed/16732292 (May 27, 2014).

Koshibu, Kyoko, Johannes Gräff, Monique Beullens, Fabrice D Heitz, Dominik Berchtold, Holger Russig, Mélissa Farinelli, Mathieu Bollen, and Isabelle M Mansuy. 2009. "Protein Phosphatase 1 Regulates the Histone Code for Long-Term Memory." *The Journal of neuroscience : the official journal of the Society for Neuroscience* 29(41): 13079–89. http://www.ncbi.nlm.nih.gov/pubmed/19828821 (August 1, 2014).

Kouzarides, Tony. 2002. "Histone Methylation in Transcriptional Control." *Current opinion in genetics & development* 12(2): 198–209. http://www.ncbi.nlm.nih.gov/pubmed/11893494.

Krishnan, Swathi, Scott Horowitz, and Raymond C Trievel. 2011. "Structure and Function of Histone H3 Lysine 9 Methyltransferases and Demethylases." *ChemBioChem : a European journal of chemical biology* 12(2): 254–63. http://www.ncbi.nlm.nih.gov/pubmed/21243713 (February 12, 2014).

Kristensen, Line H, Anders L Nielsen, Charlotte Helgstrand, Michael Lees, Paul Cloos, Jette S Kastrup, Kristian Helin, Lars Olsen, and Michael Gajhede. 2012. "Studies of H3K4me3 Demethylation by KDM5B/Jarid1B/PLU1 Reveals Strong Substrate Recognition *in vitro* and Identifies 2,4-Pyridine-Dicarboxylic Acid as an in Vitro and in Cell Inhibitor." *The FEBS journal* 279(11): 1905–14. http://www.ncbi.nlm.nih.gov/pubmed/22420752 (August 22, 2014).

Kruidenier, Laurens, Chun-wa Chung, Zhongjun Cheng, John Liddle, KaHing Che, Gerard Joberty, Marcus Bantscheff, Chas Bountra, Angela Bridges, Hawa Diallo, Dirk Eberhard, Sue Hutchinson, Emma Jones, Roy Katso, Melanie Leveridge, Palwinder K Mander, Julie Mosley, Cesar Ramirez-Molina, Paul Rowland, Christopher J Schofield, Robert J Sheppard, Julia E Smith, Catherine Swales, Robert Tanner, Pamela Thomas, Anthony Tumber, Gerard Drewes, Udo Oppermann, Dinshaw J Patel, Kevin Lee, and David M Wilson. 2012. "A Selective Jumonji H3K27 Demethylase Inhibitor Modulates the Proinflammatory Macrophage Response." *Nature* 488(7411): 404–8. http://www.ncbi.nlm.nih.gov/pubmed/22842901 (January 23, 2014).

Lachner, Monika, Roderick J O'Sullivan, and Thomas Jenuwein. 2003. "An Epigenetic Road Map for Histone Lysine Methylation." *Journal of cell science* 116(Pt 11): 2117–24. http://www.ncbi.nlm.nih.gov/pubmed/12730288 (May 23, 2014).

Lacoste, Nicolas, Rhea T Utley, Joanna M Hunter, Guy G Poirier, and Jacques Côte. 2002. "Disruptor of Telomeric Silencing-1 Is a Chromatin-Specific Histone H3 Methyltransferase." *The Journal of biological chemistry* 277(34): 30421–24. http://www.ncbi.nlm.nih.gov/pubmed/12097318 (July 23, 2014).

Laumonnier, F, S Holbert, N Ronce, F Faravelli, S Lenzner, C E Schwartz, J Lespinasse, H Van Esch, D Lacombe, C Goizet, F Phan-Dinh Tuy, H van Bokhoven, J-P Fryns, J Chelly, H-H Ropers, C Moraine, B C J Hamel, and S Briault. 2005. "Mutations in PHF8 Are Associated with X Linked Mental Retardation and Cleft Lip/cleft Palate." *Journal of medical genetics* 42(10): 780–86. http://www.pubmedcentral.nih.gov/articlerender.fcgi?artid=1735927&tool=pmcentrez&rendertype=abstract (August 15, 2014).

Lee, H J, M D Lloyd, K Harlos, I J Clifton, J E Baldwin, and C J Schofield. 2001. "Kinetic and Crystallographic Studies on Deacetoxycephalosporin C Synthase (DAOCS)." *Journal of molecular biology* 308(5): 937–48. http://www.sciencedirect.com/science/article/pii/S0022283601946492 (September 5, 2014).

Lee, KH, JW Park, HS Sung, YJ Choi, W H Kim, H S Lee, HJ Chung, HW Shin, CH Cho, TY Kim, SH Li, HD Youn, S J Kim, and YS Chun. 2014. "PHF2 Histone Demethylase Acts as a Tumor Suppressor in Association with p53 in Cancer." *Oncogene* (January): 1–13. http://www.ncbi.nlm.nih.gov/pubmed/25043306 (July 28, 2014).

Li, Haitao, Serge Ilin, Wooikoon Wang, Elizabeth M Duncan, Joanna Wysocka, C David Allis, and Dinshaw J Patel. 2006. "Molecular Basis for Site-Specific Read-out of Histone H3K4me3 by the BPTF PHD Finger of NURF." *Nature* 442(7098): 91–95. http://www.ncbi.nlm.nih.gov/pubmed/16728978 (January 21, 2014).

Liu, Wen, Bogdan Tanasa, Oksana V Tyurina, Tian Yuan Zhou, Reto Gassmann, Wei Ting Liu, Kenneth a Ohgi, Chris Benner, Ivan Garcia-Bassets, Aneel K Aggarwal, Arshad Desai, Pieter C Dorrestein, Christopher K Glass, and Michael G Rosenfeld. 2010. "PHF8 Mediates Histone H4 Lysine 20 Demethylation Events Involved in Cell Cycle Progression." *Nature* 466(7305): 508–12. http://www.pubmedcentral.nih.gov/articlerender.fcgi?artid=3059551&tool=pmcentrez&rendertype=abstract (January 24, 2014).

Lloyd, M D, H J Lee, K Harlos, Z H Zhang, J E Baldwin, C J Schofield, J M Charnock, C D Garner, T Hara, A C Terwisscha van Scheltinga, K Valegård, J A Viklund, J Hajdu, I Andersson, A Danielsson, and R Bhikhabhai. 1999. "Studies on the Active Site of Deacetoxycephalosporin C Synthase." *Journal of molecular biology* 287(5): 943–60. http://www.ncbi.nlm.nih.gov/pubmed/10222202 (September 5, 2014).

Lo, W S, L Duggan, N C Emre, R Belotserkovskya, W S Lane, R Shiekhattar, and S L Berger. 2001. "Snf1--a Histone Kinase That Works in Concert with the Histone Acetyltransferase Gcn5 to Regulate Transcription." *Science (New York, N.Y.)* 293(5532): 1142–46. http://www.ncbi.nlm.nih.gov/pubmed/11498592 (July 15, 2014).

Loenarz, Christoph, Rasheduzzaman Chowdhury, Christopher J Schofield, and Emily Flashman. 2008. "Oxygenases for Oxygen Sensing." *Pure Appl. Chem.* 80(8): 1837–47.

Loenarz, Christoph, Wei Ge, Mathew L Coleman, Nathan R Rose, Christopher D O Cooper, Robert J Klose, Peter J Ratcliffe, and Christopher J Schofield. 2010. "PHF8, a Gene Associated with Cleft Lip/palate and Mental Retardation, Encodes for an Nepsilon-Dimethyl Lysine Demethylase." *Human molecular genetics* 19(2): 217–22. http://www.ncbi.nlm.nih.gov/pubmed/19843542 (August 15, 2014).

Loenarz, Christoph, and Christopher J Schofield. 2008. "Expanding Chemical Biology of 2-Oxoglutarate Oxygenases." *Nature chemical biology* 4(3): 152–56. http://www.ncbi.nlm.nih.gov/pubmed/18277970.

———. 2009. "Oxygenase Catalyzed 5-Methylcytosine Hydroxylation." *Chemistry & biology* 16(6): 580–83. http://www.ncbi.nlm.nih.gov/pubmed/19549596 (August 8, 2014).

———. 2011. "Physiological and Biochemical Aspects of Hydroxylations and Demethylations Catalyzed by Human 2-Oxoglutarate Oxygenases." *Trends in biochemical sciences* 36(1): 7–18. http://www.ncbi.nlm.nih.gov/pubmed/20728359 (September 23, 2013).

Loh, Yuin Han, Weiwei Zhang, Xi Chen, Joshy George, and Huck Hui Ng. 2007. "Jmjd1a and Jmjd2c Histone H3 Lys 9 Demethylases Regulate Self-Renewal in Embryonic Stem Cells." *Genes & development* 21(20): 2545–57. http://www.pubmedcentral.nih.gov/articlerender.fcgi?artid=2000320&tool=pmcentrez&rendertype=abstract (July 26, 2014).

Loidl, P. 1994. "Histone Acetylation: Facts and Questions." *Chromosoma* 103(7): 441–49. http://www.ncbi.nlm.nih.gov/pubmed/7720410.

Di Lorenzo, Alessandra, and Mark T Bedford. 2011. "Histone Arginine Methylation." *FEBS letters* 585(13): 2024–31. http://www.pubmedcentral.nih.gov/articlerender.fcgi?artid=3409563&tool=pmcentrez&rendertype=abstract (July 15, 2014).

Mahon, P C, K Hirota, and G L Semenza. 2001. “FIH-1: A Novel Protein That Interacts with HIF-1alpha and VHL to Mediate Repression of HIF-1 Transcriptional Activity.” *Genes & development* 15(20): 2675–86. http://www.pubmedcentral.nih.gov/articlerender.fcgi?artid=312814&tool=pmcentrez&rendertype=abstract (July 17, 2014).

Marchler-Bauer, Aron, Shennan Lu, John B Anderson, Farideh Chitsaz, Myra K Derbyshire, Carol DeWeese-Scott, Jessica H Fong, Lewis Y Geer, Renata C Geer, Noreen R Gonzales, Marc Gwadz, David I Hurwitz, John D Jackson, Zhaoxi Ke, Christopher J Lanczycki, Fu Lu, Gabriele H Marchler, Mikhail Mullokandov, Marina V Omelchenko, Cynthia L Robertson, James S Song, Narmada Thanki, Roxanne A Yamashita, Dachuan Zhang, Naigong Zhang, Chanjuan Zheng, and Stephen H Bryant. 2011. “CDD: A Conserved Domain Database for the Functional Annotation of Proteins.” *Nucleic acids research* 39(Database issue): D225–9. http://www.pubmedcentral.nih.gov/articlerender.fcgi?artid=3013737&tool=pmcentrez&rendertype=abstract (July 13, 2014).

Martin, Cyrus, and Yi Zhang. 2005. “The Diverse Functions of Histone Lysine Methylation.” *Nature reviews. Molecular cell biology* 6(11): 838–49. http://www.ncbi.nlm.nih.gov/pubmed/16261189 (May 23, 2014).

McDonough, Michael A, Christoph Loenarz, Rasheduzzaman Chowdhury, Ian J Clifton, and Christopher J Schofield. 2010. “Structural Studies on Human 2-Oxoglutarate Dependent Oxygenases.” *Current opinion in structural biology* 20(6): 659–72. http://www.ncbi.nlm.nih.gov/pubmed/20888218 (October 17, 2013).

Metzger, Eric, Melanie Wissmann, Na Yin, Judith M Müller, Robert Schneider, Antoine H F M Peters, Thomas Günther, Reinhard Buettner, and Roland Schüle. 2005. “LSD1 Demethylates Repressive Histone Marks to Promote Androgen-Receptor-Dependent Transcription.” *Nature* 437(7057): 436–39. http://www.ncbi.nlm.nih.gov/pubmed/16079795 (May 27, 2014).

Min, Jung Hyun, Haifeng Yang, Mircea Ivan, Frank Gertler, William G Kaelin, and Nikola P Pavletich. 2002. “Structure of an HIF1-alpha-pVHL Complex: Hydroxyproline Recognition in Signaling.” *Science (New York, N.Y.)* 296(5574): 1886–89. http://www.ncbi.nlm.nih.gov/pubmed/12004076 (July 17, 2014).

Mosammaparast, Nima, and Yang Shi. 2010. “Reversal of Histone Methylation: Biochemical and Molecular Mechanisms of Histone Demethylases.” *Annual review of biochemistry* 79: 155–79. http://www.ncbi.nlm.nih.gov/pubmed/20373914 (May 27, 2014).

Mukherji, Mridul, Christopher J Schofield, Anthony S Wierzbicki, Gerbert A Jansen, Ronald J A Wanders, and Matthew D Lloyd. 2003. “The Chemical Biology of Branched-Chain Lipid Metabolism.” *Progress in Lipid Research* 42: 359–76.

Müller, Tina a, Katheryn Meek, and Robert P Hausinger. 2010. “Human AlkB Homologue 1 (ABH1) Exhibits DNA Lyase Activity at Abasic Sites.” *DNA repair* 9(1): 58–65. http://www.pubmedcentral.nih.gov/articlerender.fcgi?artid=2818486&tool=pmcentrez&rendertype=abstract (August 12, 2014).

Myllyharju, Johanna, and Kari I Kivirikko. 2004. “Collagens, Modifying Enzymes and Their Mutations in Humans, Flies and Worms.” *Trends in genetics : TIG* 20(1): 33–43. http://www.ncbi.nlm.nih.gov/pubmed/14698617 (August 10, 2014).

Niesen, Frank H, Helena Berglund, and Masoud Vedadi. 2007a. “The Use of Differential Scanning Fluorimetry to Detect Ligand Interactions That Promote Protein Stability.” *Nature protocols* 2(9): 2212–21. http://www.ncbi.nlm.nih.gov/pubmed/17853878 (January 25, 2014).

———. 2007b. “The Use of Differential Scanning Fluorimetry to Detect Ligand Interactions That Promote Protein Stability.” *Nature protocols* 2(9): 2212–21. http://www.ncbi.nlm.nih.gov/pubmed/17853878 (May 29, 2014).

Okuno, Yosuke, Fumiaki Ohtake, Katsuhide Igarashi, Jun Kanno, Takahiro Matsumoto, Ichiro Takada, Shigeaki Kato, and Yuuki Imai. 2013. “Epigenetic Regulation of Adipogenesis by PHF2 Histone Demethylase.” *Diabetes* 62(5): 1426–34. http://www.ncbi.nlm.nih.gov/pubmed/23274892 (October 7, 2013).

Olson, M O, A W Prestayko, J Olson, Archie W Prestayko, and Harris Busch. 1975. “Isolation and Characterization of Protein A24, a ‘Histone-like’ Non-Histone Chromosomal Protein.” *Journal of Biological Chemistry* 250(7): 7182–87.

Osley, Mary Ann. 2006. “Regulation of Histone H2A and H2B Ubiquitylation.” *Briefings in functional genomics & proteomics* 5(3): 179–89. http://www.ncbi.nlm.nih.gov/pubmed/16772277 (August 4, 2014).

Parker, S. P. 1997. *McGraw-Hill Encyclopedia of Science & Technology*. McGraw-Hill.

Pascual, J, M Martinez-Yamout, H J Dyson, and P E Wright. 2000. “Structure of the PHD Zinc Finger from Human Williams-Beuren Syndrome Transcription Factor.” *Journal of molecular biology* 304(5): 723–29. http://www.ncbi.nlm.nih.gov/pubmed/11124022 (February 4, 2014).

Pazin, M J, and J T Kadonaga. 1997. “What’s up and down with Histone Deacetylation and Transcription?” *Cell* 89(3): 325–28. http://www.ncbi.nlm.nih.gov/pubmed/9150131.

Peña, Pedro V, Foteini Davrazou, Xiaobing Shi, Kay L Walter, Vladislav V Verkhusha, Or Gozani, Rui Zhao, and Tatiana G Kutateladze. 2006. “Molecular Mechanism of Histone H3K4me3 Recognition by Plant Homeodomain of ING2.” *Nature* 442(7098): 100–103. http://www.pubmedcentral.nih.gov/articlerender.fcgi?artid=3190580&tool=pmcentrez&rendertype=abstract (January 30, 2014).

Perrin, F. 1926. “Polarization of Light of Fluorescence, Average Life of Molecules.” *J Phys Radium* 7: 390–401.

Plath, Kathrin, Jia Fang, Susanna K Mlynarczyk-Evans, Ru Cao, Kathleen a Worringer, Hengbin Wang, Cecile C de la Cruz, Arie P Otte, Barbara Panning, and Yi Zhang. 2003. “Role of Histone H3 Lysine 27 Methylation in X Inactivation.” *Science (New York, N.Y.)* 300(5616): 131–35. http://www.ncbi.nlm.nih.gov/pubmed/12649488 (May 27, 2014).

Qi, Hank H, Madathia Sarkissian, Gang-Qing Hu, Zhibin Wang, Arindam Bhattacharjee, D Benjamin Gordon, Michelle Gonzales, Fei Lan, Pat P Ongusaha, Maite Huarte, Nasser K Yaghi, Huijun Lim, Benjamin a Garcia, Leonardo Brizuela, Keji Zhao, Thomas M Roberts, and Yang Shi. 2010. “Histone H4K20/H3K9 Demethylase PHF8 Regulates Zebrafish Brain and Craniofacial Development.” *Nature* 466(7305): 503–7. http://www.pubmedcentral.nih.gov/articlerender.fcgi?artid=3072215&tool=pmcentrez&rendertype=abstract (May 27, 2014).

Rea, S, F Eisenhaber, D O’Carroll, B D Strahl, Z W Sun, M Schmid, S Opravil, K Mechtler, C P Ponting, C D Allis, and T Jenuwein. 2000. “Regulation of Chromatin Structure by Site-Specific Histone H3 Methyltransferases.” *Nature* 406(6796): 593–99. http://www.ncbi.nlm.nih.gov/pubmed/10949293.

Rein Aasland, Toby J. Gibson, A.Francis Stewart. 1995. “The PHD Finger: Implications for Chromatin-Mediated Transcriptional Regulation.” *Trends Biochem Sci* 20(2): 56–59.

Rice, Judd C, Scott D Briggs, Beatrix Ueberheide, Cynthia M Barber, Jeffrey Shabanowitz, Donald F Hunt, Yoichi Shinkai, and C David Allis. 2003. "Histone Methyltransferases Direct Different Degrees of Methylation to Define Distinct Chromatin Domains." *Molecular cell* 12: 1591–98.

Richmond, Robin K, David F Sargent, Timothy J Richmond, Karolin Luger, and Armin W Ma. 1997. "Crystal Structure of Thenucleosome Core Particle at 2.8A." *Nature* 7: 251–60.

Rose, Nathan R, Esther C Y Woon, Anthony Tumber, Louise J Walport, Rasheduzzaman Chowdhury, Xuan Shirley Li, Oliver N F King, Clarisse Lejeune, Stanley S Ng, Tobias Krojer, Mun Chiang Chan, Anna M Rydzik, Richard J Hopkinson, Ka Hing Che, Michelle Daniel, Claire Strain-Damerell, Carina Gileadi, Grazyna Kochan, Ivanhoe K H Leung, James Dunford, Kar Kheng Yeoh, Peter J Ratcliffe, Nicola Burgess-Brown, Frank von Delft, Susanne Muller, Brian Marsden, Paul E Brennan, Michael a McDonough, Udo Oppermann, Robert J Klose, Christopher J Schofield, and Akane Kawamura. 2012. "Plant Growth Regulator Daminozide Is a Selective Inhibitor of Human KDM2/7 Histone Demethylases." *Journal of medicinal chemistry* 55(14): 6639–43. http://www.ncbi.nlm.nih.gov/pubmed/22724510.

Rossetto, Dorine, Nikita Avvakumov, and Jacques Côté. 2012. "Histone Phosphorylation: A Chromatin Modification Involved in Diverse Nuclear Events." *Epigenetics : official journal of the DNA Methylation Society* 7(10): 1098–1108. http://www.pubmedcentral.nih.gov/articlerender.fcgi?artid=3469451&tool=pmcentrez&rendertype=abstract (August 15, 2014).

Ryle, Matthew J, and Robert P Hausinger. 2002. "Non-Heme Iron Oxygenases." *Current opinion in chemical biology* 6(2): 193–201. http://www.ncbi.nlm.nih.gov/pubmed/12039004.

Saiki, R K, D H Gelfand, S Stoffel, S J Scharf, R Higuchi, G T Horn, K B Mullis, and H A Erlich. 1988. "Primer-Directed Enzymatic Amplification of DNA with a Thermostable DNA Polymerase." *Science (New York, N.Y.)* 239(4839): 487–91. http://www.ncbi.nlm.nih.gov/pubmed/2448875 (August 14, 2014).

Sanchez, Roberto, and Ming-Ming Zhou. 2011. "The PHD Finger: A Versatile Epigenome Reader." *Trends in biochemical sciences* 36(7): 364–72. http://www.pubmedcentral.nih.gov/articlerender.fcgi?artid=3130114&tool=pmcentrez&rendertype=abstract (May 27, 2014).

Sanglier, Sarah, Cédric Atmanene, Guillaume Chevreux, and Alain Van Dorsselaer. 2008. "Nondenaturing Mass Spectrometry to Study Noncovalent Protein/protein and Protein/ligand Complexes: Technical Aspects and Application to the Determination of Binding Stoichiometries." *Methods in molecular biology (Clifton, N.J.)* 484: 217–43. http://www.ncbi.nlm.nih.gov/pubmed/18592183 (August 14, 2014).

Schalch, Thomas, Sylwia Duda, David F Sargent, and Timothy J Richmond. 2005. "X-Ray Structure of a Tetranucleosome and Its Implications for the Chromatin Fibre." *Nature* 436(7047): 138–41. http://www.ncbi.nlm.nih.gov/pubmed/16001076 (July 14, 2014).

Schindler U, Beckmann H, Cashmore AR. 1993. "HAT3.1, a Novel *Arabidopsis* Homeodomain Protein Containing a Conserved Cysteine-Rich Region." *The Plant Journal* 4(1): 137–50.

Schofield, Christopher J, and Peter J Ratcliffe. 2004. "Oxygen Sensing by HIF Hydroxylases." *Nature reviews. Molecular cell biology* 5(5): 343–54. http://www.ncbi.nlm.nih.gov/pubmed/15122348 (July 13, 2014).

Sedgwick, Barbara, Paul a Bates, Johanna Paik, Susan C Jacobs, and Tomas Lindahl. 2007. "Repair of Alkylated DNA: Recent Advances." *DNA repair* 6(4): 429–42. http://www.ncbi.nlm.nih.gov/pubmed/17112791 (August 12, 2014).

Semenza, Gregg L. 1999. “REGULATION OF MAMMALIAN O2 HOMEOSTASIS BY HYPOXIA-INDUCIBLE FACTOR 1.” *Annu. Rev. Cell Dev. Biol.* 15: 551–78.

Shi, Yujiang, Fei Lan, Caitlin Matson, Peter Mulligan, Johnathan R Whetstine, Philip A Cole, Robert A Casero, and Yang Shi. 2004. “Histone Demethylation Mediated by the Nuclear Amine Oxidase Homolog LSD1.” *Cell* 119: 941–53.

Shortle, D, D DiMaio, and D Nathans. 1981. “Directed Mutagenesis.” *Annual review of genetics* 15: 265–94. http://www.ncbi.nlm.nih.gov/pubmed/6279018.

Song, Feng, Ping Chen, Dapeng Sun, Mingzhu Wang, Liping Dong, Dan Liang, Rui-Ming Xu, Ping Zhu, and Guohong Li. 2014. “Cryo-EM Study of the Chromatin Fiber Reveals a Double Helix Twisted by Tetranucleosomal Units.” *Science (New York, N.Y.)* 344(6182): 376–80. http://www.ncbi.nlm.nih.gov/pubmed/24763583 (May 23, 2014).

Sterner, David E, and Shelley L Berger. 2000. “Acetylation of Histones and Transcription-Related Factors.” *MICROBIOLOGY AND MOLECULAR BIOLOGY REVIEWS* 64(2): 435–59.

Strahl, Brian D, and C David Allis. 2000. “The Language of Covalent Histone Modifications.” *Nature* 403(January): 41–45.

Strahl, Brian D, Patrick A Grant, Scott D Briggs, James R Bone, Jennifer A Caldwell, Sahana Mollah, Richard G Cook, Jeffrey Shabanowitz, Donald F Hunt, C David Allis, and Zu-wen Sun. 2002. “Set2 Is a Nucleosomal Histone H3-Selective Methyltransferase That Mediates Transcriptional Repression.” *Molecular and Cellular Biology* 22(5): 1298–1306.

Sun, Zu-Wen, and C David Allis. 2002. “Ubiquitination of Histone H2B Regulates H3 Methylation and Gene Silencing in Yeast.” *Nature* 418(6893): 104–8. http://www.ncbi.nlm.nih.gov/pubmed/12077605.

Tachibana, Makoto, Kenji Sugimoto, Masami Nozaki, Jun Ueda, Tsutomu Ohta, Misao Ohki, Mikiko Fukuda, Naoki Takeda, Hiroyuki Niida, Hiroyuki Kato, and Yoichi Shinkai. 2002. “G9a Histone Methyltransferase Plays a Dominant Role in Euchromatic Histone H3 Lysine 9 Methylation and Is Essential for Early Embryogenesis.” *Genes & development* 16(14): 1779–91. http://www.pubmedcentral.nih.gov/articlerender.fcgi?artid=186403&tool=pmcentrez&rendertype=abstract (August 5, 2014).

Tahiliani, Mamta, Kian Peng Koh, Yinghua Shen, William a Pastor, Hozefa Bandukwala, Yevgeny Brudno, Suneet Agarwal, Lakshminarayan M Iyer, David R Liu, L Aravind, and Anjana Rao. 2009. “Conversion of 5-Methylcytosine to 5-Hydroxymethylcytosine in Mammalian DNA by MLL Partner TET1.” *Science (New York, N.Y.)* 324(5929): 930–35. http://www.pubmedcentral.nih.gov/articlerender.fcgi?artid=2715015&tool=pmcentrez&rendertype=abstract (July 9, 2014).

Tarhonskaya, Hanna, Andrea Szöllössi, Ivanhoe K H Leung, Jacob T Bush, Luc Henry, Rasheduzzaman Chowdhury, Aman Iqbal, Timothy D W Claridge, Christopher J Schofield, and Emily Flashman. 2014. “Studies on Deacetoxycephalosporin C Synthase Support a Consensus Mechanism for 2-Oxoglutarate Dependent Oxygenases.” *Biochemistry* 53(15): 2483–93. http://www.ncbi.nlm.nih.gov/pubmed/24684493.

Taverna, Sean D, Serge Ilin, Richard S Rogers, Jason C Tanny, Heather Lavender, Haitao Li, Lindsey Baker, John Boyle, Lauren P Blair, Brian T Chait, Dinshaw J Patel, John D Aitchison, Alan J Tackett, and C David Allis. 2006. “Yng1 PHD Finger Binding to H3 Trimethylated at K4 Promotes NuA3 HAT Activity at K14 of H3 and Transcription at a Subset of Targeted ORFs.” *Molecular cell* 24(5): 785–96. http://www.ncbi.nlm.nih.gov/pubmed/17157260 (May 28, 2014).

Thomas, Jean, and Roger D Kornbergt. 1975. “An Octamer of Histones in Chromatin and Free in Solution Biochemistry :” 72(7): 2626–30.

Trewick, Sarah C, Timothy F Henshaw, Robert P Hausinger, Tomas Lindahl, and Barbara Sedgwick. 2002. "Oxidative Demethylation by *Escherichia coli* AlkB Directly Reverts DNA Base Damage." *Nature* 419(September): 174–78.

Tsai, Wen-Wei, Zhanxin Wang, Teresa T Yiu, Kadir C Akdemir, Weiya Xia, Stefan Winter, Cheng-Yu Tsai, Xiaobing Shi, Dirk Schwarzer, William Plunkett, Bruce Aronow, Or Gozani, Wolfgang Fischle, Mien-Chie Hung, Dinshaw J Patel, and Michelle Craig Barton. 2010. "TRIM24 Links a Non-Canonical Histone Signature to Breast Cancer." *Nature* 468(7326): 927–32. http://www.pubmedcentral.nih.gov/articlerender.fcgi?artid=3058826&tool=pmcentrez&rendertype=abstract (July 11, 2014).

Tsukada, Yu-ichi, Jia Fang, Hediye Erdjument-Bromage, Maria E Warren, Christoph H Borchers, Paul Tempst, and Yi Zhang. 2006. "Histone Demethylation by a Family of JmjC Domain-Containing Proteins." *Nature* 439(7078): 811–16. http://www.ncbi.nlm.nih.gov/pubmed/16362057 (May 27, 2014).

Turner, Bryan M. 1993. "Decoding the Nucleosome." *Cell* 75: 5–8.

Vivian, J T, and P R Callis. 2001. "Mechanisms of Tryptophan Fluorescence Shifts in Proteins." *Biophysical journal* 80(5): 2093–2109. http://www.pubmedcentral.nih.gov/articlerender.fcgi?artid=1301402&tool=pmcentrez&rendertype=abstract.

Walport, Louise J, Richard J Hopkinson, and Christopher J Schofield. 2012. "Mechanisms of Human Histone and Nucleic Acid Demethylases." *Current opinion in chemical biology* 16(5-6): 525–34. http://www.ncbi.nlm.nih.gov/pubmed/23063108 (September 21, 2013).

Wang, H, Z Q Huang, L Xia, Q Feng, H Erdjument-Bromage, B D Strahl, S D Briggs, C D Allis, J Wong, P Tempst, and Y Zhang. 2001. "Methylation of Histone H4 at Arginine 3 Facilitating Transcriptional Activation by Nuclear Hormone Receptor." *Science (New York, N.Y.)* 293(5531): 853–57. http://www.ncbi.nlm.nih.gov/pubmed/11387442 (July 14, 2014).

Wang, Yanming, Joanna Wysocka, Joyce Sayegh, Young-Ho Lee, Julie R Perlin, Lauriebeth Leonelli, Lakshmi S Sonbuchner, Charles H McDonald, Richard G Cook, Yali Dou, Robert G Roeder, Steven Clarke, Michael R Stallcup, C David Allis, and Scott a Coonrod. 2004. "Human PAD4 Regulates Histone Arginine Methylation Levels via Demethylimination." *Science (New York, N.Y.)* 306(5694): 279–83. http://www.ncbi.nlm.nih.gov/pubmed/15345777 (July 14, 2014).

Weake, Vikki M, and Jerry L Workman. 2008. "Histone Ubiquitination: Triggering Gene Activity." *Molecular cell* 29(6): 653–63. http://www.ncbi.nlm.nih.gov/pubmed/18374642 (July 15, 2014).

Wei, Yi, Lanlan Yu, Josephine Bowen, Martin A. Gorovsky, and C. David Allis. 1999. "Phosphorylation of Histone H3 Is Required for Proper Chromosome Condensation and Segregation." *Cell* 97(1): 99–109. http://www.ncbi.nlm.nih.gov/pubmed/10199406.

Wen, Hong, Jingzhi Li, Tanjing Song, Ming Lu, Pu-Yeh Kan, Min Gyu Lee, Bingdong Sha, and Xiaobing Shi. 2010. "Recognition of Histone H3K4 Trimethylation by the Plant Homeodomain of PHF2 Modulates Histone Demethylation." *The Journal of biological chemistry* 285(13): 9322–26. http://www.pubmedcentral.nih.gov/articlerender.fcgi?artid=2843180&tool=pmcentrez&rendertype=abstract (October 7, 2013).

Westbye, Marianne Pedersen, Emadoldin Feyzi, Per Arne Aas, Cathrine Broberg Vågbø, Vivi Anita Talstad, Bodil Kavli, Lars Hagen, Ottar Sundheim, Mansour Akbari, Nina-Beate Liabakk, Geir Slupphaug, Marit Otterlei, and Hans Einar Krokan. 2008. "Human AlkB Homolog 1 Is a Mitochondrial Protein That Demethylates 3-Methylcytosine in DNA and RNA." *The Journal of biological chemistry* 283(36): 25046–56.

http://www.pubmedcentral.nih.gov/articlerender.fcgi?artid=3259822&tool=pmcentrez&rendertype=abstract (July 11, 2014).

Whetstine, Johnathan R, Amanda Nottke, Fei Lan, Maite Huarte, Sarit Smolikov, Zhongzhou Chen, Eric Spooner, En Li, Gongyi Zhang, Monica Colaiacovo, and Yang Shi. 2006. "Reversal of Histone Lysine Trimethylation by the JMJD2 Family of Histone Demethylases." *Cell* 125(3): 467–81. http://www.ncbi.nlm.nih.gov/pubmed/16603238 (May 27, 2014).

Wyce, Anastasia, Tiaojiang Xiao, Kelly a Whelan, Christine Kosman, Wendy Walter, Dirk Eick, Timothy R Hughes, Nevan J Krogan, Brian D Strahl, and Shelley L Berger. 2007. "H2B Ubiquitylation Acts as a Barrier to Ctk1 Nucleosomal Recruitment prior to Removal by Ubp8 within a SAGA-Related Complex." *Molecular cell* 27(2): 275–88. http://www.ncbi.nlm.nih.gov/pubmed/17643376 (July 29, 2014).

Xu, Wenqing, Jessica D Podoll, Xuan Dong, Anthony Tumber, Udo Oppermann, and Xiang Wang. 2013. "Quantitative Analysis of Histone Demethylase Probes Using Fluorescence Polarization." *Journal of medicinal chemistry* 56(12): 5198–5202. http://www.pubmedcentral.nih.gov/articlerender.fcgi?artid=3724763&tool=pmcentrez&rendertype=abstract.

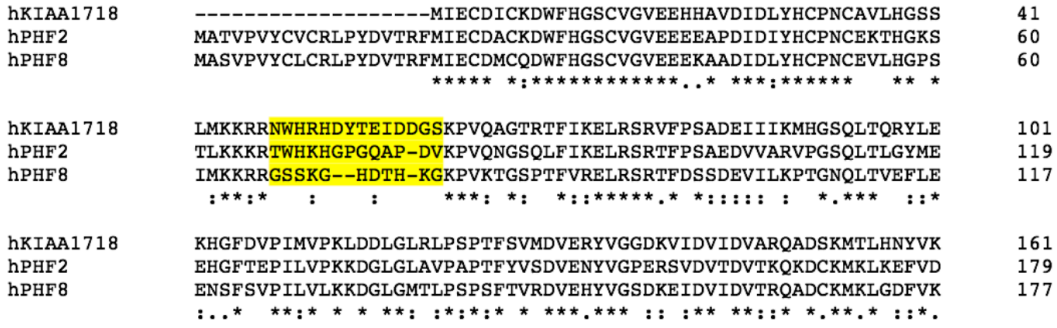
Yi, Chengqi, Guifang Jia, Guanhua Hou, Qing Dai, Wen Zhang, Guanqun Zheng, Xing Jian, Cai-Guang Yang, Qiang Cui, and Chuan He. 2010. "Iron-Catalysed Oxidation Intermediates Captured in a DNA Repair Dioxygenase." *Nature* 468(7321): 330–33. http://dx.doi.org/10.1038/nature09497 (August 18, 2014).

Yokoyama, Atsushi, Yosuke Okuno, Toshihiro Chikanishi, Waka Hashiba, Hiroki Sekine, Ryoji Fujiki, and Shigeaki Kato. 2010. "KIAA1718 Is a Histone Demethylase That Erases Repressive Histone Methyl Marks." *Genes to cells : devoted to molecular & cellular mechanisms* 15(8): 867–73. http://www.ncbi.nlm.nih.gov/pubmed/20629981 (August 15, 2014).

Zhang, Y, and D Reinberg. 2001. "Transcription Regulation by Histone Methylation: Interplay between Different Covalent Modifications of the Core Histone Tails." *Genes & development* 15(18): 2343–60. http://www.ncbi.nlm.nih.gov/pubmed/11562345 (May 24, 2014).

Zhang, Yi, Rabah Iratni, Hediye Erdjument-bromage, Paul Tempst, and Danny Reinberg. 1997. "Histone Deacetylases and SAP18, a Novel Polypeptide, Are Components of a Human Sin3 Complex." *Cell* 89: 357–64.

Supplementary figures and tables



Supplementary Figure 1 Sequence alignment of the *N*-terminal and linker regions between PHD and Jumonji domains of human KIAA1718, human PHF2 and human PHF8. Yellow indicated the linker region.

Primer	Sequence
Construct 1-6 forward primer	tacttccaatccATGGCGACGGTGCCCGTGTACTGCGTC
Construct 3-6 reverse primer	tatccacctttactgTTAAAGGAGTCGTTTCCCGTTCCGATG
Construct 1, 2, 7 and 8 reverse	tatccacctttactgtcaGACGGCTTTGGAGGCATTCTCACTGAG
Y321H SDM forward	TCATCCCCTCAGGCTGGATCCATGCCACACTCACCCCTGTGGACTGCCTG
Y321H SDM reverse	CAGGCAGTCCACAGGGGTGAGTGTGGCATGGATCCAGCCTGAGGGGATGA
Construct 7 and 8 forward	tacttccaatccatgTCCACCTTAAAGAAGAA
PHF2 specific primer 1	AACTACGTGG GGCCGGAACG
PHF2 specific primer 2	TCATCCCCTC AGGCTGGATC
PHF2 specific primer 3	TCCTGGAGAA AGTGTCCAAA
PHF2 specific primer 4	CAAGGCTCTC AGGCCCCCGA
PHF2 specific primer 5	AGCTGGCCAG GCCAAGGGGA
PHF2 specific primer 6	CAGCCTCTAC CACCCCGGCC
PHF2 specific primer 7 (Reverse)	AGCTGCCGTGGAACCAGTCC

Supplementary Table 1 The primers used in this project.